Studies on the electrodeposition of Aluminium from different air and water stable ionic liquids

Dissertation

zur Erlangung des Grades eines Doktors der Naturwissenschaften

vorgelegt von
Dipl.-Ing. Anton Fomin
aus Ramenskoe/USSR

genehmigt von der
Fakultät für Mathematik/Informatik und Maschinenbau
der Technischen Universität Clausthal

Tag der mündlichen Prüfung:
28.10.2010

Dekan: **Prof. Dr. rer. nat. habil. Jürgen Dix**

Berichterstatter: **Prof. Dr. rer. nat. Frank Endres**

Berichterstatter: **Prof. Dr.-Ing. Ulrich Kunz**

Diese Arbeit wurde am Institut für Metallurgie
der Technischen Universität Clausthal angefertigt.

Anton Fomin Datum: **01.10.2010**
Name, Vorname

EIDESSTATTLICHE ERKLÄRUNGEN

Hiermit erkläre ich an Eides Statt, dass ich die bei der Fakultät für Mathematik/Informatik und Maschinenbau der Technischen Universität Clausthal eingereichte Dissertation selbständig und ohne unerlaubte Hilfe angefertigt habe.

Die benutzten Hilfsmittel sind vollständig angegeben.

.....

Unterschrift

Hiermit erkläre ich an Eides Statt, dass ich bisher noch keinen Promotionsversuch unternommen habe.

.....

Unterschrift

Meinen Eltern, meinen Brüdern

und

meiner Tochter

Danksagung

Nach meinen zwei Diplomstudien sowie einem Promotionsstudium bin ich nun zum Ergebnis gekommen, dass es mir ohne Unterstützung und Hilfe von umgebenden Menschen sehr schwer fallen würde. Das Schreiben dieser abschließenden Worte ist der letzte Schritt beim Verfassen meiner Dissertationsschrift. Es handelt sich dabei um eine sehr dankbare Aufgabe, denn sie bietet mir die Möglichkeit, mich bei all diesen Personen nochmals aufrichtig zu bedanken.

Zunächst gilt mein Dank insbesondere meinen Eltern, meinen Brüdern Alexey und Alexander sowie meiner Tochter Nika. Meine Eltern haben mit ihrer Erziehung den Grundstein für meine Entwicklung gelegt und mich bei allen meinen Entscheidungen unterstützt. Für alle Probleme hatte meine Familie immer ein offenes Ohr für mich. Meine Tochter Nika hat mich immer schon mit ihrer Existenz unglaublich motiviert, diese Arbeit zu Ende zu bringen.

Mein Dank richtet sich an meinen Doktorvater Prof. Dr. Frank Endres für die Vergabe des interessanten Promotionsthemas und die Möglichkeit in seiner Arbeitsgruppe diese Doktorarbeit zu machen.

Ich möchte mich auch Bei Frau Dr. Natalia Borissenko für ihre hilfreichen Anregungen, Unterstützung und Korrektur der Arbeit bedanken. Außerdem danke ich Prof. Dr. Sherif Zein El Abedin, Dr. Oliver Höfft, Dr. Qunxian Liu, Dr. Giridhar Pulletikurthi für die Unterstützung und Hilfe beim Schreiben meiner Arbeit.

Als nächstes möchte ich mich bei der gesamten Arbeitsgruppe von Prof. Dr. Endres, Technikerteam vom Institut für Metallurgie sowie Institut für mechanische Verfahrenstechnik bedanken, die jeder einzelne für sich nie abgeneigt waren, einem zum Teil verzweifelten Doktoranden zu helfen. Weiterhin möchte ich ihnen für die ausgezeichnete Einarbeitung ins Laborleben danken. Besonderen Dank geht an Herrn Rüdiger Krosch für seine ständige Hilfsbereitschaft bei der Vorbereitung verschiedener Experimente.

Als letztes danke ich sehr meinem Tutor Prof. Alexander Ivanov aus Moskauer Hochschule für Stahl und Legierungen, der mir bei meinem Umzug nach Deutschland viel geholfen hat.

Ich konnte an dieser Stelle nicht alle Personen aufzählen, die mir während der Dissertation durch konstruktive Kritik, motivierende Gespräche und Ablenkung geholfen haben. Dazu zählt insbesondere auch mein Freundeskreis. All diesen Personen danke ich nochmals ganz herzlich, insbesondere Frau Nune Hovhannisyan für ihre Hilfe bei der Organisation meiner Doktorprüfung.

Content

1. Motivation

Aluminium has a high potential in various industrial applications. It plays an important role as a lightweight material in automotive and aerospace applications. Furthermore, Aluminium reacts with oxygen to form dense layers of Aluminium oxides protecting metals from corrosion. The high corrosion resistance of Al makes it an interesting coating material for steel. The commercial production of Al is carried out by electrolysis of molten cryolite (Na_3AlF_6) in which Aluminium oxide is dissolved at an elevated temperature of about 1000 °C **[1, 2]**. However it is not suitable for coating other metals with Al as the electrolysis is performed at a temperature where Al is a liquid. Currently, there are several methods available for Aluminium plating such as thermal spray coating, hot dipping, cladding, physical and chemical thermal deposition, roll binding and electroplating in e.g. organic solvents. However, all these methods except electroplating are quite expensive and technically demanding. A low-temperature electroplating process is rather cost-efficient. Furthermore the quality and the thickness of the deposits can be adjusted by controlling the parameters of the electrodeposition. Unfortunately, Aluminium cannot be obtained from aqueous baths due to its high reactivity (-1.7 V v.s. NHE). Commercially Al can be electrodeposited from organic solvents (SIGAL-process), however, a main disadvantage is a high volatility and flammability of Al species and/or organic solvents.

During the last decade ionic liquids have attracted the interest as a new generation of solvents for electrodeposition because of their attractive physicochemical properties including large electrochemical windows (up to 7 V), good chemical and thermal stabilities and low vapour pressures. Thus, ionic liquids can be applied as solvents for electrodeposition of many technically important metals which could formerly only be obtained from high temperature molten salts. By far most of studies on the electrodeposition of Aluminium from ionic liquids have been focused on tetrachloroaluminate-based ionic liquids. These ionic liquids are the simplest systems from which high quality Al deposits can be easily electrodeposited. However a main disadvantage of them is the extremely hygroscopic property of these salts. Therefore the chloroaluminate ionic liquids can only be handled under inert-gas atmosphere. The electrodeposition of Aluminium in less reactive air- and water-stable ionic liquids is of great interest. Recently it was shown that nanocrystalline and microcrystalline Al can be electrodeposited from its chloride in air- and water- stable ionic liquids, namely 1-butyl-1-methylpyrrolidinium bis(trifluoromethylsulfonyl)amide, [BMP]Tf_2N, 1-ethyl-3-methylimidazolium bis(trifluoromethylsulfonyl)amide, [EMIm]Tf_2N, and trihexyl-tetradecyl phosphonium bis(trifluoromethylsulfonyl)amide, [$P_{14,6,6,6}$]Tf_2N **[3]**. The ionic

liquids [BMP]Tf_2N and [EMIm]Tf_2N show biphasic behavior in the mixture with $AlCl_3$ and Aluminium can only be deposited from the upper phase of the biphasic mixture. In the case of [BMP]Tf_2N Aluminium deposits with very fine crystallites in the nanometer regime were obtained while in the case of [EMIm]Tf_2N Aluminium particles in the micrometer regime were electrodeposited. It was suggested that the cation of the ionic liquid influences the deposit quality.

The motivation of the present thesis was to investigate if and how the chain length of the ionic liquid cation influences there electrochemical behaviour and the grain size of Aluminium electrodeposits (Chapter 5). The phase behaviour of ILs/$AlCl_3$ and the electrodeposition of Al were studied in four different air- and water- stable ionic liquids namely 1-propyl-1-methylpyrrolidinium bis(trifluoromethylsulfonyl)amide, [PMP]Tf_2N, 1-hexyl-1-methylpyrrolidinium bis(trifluoromethylsulfonyl)amide, [HMP]Tf_2N, 1-octyl-1-methylpyrrolidinium bis(trifluoromethylsulfonyl)amide, [OMP]Tf_2N, and 1-hexyl-3-methylimidazolium bis(trifluoromethylsulfonyl)amide, [HMIm]Tf_2N.

Furthermore the Aluminium electrodeposition on a spring steel substrate was studied (Chapter 6, Chapter 7). Spring steel covered by Aluminium shows a much better corrosion resistance. Thus, it is advantageous to coat steel with an Al layer, which is self-passivated when exposed to corrosive surroundings. It is well- known that Al is oxidized rapidly by air to form an insulating oxide layer enhancing the corrosion resistance.

2 Introduction to Ionic Liquids

Ionic liquids are salt-like materials that solely consist of ions. Often with melting points of below 100 °C. Some authors limit the definition to cations with discrete anions e.g. BF_4^-, NO_3^- **[4]**. This definition however excludes the original work on chloroaluminate systems and the considerable work on other eutectic systems and is therefore unsatisfactory. Systems with anionic species formed by complex equilibria are difficult to categorise as the relative amounts of ionic species depend strongly on the composition of the different components.

Ionic liquids have were in the post classified as first and second generation liquids; where first generation liquids are those based on $AlCl_3$ and second generation are air and water stable **[4]**. The simplest ionic liquids consist of a single cation and a single anion, whereas more complex systems are formed by combining of several cations and/or anions, or complex anions, obtained in equilibrium processes. The physicochemical properties of these systems are a function of cation and anion structure and composition, therefore, a liquid with adjusted properties can be obtained by varying the type of cation and/or anion **[3]**.

2.1 Properties:

Ionic liquids possess a set of unique properties that make them very attractive for electrochemists. Due to their high thermal stability and wide electrochemical window (up to 7 V) ionic liquids can be used as solvents for the electrodeposition of metals, alloys and semiconductors which could formerly only be obtained from high temperature molten salts **[5]**.

Some of the basic physical properties of ionic liquids are presented in the following sections.

2.1.1 Ionic Conductivity

Ionic liquids have reasonably good ionic conductivities when compared with those of organic solvents/electrolyte systems (up to ~10 mS cm^{-1}) **[6]**. At elevated temperatures of e.g. 200 °C a conductivity of 0.1 Ω^{-1} cm^{-1} can be achieved for some systems. However, at room temperature their conductivities are usually lower than those of concentrated aqueous electrolytes. Based on the fact that ionic liquids are composed solely of ions, it would be

expected that ionic liquids have high conductivities. This is not the case since the conductivity of any solvent depends not only on the number of charge carriers but also on their mobility. The large size of ions of ionic liquids reduces the ion mobility leading to lower conductivities. Furthermore, ion pair formation and/or ion aggregation leads to reduced conductivity. The conductivity of ionic liquids is inversely related to their viscosity. Hence, ionic liquids of higher viscosity exhibit lower conductivity. Increasing the temperature decreases viscosity and increases the conductivity.

2.1.2 Viscosity

Generally, ionic liquids are more viscous than common molecular solvents and their viscosities usually range from 10 mPa s to about 500 mPa s at room temperature. The viscosities of some popular air- and water- stable ionic liquids at room temperature are: 312 mPa s for [BMIm]PF_6 **[7]**; 154 mPa s for [BMIm]BF_4 **[8]**; 52 mPa s for [BMIm]Tf_2N **[9];** 85 mPa s for [BMP]Tf_2N **[10].** The viscosity of ionic liquid is due to van der Waals forces and hydrogen bonding. Electrostatic forces may also play an important role. Longs alkyl chains in the cation can also lead to an increase in viscosity **[9]**. This is due to stronger van der Waals forces between cations leading to an increase in the energy required for molecular motion. Also, the ability of anions to form hydrogen bonding has a pronounced effect on viscosity. The fluorinated anions such as BF^-_4 and PF^-_6 form viscous ionic liquids due to the formation of hydrogen bonding **[11]**. In general, all ionic liquids show a significant decrease in viscosity as the temperature increases (see, e.g., ref. **11**).

2.1.3 Density

Ionic liquids in general are denser than water with values ranging from 1 to 1.6 g cm^{-3} and their densities decrease with an increase in the length of the alkyl chain in the cation **[12]**. For example, in ionic liquids composed of substituted imidazolium cations and $CF_3SO_3^-$ the density decreases from 1.39 g cm^{-3} for $[EMIm]^+$ to 1.33 g cm^{-3} for $[EEIm]^+$, to 1.29 g cm^{-3} for $[BMIm]^+$ and to 1.27 g cm^{-3} for $[BEIm]^+$ **[13]**. The densities of ionic liquids are also affected by the type of anions. For example, the densities of 1-butyl-3-methylimidazolium type ionic liquids with different anions, such as BF_4, PF_6, TFA and Tf_2N are 1.12 g cm^{-3} **[14]**, 1.21 g cm^{-3} **[9]**, 1.36 g cm^{-3} **[15]** and 1.43 g cm^{-3} **[9]**, respectively. The order of increasing

density for ionic liquids composed of a single cation at 25 °C is: $[CH_3SO_3]^-$ ≈ $[BF_4]^-$ < $[CF_3SO_3]^-$ < $[(CF_3SO_2)_2N]^-$ **[13]**.

2.1.4 Melting Point

As a class, ionic liquids were defined to have melting points of below 100 °C and many of them are liquid at room temperature. Both cations and anions contribute to the low meting points of ionic liquids. The increase in anion size leads to a decrease in melting point **[16]**. For example, the melting points of 1-ethyl-3-methylimidazolium type ionic liquids with different anions, such as $[BF_4]^-$ and $[Tf_2N]^-$ are 15 °C **[17]** and -3 °C **[9]**, respectively. Cations size and symmetry make an important impact on the melting points of ionic liquids. Large cations and increased asymmetric substitution results in a melting point reduction **[18]**.

2.1.5 Thermal Stability

Ionic liquids can be stable up to 450 °C, at least on a short time scale. The thermal stability of ionic liquids is limited by the strength of their heteroatom–carbon and their heteroatom–hydrogen bonds **[16]**. Wilkes *et al.* **[19]** reported that the ionic liquids 1-ethyl-3-methylimidazolium tetrafluoroborate, 1-butyl-3-methylimdazolium tetrafluoroborate and 1,2-dimethyl-3-propylimidazolium bis(trifluorosulfonyl)amide are stable up to temperatures of 445, 423 and 457 °C, respectively. Most of the ionic liquids have extremely low vapour pressures, thus water can be easily removed from the liquid to contents of below 1 ppm by simple heating under vacuum.

2.1.6 Electrochemical Window

The electrochemical window is an important property and plays a key role in using ionic liquids as solvents for the electrodeposition of metals and semiconductors. By definition, the electrochemical window is the electrochemical potential range over which the electrolyte is neither reduced nor oxidized at an electrode. This value determines the electrochemical stability of the solvents. As known, the electrodeposition of elements and compounds in water is limited by its low electrochemical window of only about 1.2 V. On the contrary, ionic liquids have significantly larger electrochemical windows, *e.g.*, 4.15 V for $[BMIm]PF_6$ at a platinum electrode **[20]**, 4.10 V for $[BMIm]BF_4$ **[20]** and 5.5 V for

[BMP]Tf_2N at a glassy carbon electrode **[21]**. In general, large electrochemical windows of ionic liquids give access to elements which cannot be electrodeposited from aqueous or organic solutions.

In the following section a short overview on the use of the most popular ionic liquids as solvents for electrodeposition of metals, their alloys and semiconductors is given.

2.1.7 Interface effects of Ionic Liquids

Electrodeposition from ionic liquids depends on the interaction strength of ionic liquids cation with the substrate surface. In previous work of our group, Moustafa *et al.* reported that the underpotential deposition (UPD) process was evidenced during the electrodeposition from the upper phase of [EMIm]$Tf_2N/AlCl_3$ on the Au (111) substrate and there was no clear evidence for the under potential deposition electrodeposition from the upper phase of [BMP]$Tf_2N/AlCl_3$ under the same conditions **[3]**. This behaviour is attributed to the differences in the adherence of ionic liquids cations to the substrate, which prevents the UPD process in case of [BMP]Tf_2N. Mezger *et al.* **[22]** studied ionic liquids based on imidazolium and pyrrolidium cations by high-energy x-ray reflectivity and found that these ionic liquids show strong interfacial layering, starting with a cation layer at the substrate and decaying exponentially into the bulk liquid **[22]**. Using an atomic force microscope (AFM), Atkin and Warr detected that the surface charge, roughness and the orientation of cations at the interface are critical determinants of solvation layer formation in ionic liquids **[23]**.

In the work of **[24]**, the surface interaction of [EMIm]Tf_2N and [BMP]Tf_2N with Au(111) substrate has been studied using AFM. They observed that the interaction strength of the interfacial layer is dependent on the cation type, with greater force required for the AFM tip to rupture the innermost layer for [BMP]Tf_2N than for [EMIm]Tf_2N. This difference is attributed to stronger cation surface electrostatic interactions for [BMP]Tf_2N compared to [EMIm]Tf_2N because the positive charge is localized in the case of $[BMP]^+$ and delocalized for $[EMIm]^+$ **[24]**.

2.2 Electrodeposition of Metals, Alloys and Semiconductors from Ionic Liquids

In this section recent efforts on the electrodeposition of less reactive metals (such as Cu, Cd, Zn, Ag, etc.), highly reactive metals (such as Al. Li, and Mg), refractory metals (such as Ta and Ti), some alloys, elemental semiconductors (such as Si and Ge), their mixtures (Si_xGe_{1-x}) and compound semiconductors (CdTe, InSb, etc.) in the ionic liquids is reviewed.

Katayama et al. **[25]** have reported that the room temperature ionic liquid 1-ethyl-3-methylimidazolium tetrafluoroborate ([EMIm]BF_4) is applicable as an alternative electroplating bath for silver. The ionic liquid [EMIm]BF_4 is superior over chloroaluminate systems since the electrodeposition of silver can be performed without the risk of Aluminium codeposition. Electrodeposition of silver from the ionic liquids 1-butyl-3-methylimidazolium tetrafluoroborate ([BMIm]BF_4) and [BMIm]PF_6 was also reported in ref. **[26]**. It was also stated that Cd **[27]**, Cu **[28]** and Sb **[29]** can be electrodeposited in a mixture of 1-ethyl-3-methylimidazolium tetrafluoroborate ([EMIm]BF_4) and [EMIm]Cl. Recently, Sun et al. have demonstrated that compound semiconductors such as indium antimonide (InSb) **[30]** and cadmium telluride (CdTe) **[31]** can be electrodeposited in the 1-ethyl-3-methylimidazolium tetrafluoroborate ionic liquid [BMIm]BF_4. InSb is a III–V compound semiconductor and CdTe is a II–VI semiconductor, both are widely used in many fields such as electronic devices and solar cells. It was stated in ref. **[32]** that titanium can be electrodeposited in thin layers at room temperature in the ionic liquid 1-butyl-3-methylimidazolium bis (trifluoromethylsulfonyl) amide [BMIm]Tf_2N.

It has been shown that ionic liquids can be formed by the combination of zinc chloride with pyridinium- **[33]**, dimethylethylphenyl-ammonium- **[34]**, 1-ethyl-3-methylimidazolium chloride, [EMIm]Cl, and 1-butyl-3-methylimidazolium chloride, [BMIm]Cl **[35-37]**. These ionic liquids are quite easy to prepare and do not decompose in the presence of water and air. It was reported in **[38]** that the potential limits for a basic 1 : 3 $ZnCl_2$–[EMIm]Cl ionic liquid corresponds to the cathodic reduction of $[EMIm]^+$ and anodic oxidation of Cl^-, giving an electrochemical window of approximately 3.0 V. For acidic ionic liquids that have a $ZnCl_2$–[EMIm]Cl molar ratio higher than 0.5 : 1, the negative potential limit is due to the deposition of metallic zinc, and the positive potential limit is due to the oxidation of the chlorozincate complexes. As a result of this fact, the electrodeposition of Zn and its alloys is possible in the Lewis acidic liquids. It was shown that Lewis acidic $ZnCl_2$–[EMIm]Cl (in which the molar ratio of $ZnCl_2$ is higher than 33 mol%) are potentially useful for the electrodeposition of zinc and zinc containing alloys **[39-41]**. Huang and Sun have reported that Pt–Zn alloy **[42]**, iron

and Zn–Fe alloy **[43]**, tin and Sn–Zn alloy **[44]**, cadmium and Cd–Zn alloy **[45]** can be electrodeposited in Lewis acidic $ZnCl_2$–[EMIm]Cl ionic liquids.

Abbott et al. **[46]** have shown the synthesis and characterization of new moisture stable, Lewis acidic ionic liquids/deep eutectic solvents made from metal chlorides and quaternary ammonium salts, which are commercially available. They have shown that mixtures of choline (2-hydroxyethyltrimethylammonium) chloride $[(H_3C)_3NC_2H_4OH)Cl]$ and MCl_2 (M = Zn, Sn) give conducting and viscous liquids at or around room temperature. These liquids are easy to prepare, they are water and air insensitive and their low costs enable their use in large scale applications. Furthermore, they have reported **[47]** that a dark green, viscous liquid can be formed by mixing choline chloride with chromium(III) chloride hexahydrate and the physical properties of this liquid are characteristic of an ionic liquid. The eutectic composition is found to be 1 : 2 choline chloride/chromium chloride. From this ionic liquid chromium can be electrodeposited efficiently to yield a crack-free deposit **[47]**. Addition of LiCl to the choline chloride/$CrCl_3 \cdot 6H_2O$ mixture was found to allow the deposition of nanocrystalline black chromium films **[48]**. The use of this ionic liquid might offer an environmentally friendly process for electrodeposition of chromium instead of the currently used chromic acid based baths.

Endres et al. have studied the electrodeposition of Ta **[49],** Li **[50]**, Mg **[51]**, Se**[52],** In**[52]**, Cu **[52]**, Si **[53-55]**, Ti **[54]** and Ge **[55, 56]** in ionic liquids.

The electroreduction of 0.5 M TaF_5 **[49]** on Au(111) and on polycrystalline gold substrates was investigated at room temperature in the ionic liquid 1-butyl-1-methylpyrrolidinium bis(trifluoromethylsulfonyl)amide, [BMP]TF_2N. The electrochemical reduction of TaF_5 in the employed ionic liquid occurs in several steps. The first redox process is attributed to the reduction of TaF_5 to TaF_3, which likely occurs in the solution, as EQCM indicates no mass change. The electrodeposition of tantalum occurs only in a very narrow potential window and is preceded by the formation of various non-stoichiometric tantalum subhalides.

The underpotential deposition (UPD) of lithium **[50]** was made on Au(111) from 0.5 mol/L $LiTf_2N$ in the air- and water stable ionic liquid 1-butyl-1-methylpyrrolidinium bis(trifluoromethylsulfonyl)amide, [BMP]Tf_2N. The pure [BMP]Tf_2N was found to be inert in the potential regime investigated. The results show that the lithium UPD on Au(111) in [BMP]Tf_2N begins at potentials considerably positive to the electrode potential of bulk deposition and follows a layer-by-layer mechanism with the formation of at least two monolayers. A large number of monoatomically deep pits appears when the potential reaches

positive values, which is an indication that a Li–Au alloy was formed. In a more negative potential regime a less defined layer is formed on the surface that prevents reproducible STM images. This observation might be explained on the basis of initial SEI formation.

The electrochemical deposition of magnesium **[51]** was investigated in the ionic liquids 1-ethyl-3-methylimidazolium tetrafluoroborate [EMIm]BF_4, 1-butyl-1-methylpyrrolidinium triflate [BMP]TfO, and 1-butyl-1-methylpyrrolidinium bis(trifluoromethylsulfonyl)amide [BMP]Tf_2N. The reduction of $Mg(ClO_4)_2$ in 1-butyl-1-methylpyrrolidinium triflate is followed by an anodic process showing typical stripping peak behaviour; however, the current efficiency for magnesium deposition is not very high. In comparison studies, deposition of magnesium from propylene carbonate/tetraethylammonium tetrafluoroborate was observed only after a potential hold at −2.60 V. Magnesium deposition was observed from a THF/1.0 M phenylmagnesium bromide solution; however, additions of [BMP]TfO gradually prevented observation of a magnesium stripping peak. Experiments carried out in solutions of phenyl magnesium Grignard reagents in [BMP]Tf_2N showed possible magnesium deposition; however, removal of the THF in the Grignard reagent solution results in anodic stripping peaks for magnesium at 150 °C.

The electrodeposition of Se, In and Cu **[52]** in the in the air- and water-stable ionic liquid 1-butyl-1-methylpyrrolidinium bis(trifluoromethylsulfonyl)amide ([BMP]Tf_2N) was investigated. The results show that grey selenium can be obtained at temperatures ≥100 °C. XRD patterns of the electrodeposit obtained at 100 °C show the characteristic peaks of crystalline grey selenium. Nanocrystalline indium with grain sizes between 100 and 200 nm was formed in the employed ionic liquid, containing 0.1 M $InCl_3$, at room temperature. It was also found that copper(I) species can be introduced into the ionic liquid [BMP]Tf_2N by anodic dissolution of a copper electrode and nanocrystalline copper with an average crystallite size of about 50 nm was obtained without additives in the resulting electrolyte.

The electrodeposition of silicon was studied on Au (111) **[53]** in the room temperature ionic liquid 1-butyl-1-methylpyrrolidinium bis(trifluoromethylsulfonyl)amide with a $SiCl_4$ concentration of 0.1 mol/L. A main reduction process begins in the cyclic voltammogram at about -1.8 V versus ferrocene/ferrocinium, which is correlated to the electrodeposition of elemental semiconducting silicon. It has been found that at an electrode potential more negative than the open circuit potential (OCP), the Au(111) surface is subject to a restructuring/reconstruction both in the case of the pure ionic liquid and in the presence of $SiCl_4$. The first STM-probed silicon islands with 150-450 pm in height appear at about -1.7 V versus ferrocene/ferrocinium. Their lateral and vertical growth leads to the formation of a

rough layer with silicon islands of up to 1 nm in height. At about -1.8 V the islands merge and form silicon agglomerates. In situ I/U tunneling spectroscopy reveals a band gap of 1.1 ± 0.2 eV for layers of about 5 nm in height, a value that has to be expected for semiconducting silicon.

The investigation of titanium electrodeposition from its halides ($TiCl_4$, TiF_4, TiI_4) in different ionic liquids, namely 1-ethyl-3-methylimidazolium bis(trifluoromethylsulfonyl)amide ([EMIm]Tf_2N), 1-butyl-1-methylpyrrolidinium bis(trifluoromethyl-sulfonyl)amide ([BMP]Tf_2N), and trihexyltetradecyl-phosphonium bis(trifluoromethylsulfonyl)amide ([$P_{14,6,6,6}$]Tf2N) was presented in ref. **[54]**. Cyclic voltammetry and EQCM measurements show that, instead of elemental Ti, only non-stoichiometric halides are formed, for example with average stoichiometries of $TiCl_{0.2}$, $TiCl_{0.5}$ and $TiCl_{1.1}$. In situ STM measurements show that—in the best case—an ultrathin layer of Ti or $TiCl_x$ with thickness below 1 nm can be obtained. In addition, results from both electrochemical and chemical reduction experiments of $TiCl_4$ in a number of these ionic liquids support the formation of insoluble titanium cation–chloride complex species often involving the solvent. Solubility studies suggest that $TiCl_3$ and, particularly, $TiCl_2$ have very limited solubility in these Tf_2N based ionic liquids. Therefore it does not appear possible to reduce Ti^{4+} completely to the metal in the presence of chloride. Successful deposition processing for titanium in ionic liquids will require different maybe tailor-made titanium precursors that avoid these problems **[54]**.

In the paper **[55, 56]** it has been shown for the first time that Ge and Si nanowires with diameters of 90–400 nm can be made by a simple electrochemical template synthesis in an ionic liquid.–Nanosized Si, Ge and Si_xGe_{1-x} films can be made at room temperature by a relatively simple electrochemical process (compared with ultra-high vacuum techniques) in the air- and water-stable ionic liquid [BMP]Tf_2N containing $GeCl_4$ and/or $SiCl_4$ as precursors. The simplicity and the mild reaction conditions of the synthesis process, compared to the traditionally used ultra-high vacuum techniques, make it an attractive method for the manufacture of such materials. The only restriction in this method is the need to perform the synthesis under inert gas conditions because of the hygroscopic nature of the precursors $GeCl_4$ and $SiCl_4$.

The electropolymerization of benzene in the air and water-stable ionic liquid 1-hexyl-3-methylimidazolium tris(pentafluoroethyl)trifluorophosphate, [HMIm]FAP has been shown in **[57]**. The IR results indicate that poly(para)phenylene is the end product of the electropolymerization of benzene in the employed ionic liquid. The resulting conjugation

lengths of the product fall between 19 and 21. A polymer reference electrode is used successfully for the electrochemical polymerization of benzene. The first in situ STM results show that the electropolymerization of benzene in the ionic liquid can be probed on the nanoscale and the band gap of the prepared polymer can be determined. The electrodeposited polymer film obtained at a constant potential of 1.0 V vs PPP (polyparaphenylene) exhibits a band gap of 2.9±0.2 eV.

A short overview on the use of the ionic liquids as solvents for the electrodeposition of Aluminium is given in Chapter 2.4.

2.3 Ionic Liquids Employed in the Present Thesis

In the present study four different air- and water- stable ionic liquids based on the same anion bis(trifluoromethylsulfonyl)amide, Tf_2N^-, and four different cations, namely, 1-hexyl-3-methylimidazolium, $[HMIm]^+$, 1-hexyl-1-methylpyrrolidinium, $[HMP]^+$, 1-octyl-1-methylpyrrolidinium $[OMP]^+$, and 1-propyl-1-methylpyrrolidinium, $[PMP]^+$, were applied to investigate if/how the cation of the ionic liquid influence the quality of aluminum electrodeposits (Figure 1).

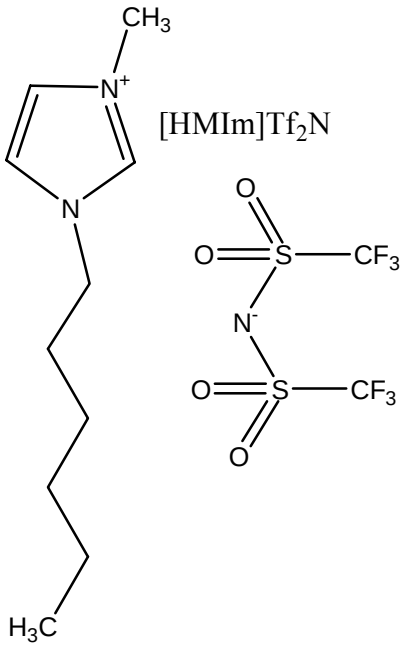

[HMIm]Tf_2N

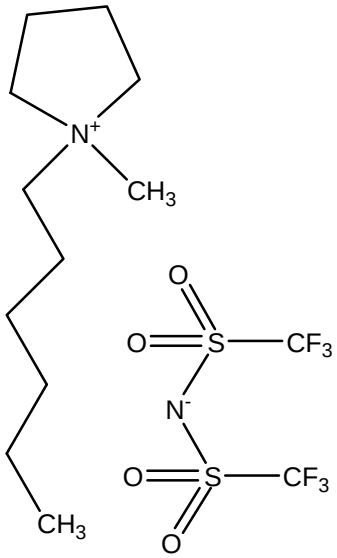

[HMP]Tf_2N

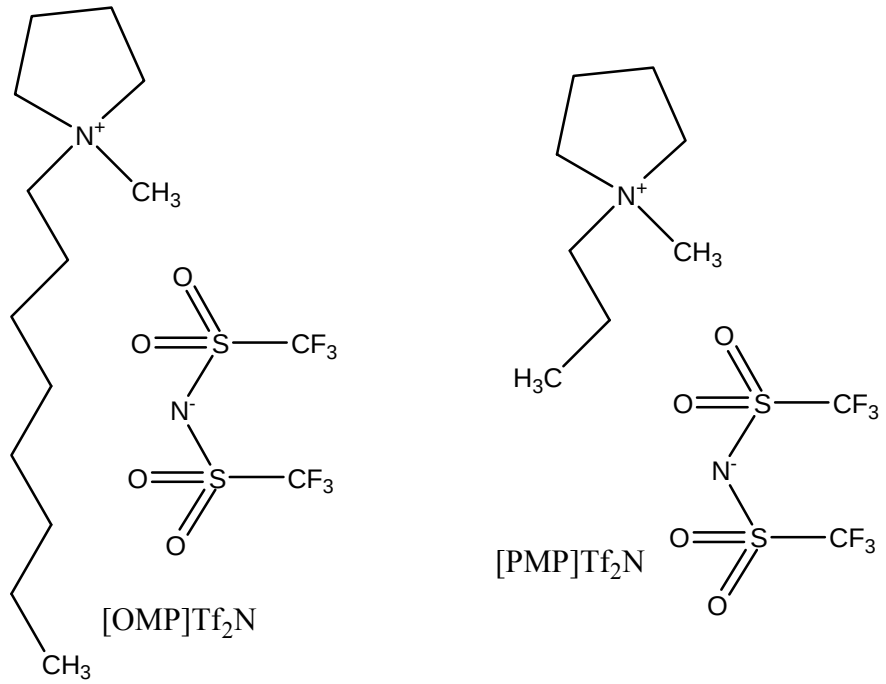

Fig.1: Chemical formulas of the ionic liquids employed to study the influence of the cation on the quality of Al electrodeposit.

The ionic liquids were purchased from Io-Li-Tec in the highest available quality. They were dried under vacuum for 12 h at a temperature 100 °C to water contents of below 2 ppm and stored in a closed bottle in an argon-filled glove box with water and oxygen below 1 ppm (OMNI-LAB from Vaccum Atmospheres). Anhydrous $AlCl_3$ grains (Fluka, 99%) were used without further purification as a source of Al. All electrochemical experiments were performed inside the glove box. Studies have been carried out on phase behavior, electrochemical deposition of Aluminium in the mixtures of these liquids with $AlCl_3$. Furthermore viscosity measurements of the upper phase of $[PMP]Tf_2N$ / $AlCl_3$ were performed. The physicochemical properties of these ionic liquids are given in the Table 1.

Table 1: *The physical properties of the ionic liquids presented in fig. 1 at 25°C*

Ionic Liquid	**[PMP]Tf_2N**	**[HMP]Tf_2N**	**[OMP]Tf_2N**	**[HMIm]Tf_2N**
Formula	$C_{10}H_{18}F_6N_2O_4S_2$	$C_{13}H_{24}F_6N_2O_4S_2$	$C_{15}H_{28}F_6N_2O_4S_2$	$C_{12}H_{19}F_6N_3O_4S_2$
Molar Mass, g/mol	408.38	450.47	478.53	447.42
Melting point, °C	12.1[58]	3[59]	-	-7[61]
Decomposition Temperature, °>C	-	320[60]	-	275[60]
Viscosity, mPa·s	-	108[60]	-	68[61]
Density, g/ml	-	1.34[60]	-	1.37[60]
Conductivity, mS/cm	1.6[58]	-	-	2.2[61]

Three different air- and water- stable ionic liquids, namely 1-ethyl-3-methylimidazolium bis(trifluoromethylsulfonyl)amide, [EMIm]Tf_2N, 1-ethyl-3-methylimidazolium chloride, [EMIm]Cl, and 1-butyl-1-methylpyrrolidinium bis(trifluoromethylsulfonyl)amide, [BMP]Tf_2N were used for Aluminium electroplating of the spring steel substrates (Figure 2).

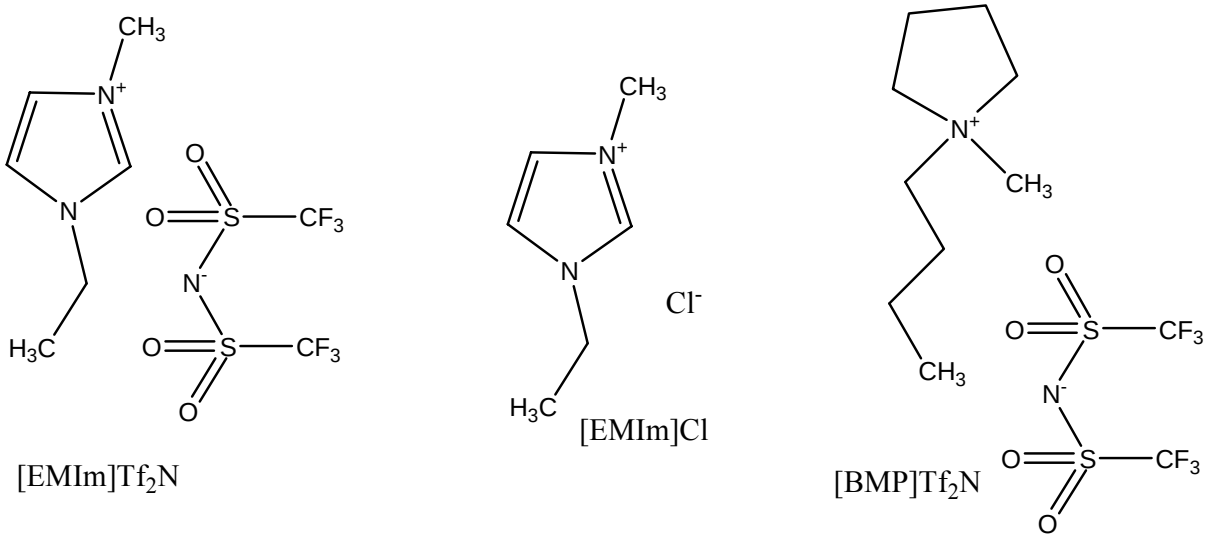

Fig.2: Chemical formulas of the ionic liquids employed for Aluminium electroplating of the spring steel substrates.

The ionic liquids were purchased from MERCK in the highest available (ultrapure) quality. They were dried under vacuum for 12 h at a temperature 100 °C to water contents of

below 2 ppm and stored in a closed bottle in an argon-filled glove box with water and oxygen of below 1 ppm (OMNI-LAB from Vaccum Atmospheres). Anhydrous $AlCl_3$ grains (Fluka, 99%) were used without further purification as a source of Al. All electrochemical experiments were performed inside the glove box. All these liquids were employed as solvents for Aluminium electroplating of the spring steel substrates. The physicochemical properties of these ionic liquids are presented in Table 2.

Table 2: *The physical properties of the ionic liquids presented in fig. 2 at 20°C*

Ionic Liquid	**[BMP]Tf_2N**	**[EMIm]Tf_2N**	**[EMIm]Cl**
Formula	$C_{11}H_{20}F_6N_2O_4S_2$	$C_8H_{11}F_6N_3O_4S_2$	$C_6H_{11}N_2Cl$
Molar Mass, g/mol	422.41	391.31	146.62
Melting point, °C	-18[60]	-3[8]	61.1[62]
Decomposition Temperature,°>C	310[61]	280[61]	-
Viscosity, mPa·s	85[9]	36[63]	-
Density, g/ml	1.4[60]	1.53[60]	1.19[64]
Conductivity, mS/cm	2.2[60]	8.8[60]	-

All the liquids employed in this work and their solutions with $AlCl_3$ exist in liquid state at room temperature. The ionic liquids [PMP]Tf_2N, [HMP]Tf_2N, [OMP]Tf_2N, [HMIm]Tf_2N, [BMP]Tf_2N and [EMIm]Tf_2N exhibit biphasic behavior in the $AlCl_3$ concentration range from 1.6 to 2 mol/L, 1.3 to 1.8 mol/L, 2 to 3 mol/L, 4.5 to 6.5 mol/L, 1.6 to 2 mol/L, 4.5 to 6.5 mol/L, respectively. The ionic liquid [EMIm]Cl shows monophase behavior by adding of $AlCl_3$. Aluminium can only be electrodeposited from the upper phase of the biphasic mixtures as the reducible Aluminium-containing species exists only in the upper phase of the biphasic mixtures **[65]**.

3 Introduction to Aluminium Electrodeposition

Aluminium can not be electrodeposited from an aqueous solution because of its reactivity ($E° = -1,7$ V *vs.* NHE). The electrodeposition process would be restricted by hydrogen evolution at the cathode surface; consequently, Aluminium can only be electrodeposited from non-aqueous aprotic electrolytes such as molten salts and organic solvents. Many of these electrolytes are sensitive to air and moisture so that the electrodeposition process must be carried out in inert atmosphere such as argon or nitrogen.

Before introducing the various baths used for electrodeposition of Aluminium, the requirements for Aluminium electrodeposition are shortly mentioned.

3.1 Requirements for Aluminium Electrodeposition Baths

The baths for Aluminium electrodeposition should have the following requirements **[67, 68, 69]**:

a) The electrolyte should consist of a solvent acting as a mild Lewis base and a solute acting as a Lewis acid that mutual coordination and dissolution of the solute can take place.
b) The solute that is used as an Al source should exhibit a high solubility in the solvent. A stable complex must be formed in the plating solution.
c) For some applications, it is desirable that the composition of the bath remains constant during the operation. This implies that the electrode process has to be chemically reversible. This permits the long-term operation of the bath without a change in the electrodeposition characteristics.
d) The medium must exhibit reducing and water-consuming properties.

Also a potentially suitable solvent for the preparation of Al-electrodeposition baths must comply with the following criteria **[67, 69]**:

a) The solvent must be electrochemically stable in order to permit the reduction of Al(III) compound without electrolysis of the solvent. This requires that the standard potential that characterizes the electrochemical equilibrium between metallic Aluminium and the Aluminium complex in solution lies within the existence regime of the solvent.
b) The electrode reaction has to be kinetically feasible (low overpotential) and mass-transport process has to favor a controllable surface morphology. The free energy

of the co-ordination complex of the solvent and Aluminium solute, e.g. Aluminium halide, should be sufficiently low to ensure a good solubility of the salt.

c) The dissociated Al complex ion must release Aluminium at a less negative potential than that of possible electrode reactions involving the solvent.

3.2 Aluminium Electrodeposition Baths

3.2.1 Electrodepostion of Aluminium from Organic Solvents

The first attempt to electrodeposit Aluminium from organic solvents was made by Plotnikov in 1899 **[70, 71]**. He used solutions of Aluminium bromide and alkali bromide in bronze, toluene and xylene.

To date, there are three classes of organic solvents, which have been successfully used for Aluminium electrodeposition **[72]**.

3.2.1.1 Etheric Solvents or Hydride Baths

In etheric baths the solvents, such as diethyl ether (Et_2O) and tetrahydrofurane (THF), $AlCl_3$ and LiH or $LiAlH_4$ are mixed together to form solutions containing the electroactive species from which Aluminium can be electrodeposited. The resulting solutions are called hydride baths and they are classified into two ways, NBS (National Bureau of Standards) and THF baths.

a) The NBS baths

In 1932, Brenner and co-workers at the NBS succeeded to electrodeposit Aluminium on an industrial scale by using solutions made by dissolving Aluminium chloride and lithium hydride in diethylether (Et_2O) **[73-76]**. Later, lithium hydride was replaced by lithium Aluminium hydride, which can be dissolved more easily in diethylether **[77]**. The addition of $LiAlH_4$ instead of LiH increases the bath lifetime. The obtained cathodic current efficiency at current densities 2-5 A/dm^2 and ambient temperatures was 90%. The anodic current efficiency was 100%, but the anodically dissolved Aluminium could not be deposited onto the cathode, therefore the Aluminium content of the bath decreased during the electroplating process and $AlCl_3$ had to be added from time to time to increase the bath lifetime.

NBS electrolyte was used on a pilot plant scale at General Electric by Schmidt and co-workers **[78-81]** who electroformed parabolic mirrors. The cathode current densities were 1,5-10 A/dm^2. Both the micro and the macro throwing powers were reported to be excellent. Adherent Aluminium coatings of 300 μm in thickness were deposited on various Aluminium alloys, titanium alloys and copper alloys as well as steel in NBS baths **[82]**. The application of the NBS bath to Electro-Optical Systems **[83]** was similar to the application at General Electric, namely the electroforming of solar mirrors. Wither and Abrams **[84]** electroformed composites containing boron filaments. To strengthen the Aluminium deposit they added magnesium solution to the NBS bath, probably as ethylmagnesium bromide. By using bare Al anodes, Clay et al. **[85]** succeeded in determining the optimum conditions such as agitation, low current densities (up to 2 A/dm^2) and somewhat higher temperature (40 °C) to prolong lifetime of the bath. Under these circumstances the anodic current efficiency was found to be 100%. Levinskas and co-workers **[86]** studied the relation between the geometry of the cell and the pre-treatment of the cathode surface on the one hand and the optimum current density

on the other hand. They also studied the influence of additives such as diethylamine, butylamine and piperidine on the deposit and bath quality **[87]**.

The NBS bath possessed several drawbacks such as flammability, limited lifetime, variation of the composition, low anodic current efficiency and hydrogen embrittlement due to excessive hydrogen evolution **[88, 89]**. Nevertheless, the process has been a commercial reality for a long time, and has also been adopted by NASA **[90]**.

b) The THF baths

The use of THF alone or THF with a combination with benzene instead of diethylether has been suggested by Ishibashi and Yoshio **[91, 92]**. It was not only less inflammable but also less volatile. Furthermore, it showed better anode dissolution and therefore longer bath lifetime. Ishibashi and Yoshio were able to apply successfully current densities above 10 A/dm^2 with agitation. The composition of the bath was roughly 60 vol.% THF, 40 vol.% benzene with 0,7-1,3 mol/l $AlCl_3$ and $LiAlH_4$. Excellent deposits were obtained with an $AlCl_3$: $LiAlH_4$ molar ratio 3 : 1. Other hydrocarbons were tried in addition to benzene, such as 1,2-dichloroethane and toluene, in these cases the deposit on the cathode was obtained, but a white precipitate was observed on the anode. An unsuccessful attempt was made to improve the operation of the NBS electrolyte by adding some aromatic hydrocarbons **[92]**. Yoshio and Ishibashi have suggested a rather complicated pretreatment of the cathode surface prior to the electrolysis but Eckert and Kölling **[93]** have shown it to be less useful. Kurata et al. **[94-96]** have also studied special pre-treatment of iron and steel surface in order to obtain purer and adherent deposits.

The THF electrolyte has been utilized by the Nisshin Steel Co. in Japan for the continuous Aluminium coating of steel wires and strips used, for example, in integrated circuits **[97]**. Also, it has been used for the electroplating of carbon fibres **[98]**. Graef studied the mechanism of Aluminium electrodeposition from solutions of $AlCl_3$ and $LiAlH_4$ in THF **[68]**. Moreover, Al-Mg alloys, containing up to 13% Mg could be obtained from THF bath with $MgBr_2$ **[99]**. In 2000, Lefebre and Conway reported in two papers that Aluminium can be electrodeposited from plating baths of varying ratios of $AlCl_3$ and $LiAlH_4$ dissolved in THF. They studied the kinetics, mechanisms, nucleation and surface morphologies in the process of electrocrystallization of Aluminium on smooth gold and glassy-carbon substrates **[100, 101]**.

3.2.1.2 Aromatic Hydrocarbons Baths

These electrolytes are also known as bromide baths because $AlBr_3$ is the Aluminium-containing compound. The aromatic hydrocarbons are usually benzene, toluene, xylene, and their mixtures and derivatives.

a) $AlBr_3$+MBr as the electroactive components

Attempts were made to increase the conductivity of $AlBr_3$ solution by the addition of quaternary ammonium or pyridinium salts such as ethylpyridinium bromide **[102]**, ethylenepyridinium dichloride and ethylenepyridinium dibromide **[103]**. The cathode efficiencies ranged from 80 to 92% at current densities from 0.2 to 2 A/dm^2, the deposit was about 6 μm thick. Also, this type of electrolyte has been studied by Simanavicius and Dobrovolskis **[104-106]**. The best deposits were obtained with quaternary pyridinium or dimethylaniline salts in toluene. The anodic species was assumed to be $Al_2Br_7^-$ on the basis of conductivity measurements. These electrolytes are complicated to operate and the results obtained are rather poor. In small amounts, the quaternary salts can improve the brightness of the deposit, but higher concentrations lead to the incorporation of the quaternary salt into the deposit and eventually leads to low purity and corrosion resistance. Better results were obtained using alkali bromide (MBr), mainly KBr, in combination with $AlBr_3$ **[107, 108]**. The function of each component of the bath can be characterized as follows. $AlBr_3$ is the Aluminium-containing component. The alkali bromide has to increase the solution conductivity to the value required for electrolysis, i.e. 1 – 6 mS/cm, and to improve the throwing power of the solution by forming anions of the types $Al_2Br_7^-$ or $AlBr_4^-$. The concentration of the alkali bromide must not exceed 1 mol/l because co-deposition of the alkali metal can occur. The function of the solvent itself, apart from its dissolution properties, consists in its ability to bind protons formed in contact with surroundings. The stability of the σ complexes of aromatic hydrocarbons with protons increases in the following sequence: benzene < toluene < m-xylene < mesitylene. In general, the longer and more branched chain or the higher the number of aromatic rings, the better the reactivity of the hydrocarbon towards protons. The deposits obtained from such electrolytes were smooth, homogeneous and microcrystalline with good adherence. Both the cathode and the anode efficiencies were 100% and the current density was 10 A/dm^2. The purity of the deposits was 99,5%. The metals coated were copper, brass and steel. The anode was 99,5% Aluminium. Simanavicius

et al. reported comparative studies on the co-deposition of Al with Co, Cr, Zn or Mn from $AlBr_3$-dimethylethylphenylammonium bromide solutions in toluene containing the acetylacetonate complex of the corresponding metal **[109]**.

Although, there are no reports concerning the industrial application of this bath, the results of laboratory experiments regarding plating quality and long-term performance appeared to be very promising. Its use would permit easier and more economical operation than the baths containing lithium Aluminium hydride or Aluminium organic compounds.

b) $AlBr_3$+HBr as the electroactive components

This combination has been used by Capuano and Davenport **[110-113]**. The electrolyte consisted of 36 – 45 vol.% $AlBr_3$ in a 1:1 mixture of ethylbenzene or diethylbenzene and toluene. The solution was prepared as follows. An inert gas saturated with water vapour was passed through the solution to saturate the solvent with water, prior to dissolution of the $AlBr_3$, which would give rise to HBr. The solution thus prepared must be carefully protected against moisture and oxygen by an inert atmosphere. The presence of HBr in the solution ensures the required specific conductivity of 3 – 4 mS/cm. The coated surfaces were copper and steel. The anode was pure Aluminium. At 1 A/dm^2 the anodic efficiency was 100% and the cathodic efficiency 80%. With increasing current density the cathodic efficiency decreased. The low cathodic efficiency compared with the anodic efficiency caused an enrichment of the solution with Aluminium, which successfully formed bonds with Br^- from the HBr. The deposits were up to 25 pm thick and it was claimed to be very good with regard to mechanical strength and corrosion resistance. The bath life was also excellent, during one year of operation under optimum conditions the bath composition and function remains unchanged. Although Davenport and Capuano **[112]** regarded their electrolyte as highly suitable for an application, no industrial use is known as yet. The system $AlBr_3$ + HBr in o-, m- and p-xylene has been investigated in detail by Simanavicius and co-workers **[114-117]**. Current efficiencies of 90% were attained. After the Aluminium had been deposited on the cathode, hydrogen evolution and decomposition of the solvent were observed. Some experiments have been performed to electroplate Aluminium from a solution of $AlBr_3$ in ethylbenzene without the addition of any further components **[118-120]**. The freshly prepared solution was light yellow in color and had a conductivity that was of the order of 10^{-8} S/cm. With time the solution turned to dark brown and the conductivity increased to 10^{-3} S/cm. These changes, caused by traces of water present in the electrolyte, have been ascribed to the

formation of well-dissociated complexes of the type $Al_2Br_4OH.C_8H_{10}^+$ **[120]**. In 2003, Shavkunov and Strugova reported that Aluminium could not be deposited electrochemically from a benzene solution of Aluminium bromide even after a prolonged electrochemical aging. However Aluminium was deposited from a solution of toluene with a low current efficiency in the form of individual crystals, and for the electrolyte a prolonged electrochemical aging was required. They succeeded to obtain high-quality Aluminium coatings at a current efficiency of 60-80% from xylene, ethylbenzene, xylene-durene electrolytes containing Aluminium bromide. They have also studied the kinetics of Aluminium electrodeposition from such solutions **[121]**.

Capuano has not only electrodeposited Aluminium and Aluminium alloys, such as Al-Cu, Al-Sn, Al-Zn alloys, from alkylbenzene-HBr electrolytes but also reviewed theoretical considerations pertaining to the electrodeposition process. He reported that, Aluminium bromide produces π complexes when dissolved in alkylbenzenes. When the solvent has a large number of radicals attached or larger chains, a monomeric dicomplex (Al cation) is produced. A study of the interaction between Al_2Br_6 and alkylbenzenes showed that toluene produces the highest amount of open dimer, m-xylene, the highest quantity of closed dimer, and 1-2-4-trimethylbenzene is the richest in Aluminium cations. The Aluminium cation is responsible for the electrodeposition of Aluminium. Hydrobromic acid enhances the conductivity of the electrolyte and the formation of monomeric π complexes. The content of the minor constituents, Cu, Sn or Zn, in Aluminium alloy coating can be controlled by using Aluminium alloy anodes of specified composition if the current density, agitation and specific conductivities are maintained constants. The codeposition of Cu, Sn and Zn in the electrodeposition of Aluminium alloy was found to be a diffusion-rate controlling process. The use of pulse plating permits to deposit thicker Aluminium alloy coatings. Barrel plating of steel and titanium fasteners was shown to be possible from organic electrolytes. The corrosion resistance of Aluminium-plated fasteners was shown to be increased considerably by chromating **[122]**.

c) OrganoAluminium compounds as the electroactive components

This type of electrolyte was developed by Ziegler and Lehmkuhl **[123-125]**. The bath is based on the compounds: $(C_2H_5)_4NCl/2Al(C_2H_5)_3$, $NaF/2Al(C_2H_5)_3$ and $NaF/2Al(C_2H_5)_3/3.3C_7H_8$. Toluene was used as a solvent. The bath was operated at 60 – 90 °C with current densities of 1 – 5 A/dm^2. The purity of the deposit is 99,9999%, which was the

best obtained purity so far. The composition of the bath and the influence of additives on the brightness of the deposit have been studied by Dötzer and co-workers **[126-128]**. Electrolytes with organoAluminium compounds were used by SIGAL (Siemens-Galvano-Aluminium) in discontinuous operation for manufacturing reflectors as well as light and heat radiators. The electrolytic cell is put in a double-walled chamber filled with inert gas to prevent the influence of air and moisture on the electrodeposition process.

3.2.1.3 Electrodeposition of Aluminium from Dimethylsulfone ($DMSO_2$)

Such solutions have a number of attractive features, such as: high conductivity, good thermal stability **[129]**, ability to dissolve numerous metallic cations **[130, 131]**. Dimethylsulfone ($DMSO_2$) has been considered as a promising organic solvent for rechargeable cells **[132]**. Recent investigations **[133, 134]** have shown that Aluminium can be reversibly plated and stripped in a mixture (2:1 mole ratio) of $AlCl_3$: LiCl dissolved in $DMSO_2$ while no Aluminium plating was observed in that of a 1:1 mole ratio. Analysis of chronoamperograms indicated that the Aluminium deposition process at a tungsten electrode from the mixtures of $AlCl_3$/LiCl/$DMSO_2$ involved progressive nucleation with diffusion-controlled growth of the nuclei **[133]**. SEM observations **[133]** showed that smooth and continuous Aluminium deposits could be obtained from the $DMSO_2$ baths by potential step technique. A Raman study **[135]** revealed:

a) $AlCl_4^-$ ion was always the main Al(III) species.

b) $Al_2Cl_7^-$ was never found even in the more acidic baths, i.e. with $AlCl_3$/LiCl mole ratio greater than one.

c) A coordination complex, $Al[(CH_3)_2SO_2]_3^+$ was formed in the acidic melts between $DMSO_2$ and Al(III).

This complex was responsible for Aluminium deposition on tungsten electrode from $AlCl_3$/LiCl/$DMSO_2$ bath through the following reactions **[133]**:

$$Al[(CH_3)_2SO_2]_3^{3+} + 3e^- \rightarrow Al + 3(CH_3)_2SO_2$$

No Aluminium plating process occurred in a mixture (2:1 mole ratio) of $AlCl_3$: LiCl, indicating that as a Lewis base, $DMSO_2$ was weaker than Cl^- but stronger than $AlCl_4^-$, leading to the following equilibrium for $DMSO_2$- based electrolytes:

$$AlCl_3 + Cl^- \rightarrow AlCl_4^-$$

$$4AlCl_3 + 3(CH_3)_2SO_2 \rightarrow Al[(CH_3)_2SO_2]_3^{3+} + 3AlCl_4^-$$

In 2002, Fransaer et al. **[136]** have achieved the electrolytic codeposition of micro- and nano-sized particles with Aluminium from $DMSO_2$ baths. SiC, SiO_2, Al_2O_3, TiB_2 and hexagonal BN particles were co-deposited with Aluminium from $AlCl_3/DMSO_2$ electrolyte. Moreover, he studied the effect of particle concentration and current density on the co-deposition rate of SiO_2 with Aluminium. He also found that the co-deposition of the various particles with Al from $AlCl_3$: $DMSO_2$ solutions was very high.

The large degree of co-deposition of hydrophilic particles (SiO_2 and Al_2O_3) confirms that elimination of the hydration sheath achieved by using non-aqueous electrolytes can significantly enhance the co-deposition of such particles and can avoid the agglomeration that takes place in aqueous electrolytes. This opens new fields of applications for the synthesis of composite coatings containing homogeneously dispersed nanometer-sized particles with compositions that cannot be obtained from aqueous electrolytes.

Unfortunately, the common feature of all organic baths for the electrodeposition of Aluminium is the absolute necessity of operating in an inert atmosphere and therefore in closed systems. All the organic solvent baths have many disadvantages: they are inflammable, volatile, hygroscopic and are consequently relatively complicated to handle. For example, from the disadvantages of the organoAluminium baths, their self-ignition in air and their vigorous reaction with water.

To avoid the prevail disadvantages of organic solvents baths, the investigation of new nonaqueous electrolytic systems for the electrodeposition of Aluminium has continued. Among them, high temperature chloroaluminate molten salts such as $AlCl_3$-NaCl and related lower melting chloroaluminates based on quaternary ammonium chloride salts (ionic liquids) such as N-butylpyridinium chloride (N-BPC) and 1-ethyl-3-methylimidazolium chloride [EMIm]Cl. These ambient temperature molten salts have received more attention as promising Aluminium plating baths for industrial applications.

3.2.2 Electrodeposition of Aluminium from Chloroaluminate Molten Salts

Electrodeposition of Aluminium from ionic liquids would have many advantages. The low working temperature (120 °C and higher) compared with the hot plating process suppresses the formation of brittle intermetallic compounds in the underlayer. The higher electrical conductivity of the electrolyte (by 1 to 2 orders) makes it possible to carry out the electrolysis at higher current densities. There is a low toxicity, no danger of explosion and

control of the thickness of the Aluminium layer make it potentially attractive for wider application.

Aluminium can be electrodeposited from molten salts (chloroaluminate molten salts), mainly chlorides, where Aluminium can be deposited either by using a soluble Aluminium anode or the electrochemical decomposition of the electroactive species, $Al_2Cl_7^-$, which was formed in the Lewis acidic molten $AlCl_3$: Alkali metal chloride mixture of the molar ratio 2:1. The electrochemical reduction of the electroactive species occurs by the following reactions **[137]**:

$$4Al_2Cl_7^- + 3e^- \rightarrow Al + 7AlCl_4^-$$

Extensive work has been reported on the electrodeposition of Aluminium from such type. The first paper on the electrolytic Aluminium deposition from a molten $AlCl_3$-NaCl mixture was published at the mid of nineteenth century **[138]**.

The first attempt to use this electrolyte for the deposition of Aluminium on an iron base was made by Plotnikov and co-workers **[139-141**]. Chittum **[142]** proposed LiCl instead of NaCl. The quality of the Al layers deposited in molten electrolytes containing Aluminium and alkali chlorides was examined by Orleva and Lainer **[143]**. Bromides as well as chlorides have been tested as possible electrolytes for the deposition of Al layers **[144-146]**. A systematic investigation of electrolytic Aluminium plating in molten chlorides was carried out by Delimarskii and co-workers **[147-149]**. Of the different mixtures containing Aluminium and alkali chlorides, the binary mixture with a composition corresponding to the compound 2 $AlCl_3$.NaCl was found to be the most suitable electrolyte. As the electrolyte is hygroscopic, electrolysis is carried out in an inert atmosphere. Furthermore, dehydrating substances such as silica gel and activated charcoal should be added directly to the electrolyte. This increases the current efficiency of the electrolysis **[150, 151]**.

The results of the electrolysis of the binary Aluminium chloride – alkali chloride ($AlCl_3$-MCl) mixtures, however, were disappointing as in all cases Al was deposited in the form of a dull, coarse-grained layer with low corrosion resistance. Therefore, numerous attempts were made to influence the process of electrocrystallization of Aluminium, mainly by addition of different metals, either in the form of compounds (chlorides or oxides), or as auxiliary anodes of respective metals. The influence of Sn, Pb **[147, 149, 152-154]**, Zn, Sb, Bi **[155]**, Mn **[156]**, Cu, Ag, Cd, Ga, In, Tl, Ge **[157]** and V **[158]** has been studied. It was found that only Sn, Pb and Mn have a favorable influence on the properties of the deposited layer. In all cases, however, instead of pure Aluminium the corresponding Aluminium alloy was deposited.

Paucirova and Matiasovsky **[159]** in 1975 have succeeded to electroplate iron substrates by a fine-crystalline, silver-bright and non-porous Aluminium layer from molten salts based on chlorides. They also found that the suitable electrolyte for Aluminium electroplating in molten salts was a quaternary mixture of 80 wt.% $AlCl_3$ + 10 wt.% KCl + 5 wt.% NaCl + 5 wt.% NaI and in the temperature range 150 – 200 °C with a cathodic current density of up to 7 A/dm^2. G.R. Stafford has reported that Aluminium, Aluminium-manganese and Aluminium-titanium alloys can be electrodeposited from $AlCl_3$ – NaCl molten salt at 150 °C **[137, 160]**.

The drawbacks of the $AlCl_3$ – NaCl molten salt are its high $AlCl_3$ vapour pressure, which may result in explosions at elevated temperatures and the fact that the melt is very corrosive. Therefore ionic liquids might be an alternative.

3.2.3 Electrodeposition of Aluminium from Ionic Liquids

Electrodeposition of Aluminium from ionic liquids can be performed at room temperature. The Aluminium deposits obtained are usually of good quality, high purity, of low porosity and heat resistant. Popular examples of ionic liquids include the chloroaluminates, which are prepared by mixing anhydrous $AlCl_3$ with a suitable organic halide. It is the simplest system from which Aluminium can be easily electrodeposited. Depending upon the molar ratio of $AlCl_3$ and organic halide, they can be classified into basic, neutral or acidic in the sense of Lewis acidity. In the neutral 1:1 melt Aluminium is present almost entirely as $AlCl_4^-$ ions, whereas in the 2:1 melt it is present as $Al_2Cl_7^-$. In melts having a molar ration between 1:1 and 2:1, both $Al_2Cl_7^-$ and $AlCl_4^-$ ions will be present. The acid-base properties of the melt at ambient temperature may be described by following equilibrium **[161, 162]**:

$$2AlCl_4^- \leftrightarrow Al_2Cl_7^- + Cl^-$$

with an equilibrium constant K=3,8 x 20-13 at 30 °C. In acidic melts, the $Al_2Cl_7^-$ ion is the only species from which Aluminium can be electrodeposited according to the following reaction:

$$4Al_2Cl_7^- + 3e^- \rightarrow Al + 7AlCl_4^-$$

In presence of an excess of $AlCl_3$, the following reaction is virtually complete:

$$AlCl_4^- + AlCl_3 \rightarrow Al_2Cl_7^-$$

A lot of work has been done using chloroaluminate ionic liquids to get high quality Aluminium deposits by several authors. For example, $AlCl_3$ / 1-ethyl-3-methylimidazolium chloride and the ionic liquids $AlCl_3$ / N-butylpyridinium chloride have been widely used in electrodeposition of Aluminium and its alloys.

It is known that by some ionic liquids nano- or microcrystalline Al can be electrodeposited only from the upper phase of $AlCl_3$ / ionic liquid mixtures **[65]**. The biphasic behavior of two ionic liquids mixtures with $AlCl_3$ has been studied in ref. **[163]**. The ionic liquids 1-butyl-1-methylpyrrolidinium bis(trifluoromethylsulfonyl) amide ([BMP]Tf_2N) and 1-ethyl-3-methylimidazolium bis(trifluoromethylsulfonyl) amide ([EMIm]Tf_2N) form two phases with higher formal concentrations of $AlCl_3$. The addition of $AlCl_3$ to the liquids first leads to complexation with $[Tf_2N]^-$ and then disproportionation of the initial $[AlCl_x(Tf_2N)_y]^-$ complexes give $Al(Tf_2N)_3$ and $[AlCl_4]^-$. At high concentration of $AlCl_3$ (1.6 mol/L for [BMP]Tf_2N and 2.5 mol/L for [EMIm]Tf_2N), which are required for Al electrodeposition, the lower phase consists almost completely of $Al(Tf_2N)_3$, whereas in the upper phase cation-$[AlCl_4]^-$ is the dominant species. [BMP]$AlCl_4$ with a melting point of 74 °C is solid at room temperature and dissipates in the upper phase. Electrodeposition of Aluminium in the upper phase occurs from mixed $(AlCl_x[Tf_2N]_y)^-$ species, which is supposed to be formed at the boundary between $Al(Tf_2N)_3$ and $[AlCl_4]^-$ **[163]**.

3.2.3.1 Electrodeposition of Aluminium in $AlCl_3$ / imidazolium halide Ionic Liquids

The $AlCl_3$/[EMIm]Cl mixture is specially attractive for the electrodeposition of Aluminium and its alloys because it has a very low melting point over a wide range of compositions, high intrinsic electrical conductivity at room temperature, and a low vapour pressure **[164]**. This system was widely used by several researchers to electrodeposit Aluminium and its alloys. Hussey and co-workers have carried out intensive studies on the electrodeposition of Aluminium and Aluminium alloys from $AlCl_3$/[EMIm]Cl. They succeeded to electrodeposit transition metal-Aluminium alloys such as Al-Mo **[165]**, Al-Ti **[165]**, Al-Zr **[166]**, Ag-Al **[167]**, and ternary Al-Mo-Mn **[168]** alloys. These alloys are technologically important because of their corrosion resistance, particularly pitting corrosion, and in some cases, their interesting magnetic properties.

Jiang et al. **[169]** have studied the electrodeposition, electrochemical nucleation and surface morphology of Aluminium on both tungsten and Aluminium electrodes from 2:1

molar ratio $AlCl_3$: [EMIm]Cl ionic liquid. The electrodeposits obtained on both tungsten and Aluminium electrodes were dense, continuous and well adherent.

The $AlCl_3$/[EMIm]Cl (60/40 mol.%) mixture was used to electroplate mild steel by well adherent and highly resisted to scratches Aluminium coatings **[170]**. However, the quality of the deposit can be greatly improved by utilizing pulse plating techniques **[171, 172]** or by addition of some organic solvents such as benzene or methyl *tert*-butyl ether **[172]** that improve the deposit surface morphology. It is possible that the organic molecules play the role of brighteners.

Endres et al. reported that nanocrystalline Aluminium can be made electrochemically in Lewis acidic ionic liquids based on $AlCl_3$ and [EMIm]Cl under galvanostatic conditions by addition of nicotinic acid **[173]**. Also the $AlCl_3$/1-ethyl-3-methylimidazolium chloride melt is a viscous and transparent liquid at room temperature when the molar composition is in the range of 0.3:1 to 2:1 **[174]**.

Lai **[175]** have electrodeposited Aluminium in room temperature $AlCl_3$/[EMIm]Cl ionic liquid on glassy carbon, platinum and tungsten. Moreover, he has studied the mechanism of the electrodeposition and dissolution processes in such ionic liquid. The obtained results indicated that the Aluminium deposition process at the above-mentioned substrates was preceded by a nucleation step and was kinetically complicated. The deposited Aluminium was found to be unstable and subject to a slow corrosion process. This is most likely due to impurities and organic cations present in the melt.

Also, Aluminium deposition from the $AlCl_3$/1-ethyl-3-methylimidazolium chloride was studied employing an inverted optical microscope to perform in situ optical observations during the deposition process at tungsten electrode. Thin, continuous Aluminium coatings with crystal sizes below optical microscopic resolution were produced from a 1.1:1 $AlCl_3$: [EMIm]Cl molten salt at potentials < -0.2 V vs. an Al(III)/Al reference electrode. Analysis of chronoamperograms indicated that the deposition process involves progressive nucleation with diffusion-controlled growth of the three-dimensional nuclei **[176]**.

Liao et al. **[177]** have improved the quality of the Aluminium deposit obtained in Lewis acidic $AlCl_3$/[EMIm]Cl mixture by addition of benzene as a “cosolvent”.

3.2.3.2 Electrodeposition of Aluminium in ($AlCl_3$/N-BPC) System

The $AlCl_3$ / N-butylpyridinium chloride system is liquid at ambient temperatures over a wide composition range; molar ratio from 0.75:1 to 2:1 $AlCl_3$/N-BPC **[178]**.

Kazacos and co-workers employed different electrodes such as glassy carbon, tungsten **[179]**, and platinum **[64]** to investigate the mechanism of Aluminium deposition and dissolution reactions in $AlCl_3$/N-BPC melts at ambient temperature. The results showed that the electrodeposition of Aluminium from that liquid at glassy carbon and tungsten electrodes was kinetically complicated and the corrosion rate of Aluminium was linearly proportional to the acidity of the melt at 40 °C. Besides impurities, the major reason for the corrosion of the deposited Aluminium in that melt was also found to be due to the organic butylpyridinium cation (BuPy+) **[179]** while at platinum electrodes, the results indicated that the Aluminium deposition reactions was a quasi reversible process and there was an evidence for formation of Pt-Al alloy in the initial stages of Aluminium deposition **[64]**.

In 1980, Robinson and Osteryoung **[180]** studied the electrodeposition and stripping process of Aluminium in $AlCl_3$/N-BPC melts with and without benzene at tungsten, platinum and glassy carbon electrodes. In acidic liquids, at all three electrodes, the reduction of Al_2Cl_7-ions was found to involve a nucleation process while at the tungsten and platinum electrodes, an under potential deposition was also observed. Studies of the stripping of Aluminium from inert substrates showed that Aluminium is very slowly corroded in acidic melts, and melt-benzene mixtures, by traces of oxidizing impurities while in basic systems Aluminium reduces the n-butyl pyridinium cation.

Yang **[181]** has electrodeposited Aluminium from an acidic liquid of this system by using a DC constant current and pulse current methods at 30 °C. The quality of the deposited Aluminium layer was improved by applying pulse current: the particle size decreased and the adhesion became much better.

Furthermore, alloys such as Co-Al **[182]** and Al-Cr **[183]** can be electrodeposited on different substrates in the acidic melt of this system.

3.3 Electrodeposition of Aluminium on the Nanoscale

Nanometals are of great interest for nanotechnology. The hardness of nanocrystalline metals is found to increase with decreasing particle size, which is explained by increasing fraction of atoms located at the grain boundaries. Furthermore, it is found that the corrosion resistance often gets better for nanocrystalline metals **[65]**. Adjusting the hardness of a material simply by varying the grain size opens many interesting perspectives for technical applications: nanocrystalline Ni is used as a hard coating material to achieve the high

hardness and strength of steel without the usual corrosion problems, and nanocrystalline Co might replace the more expensive titanium.

Electrochemistry is a powerful tool for making nanocrystalline materials because the grain size can be adjusted by varying the electrochemical parameters such as overvoltage, current density, pulse parameters in pulse electrodeposition, bath composition and temperature.

Liu et al. reported in **[170]** that, besides microcrystalline Aluminium, nanocrystalline Aluminium can also be electroplated from [EMIm]$Tf_2N/AlCl_3$ and [EMIm]$Cl/AlCl_3$ at room temperature without any additives. The crystal refinement is due to a cathodic decomposition of the imidazolium ions to a certain extent giving rise to nanocrystalline Aluminium. The electrochemical behavior was studied by cyclic voltammetry, galvanostatic and potentiostatic polarization experiments complemented by scanning electron microscopy/energy-dispersive X-ray analysis. It was found that the upper phase of the biphasic ionic liquid [EMIm]$Tf_2N/AlCl_3$ and the Lewis acidic [EMIm]$Cl/AlCl_3$ ionic liquid are both subject to some decomposition at low electrode potentials and the decomposition products play an important role as a crystal size refiner. Aluminium deposits obtained in [EMIm]$Tf_2N/AlCl_3$ (undecomposed) on a mild steel surface form a dense and compact layer of about 30-50 μm thick at a current densities of less than 5 mA/cm^2. It was shown that Al deposits made at relatively low current densities consist of coarse crystallites. At the current densities of more than 5 mA/cm^2 the deposits obtained in [EMIm]$Tf_2N/AlCl_3$ are no longer metallic bright and, with further rising of the current density to 10 mA/cm^2 and higher, the Al deposit is no longer a compact dense layer but rather a black powder loosely adhering to the electrode surface. At the same time the Aluminium deposits obtained on a mild steel at -0.45 V for 3h in [EMIm]$Tf_2N/AlCl_3$ (upper phase) after decomposition at 10 mA/cm^2 for about 90 min (0.2% of $[EMIm]^+$ decomposed) confirms that decomposition products of imidazolium ion alter the electrodeposition. These deposits contain only fine crystallites in the nanometer regime. They have a goldish shining surface and are estimated to be about 10 μm thick. In [EMIm]$Cl/AlCl_3$, compact Al layers on mild steel substrate can be obtained up to about 20 mA/cm^2. Similar to [EMIm]$Tf_2N/AlCl_3$, Al deposits obtained on mild steel at -0.4 V for 2h in [EMIm]$Cl/AlCl_3$ after decomposition at 50 mA/cm^2 for 2h (1.3% of $[EMIm]^+$ decomposed) contains fine crystallites with average grains size in the nanometer regime. The obtained Al films with the thicknesses of more than 10 μm possess a shining goldish appearance [**170**].

Endres et al. have reported in **[65]** that nanocrystalline Aluminium can be electrodeposited from the upper phase of the biphasic mixture $AlCl_3$ / 1-butyl-1-

methylpyrrolidimium bis(trifluoromethylsulfonyl)amide on gold substrates at different temperatures. The deposits appear to be thick, shiny and well-adhering to the substrate. XRD measurements using Scherrer equation show the average grain size of Aluminium 40 and 34 nm at 50 and 100 °C, respectively.

The previous studies show that the decomposition of the ionic liquids can alter the deposit morphology tremendously. Unexpected alterations of deposit morphology and grain size might occur. Further studies are needed in order to get more insight on the processes. Therefore the aim of the present study is to investigate if and how the cations of different ionic liquids influence the electrodeposition of Aluminium.

4 Experimental

4.1 Cyclic Voltammetry

Cyclic voltammetry (CV) is a common technique in electrochemistry. This method is very useful to obtain information about the reaction rate, mechanism of the reaction and the types of possible intermediates.

In CV the potential swept between two given values (E_{min} and E_{max}) at a constant scan rate υ, while the corresponding current is recorded, as shown in Figure 3.

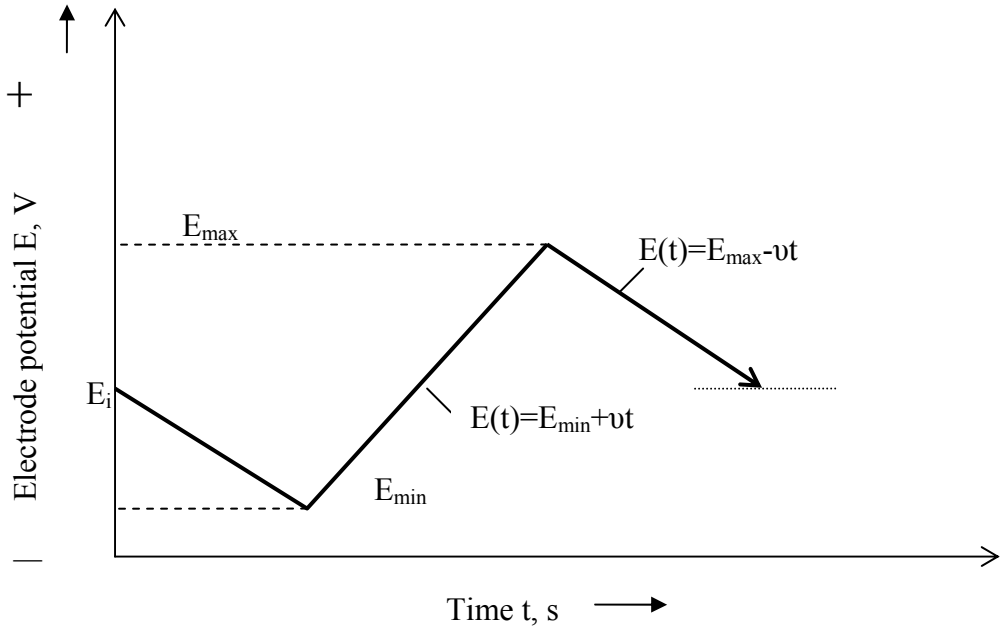

Fig.3: Potential-time behavior (Potential sweep)

E_i is the initial potential, where no electrode reaction occurs and therefore no faradaic current flows. During the measurement, the electrode potential E(t) is changing linearly with a time t. Single or multiple cycles can be acquired. The resulting cyclic voltammogram is presented in Figure 4.

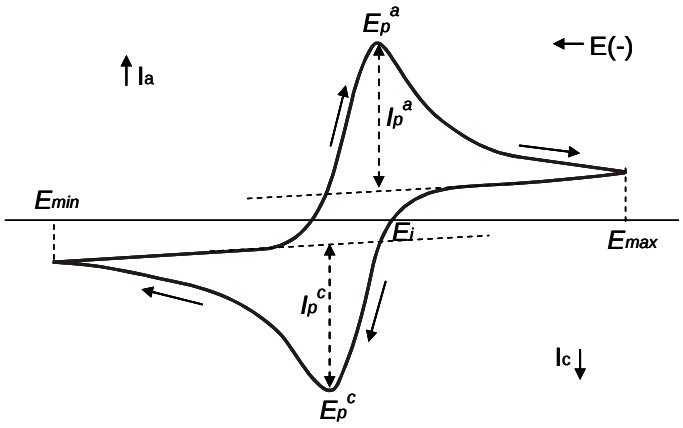

Fig.4: A typical cyclic voltammogram for a solely diffusion controlled process **[184]**

The cyclic voltammogram is characterized by two parameters: the difference of potentials, at which anodic and cathodic peak currents occur, $\Delta E_p = E_p^a - E_p^c$; and the ratio of anodic and cathodic peak currents, I_p^a / I_p^c. It has to be mentioned that by changing the electrode potential, a capacitive current flows, which leads to a mistake in the determination of the faradaic current. The charge current is directly proportional to the scan rate and thus its influence significantly increases at faster scan rates. Therefore, I_p^a and I_p^c are measured from the decaying anodic and cathodic currents as a baseline, respectively, as shown in figure 4. For a reversible reaction the $I_p^a / I_p^c = 1$; the parameter ΔE_P is independent on a scan rate, slightly depends on the switching potential and its value is close to $2.3\frac{RT}{nF}$ for a solely diffusion controlled process. Therefore, CV is used to indicate whether a reaction occurs and at which potential, to make a conclusion on the type of electron transfer mechanism and on the type of the reaction, to measure the diffusion coefficients. For reversible processes the number of electrons taking part in the reaction may be calculated.

A standard cell configuration consists of three electrodes immersed in the electrolyte of interest: the working electrode (WE), the reference electrode (RE) and the counter electrode (CE). During the potential sweep the current is measured between counter and working electrodes, while potential is measured across reference and working electrodes.

All electrochemical experiments were performed inside an argon filled glove box (Vacuum Atmospheres OMNILAB) with water and oxygen below 2 ppm. The electrochemical measurements were carried out using a PARSTAT 2263

potentiostat/galvanostat controlled by a PowerCV software.

The electrochemical cell applied to study Al electrodeposition at room temperature was made of Teflon and clamped over a Teflon covered Viton o-ring onto the substrate, thus yielding a geometric surface area of the working electrode of 0.3 cm^2 (Figure 5a). At elevated temperature a round glass flask with a Teflon cover was used as the electrochemical cell (Figure 5b). All parts of the electrochemical cell in contact with the electrolyte were formerly cleaned in a mixture of 50/50 vol. % H_2SO_4/H_2O_2 followed by refluxing in pyrogene free water (aqua destillata ad iniectabilia) prior to use.

Au(111) substrates purchased from Arrandee Inc. with a dimension of 10x10 mm^2 were used as a working electrode (WE). Prior to use the Au(111) substrates were carefully heated in a hydrogen flame to minimize surface contaminations. Owing to the major part of (111)-oriented gold *terraces* electrochemical experiments were very reproducible. Al-wires (99.999%, ø 0.5 mm) were applied as a counter (CE) and a reference (RE) electrodes. Before use the Al-wires were grinded with 800 SiC-sandpaper and rinsed in isopropanol in ultrasonic bath.

a) **b)**

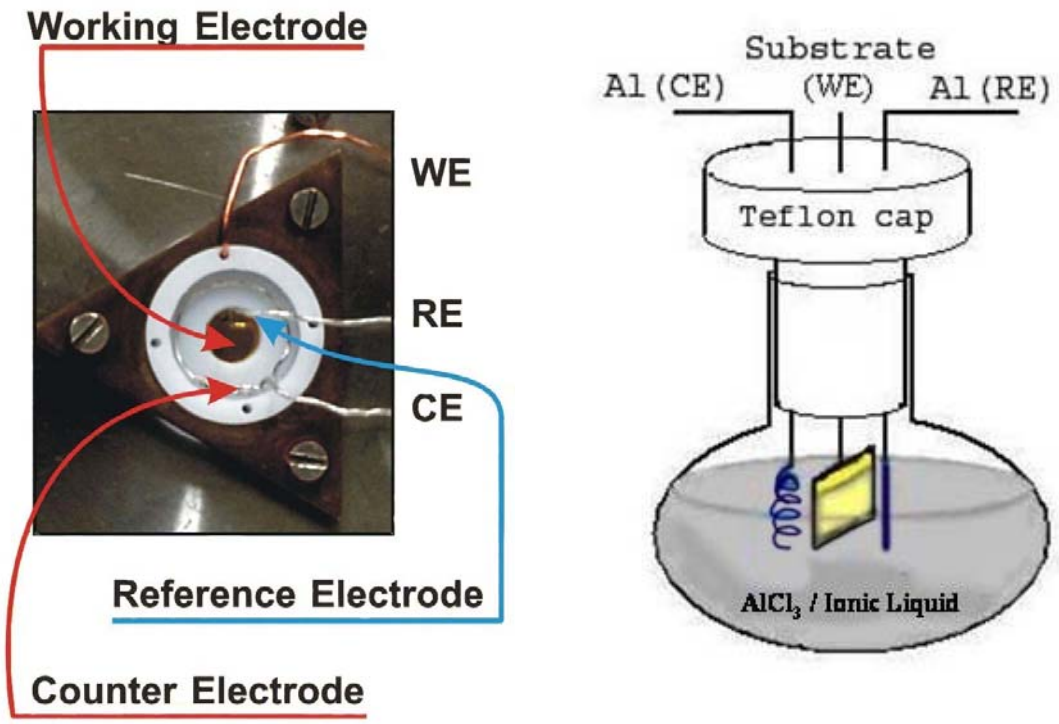

Fig.5: (a) The photograph of the electrochemical cell applied for Aluminium electrodeposition on Au (111) at room temperature; (b) A schematic view of the electrochemical cell used for Aluminium electrodeposition on Au (111) at high temperatures.

For electroplating a standard glass beaker was applied as an electrochemical cell (Figure 6).

Spring steel plates of 10 mm long, 30 mm wide and about 0.2 mm thick were applied as a working electrode (WE). Spring steel is a medium carbon steel with very high yield strength. The objects made of spring steel may return to their original shape despite significant bending or twisting. Silicon is the key component of the most spring steel alloys. An example of a spring steel used for cars would be AISI 9255 (DIN and UNI: 55Si7, AFNOR 55S7), containing 1.50%-1.80% silicon, 0.70%-1.00% manganese and 0.52%-0.60% carbon. In this work, spring steel supported by "Firma Andritz" with chemical composition0.75% C, 0.3% Si, 0.7% Mn and 0.25% Cr was employed as substrate. Prior to use the spring steel plates were grinded with 800 SiC-sandpaper followed by subsequent polishing with 3 µm diamond solution until no traces of the grinding on the substrate can be seen. Al-wire (99.999%, ø 0.5 mm) was used as a reference electrode (RE). Two Al plates were employed as a sacrificing counter electrode (CE). Before use Al-wire and Al plates were grinded with 800 SiC-sandpaper and rinsed in isopropanol in ultrasonic bath to minimize surface contaminations.

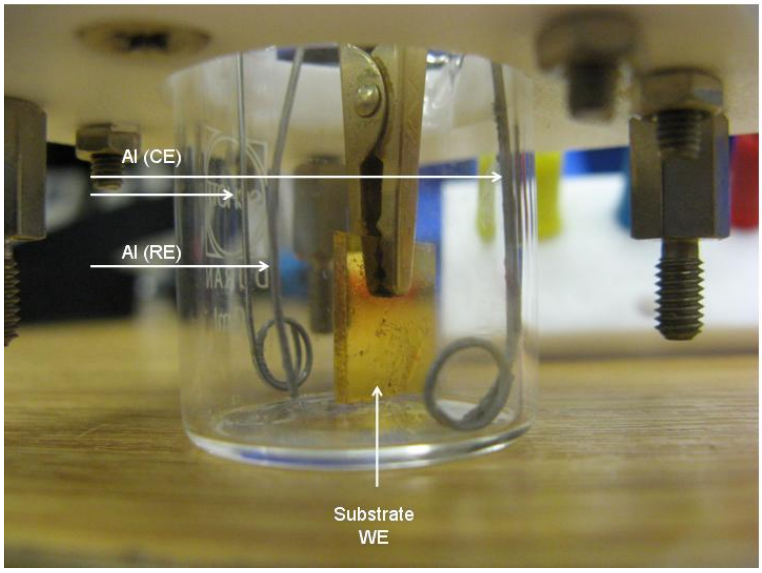

Fig.6: The photograph of the electrochemical cell applied for the electroplating.

The spring steel substrates coated with Aluminium have to be cleaned from the residues of the electrolyte immediately after the electroplating, otherwise within two hours corrosion takes place. In order to prevent it, the electroplated samples were washed in isopropanol in Sohxlett extraction. To analyze the morphology of the electrodeposits the cross section view of the films was obtained using an optical microscope Zeiss Axio Scope. For this

purpose the deposits were cut with scissors and mounted on the sample holder of the microscope. Then the specimens were grinded with 80, 300 and 800 SiC-sandpaper, polished with a diamond suspension (3 μm) for 6 minutes and thoroughly washed with ethanol in ultrasonic bath.

4.2 Scanning Electron Microscopy

The first Scanning Electron Microscope (SEM) image was obtained by Max Knoll in 1935. Nowadays SEM is applied for a numerous applications in various fields of science **[185]**. SEM allows studying the sample surface directly. The SEM images are obtained by scanning with a high-energy beam of electrons. The electrons interact with the atoms of the sample producing signals that contain information about topography and morphology of the surface, crystallography and elemental composition of the sample.

The types of signals produced by SEM include secondary electrons, backscattered electrons, characteristic X-rays, light (cathodoluminescence), Auger electrons, bremsstrahlung- all these types of signals require specific detectors for their determination, which are not usually available in a single machine. The most common (standard) detection mode is secondary electron imaging, where the SEM can produce a high-resolution image of a sample surface, revealing details in the nanometer regime.

Characteristic X-rays are emitted when the electron beam removes an inner shell electron from the sample causing a higher energy electron to fill the shell and release energy. The wavelength increases with decreasing of atomic number. This dependence is used in an energy dispersive X-ray analysis (EDX), which provides information about elemental composition of the sample.

In this work SEM and EDX analysis of the deposited Aluminium were performed to obtain information about the surface morphology of the deposited Aluminium and elemental composition of the sample. For these purposes high resolution field emission scanning electron microscopes (Camscan 44 and Carl Zeiss DSM 982 Gemini) were used.

4.3 Viscometer

A falling-ball viscometer from RheoTec GmbH was used to measure the viscosity of different ionic liquids (Figure 7). The viscosity of the liquid was measured by recording the time consumed by ball falling between two marks on the tube.

Fig.7: A falling-ball viscometer **[186]**

All the viscosity measurements were performed inside the glove box under argon atmosphere. For calculating the viscosity the following equation was used:

$$\eta = t(\rho_1 - \rho_2) \cdot K \cdot F$$

where: η – dynamic viscosity [mPa s]

t – falling time of the ball [s]

ρ_1 – density of the ball [g/cm^3]

ρ_2 – density of the liquid [g/cm^3]

K – constant of the ball [mPa cm^3 g^{-1}]

F – Constant of working angle [-]

Constant of the ball and ball density are known from the viscometer chart. Falling time of the ball and liquid density were measured.

4.4 X-Ray Diffraction

After discovery of X-rays by Wilhelm Röntgen in 1895, X-Ray Diffraction (XRD) technique found a broad application in various fields. Seventeen years later Max von Laue suggested that X-rays might be diffracted when passed through a crystal, and he had realized that their wavelengths are comparable to the distance of the lattice planes. The earliest approach to the analysis of diffraction patterns produced by crystals are treated regard a lattice plane as a mirror, and to model a crystal as stacks of reflecting lattice planes of distance *d* (Figure 8).

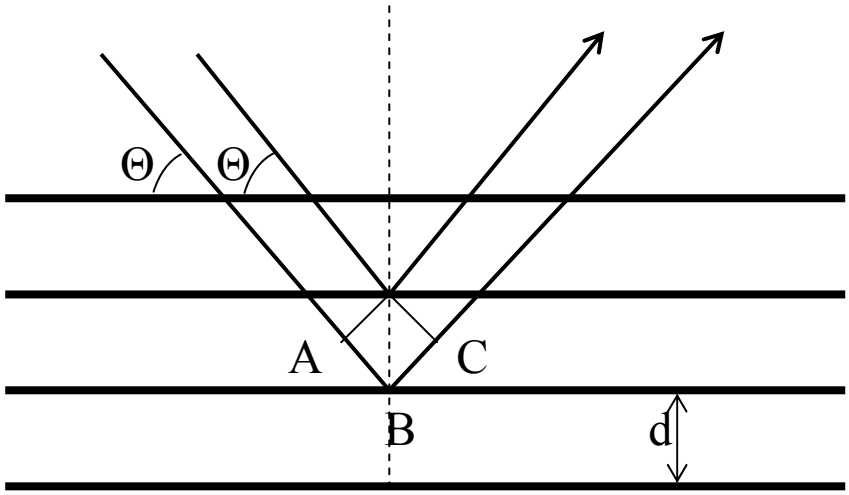

Fig.8: Reflection of X-rays in lattice planes

The difference in path-length of the two rays in previous figure can be presented as:

$$AB + BC = 2d \sin \Theta ,$$

where Θ is the glancing angle.

However, when the path-length difference is an integral number of wavelengths

$$AB + BC = n\lambda ,$$

the reflected waves are in phase and interfere constructively. It follows that a brought reflection should be observed when the glacing angle satisfies the Bragg law:

$$n\lambda = 2d\sin\Theta\,.$$

The grain size of Aluminium particles of the electrodeposits was calculated by a formalism for the evaluation of line widths of Bragg peaks. The calculation by Scherrer method is built on the dependence of the full width at half-maximum of the peak (FWHM) and grain size. The Scherrer grain size τ is equal **[187]**:

$$\tau = \frac{K\lambda}{\beta\cos\Theta}$$

where K is Scherrer constant equals to 0.9 for spherical particles, λ is wave-length equals to 1.79 for Co $K\alpha_1$ rays, Θ is the Bragg angle and β is the full width at half-maximum of the peak.

XRD diffractograms of the deposited Aluminium were recorded using a Siemens Diffraktometer D5000 with Cu-K_α radiation.

5 Results

5.1 Influence of Cation of Ionic Liquid on Aluminium Deposition

Previous studies show that the average grain size of Aluminium deposit depends on the type of the ionic liquid used for the electrodeposition **[65]**. To understand this phenomenon four different air- and water- stable ionic liquids based on the same anion bis(trifluoromethylsulfonyl)amide, Tf_2N^-, and four different cations, namely, 1-hexyl-3-methylimidazolium, $[HMIm]^+$, 1-hexyl-1-methylpyrrolidinium, $[HMIP]^+$, 1-octyl-1-methylpyrrolidinium $[OMP]^+$, and 1-propyl-1-methylpyrrolidinium, $[PMP]^+$, were applied to investigate how the cation of the ionic liquid influences the quality of aluminum electrodeposits.

5.1.1 $[PMP]Tf_2N/AlCl_3$

5.1.1.1 Phase Behaviour of $[PMP]Tf_2N/AlCl_3$

To study the phase behaviour of the $[PMP]Tf_2N/AlCl_3$ liquid three solutions of $[PMP]Tf_2N$ containing of 1.5 mol/l, 2.0 mol/l and 2.5 mol/l $AlCl_3$ have been made by simple dissolving of the Aluminium chloride in the employed ionic liquid. All mixtures were carefully heated at 100 °C for 1h in order to dissolve $AlCl_3$ thoroughly. After 24 hours all mixtures exhibited a monophasic behaviour, however the viscosity of the liquids varied depending on $AlCl_3$ content. As no changes were found after 3 days, the concentration of $AlCl_3$ in the first mixture was increased from 1.5 to 1.6 mol/l, while the concentration of $AlCl_3$ in the two other solutions were decreased from 2.0 to 1.7 mol/l and from 2.5 to 1.9 mol/l, respectively. After that all the bottles were heated at about 100 °C for 1h. After 5 days biphasic mixtures are formed in all solutions of $AlCl_3$/$[PMP]Tf_2N$, furthermore the quantity of the more viscous phase is increased by increasing the molar ratio of $AlCl_3$ in the solution. Thus in $[PMP]Tf_2N$ containing 1.6 M $AlCl_3$ only a very thin layer of the more viscous phase is formed, while the volume of this phase in mixtures containing 1.7 M $AlCl_3$ and 1.9 M $AlCl_3$ are about 25 vol.% and 40 vol.%, respectively Similar to $[BMP]Tf_2N/AlCl_3$ **[3]**, the upper phase is “milky” and looks to have a colloidal structure. It is not clear, whether $[PMP]Tf_2N$ ionic liquid shows a similar solvation behaviour to $[BMP]Tf_2N$ or that might be due to organic impurities present in the employed ionic liquid.

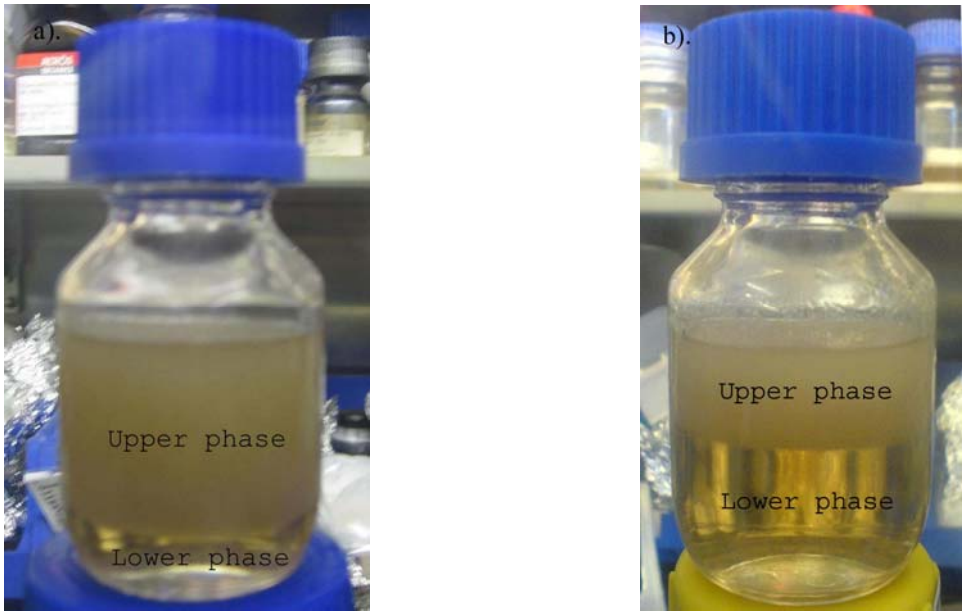

Fig.9: The photographs of the mixture of 1.9 M $AlCl_3$/[PMP]Tf_2N taken (a) 24h after the preparation; (b) 120h after the preparation.

5.1.1.2 Electrodeposition of Aluminium on Au (111)

Aluminium deposition was carried out from [PMP]Tf_2N/$AlCl_3$ containing 1.6, 1.7 and 1.9 mol/l of $AlCl_3$ at elevated temperature of more than 50 °C. Similar to [BMP]Tf_2N/$AlCl_3$ **[65]**, the Al deposition is possible only from the upper phase of the ionic liquid. The best quality of the electrodeposit was obtained in [PMP]Tf_2N/$AlCl_3$ (1.9 mol/l) at 100 °C.

Figure 10 shows the typical cyclic voltammogram of the upper phase of the biphasic mixture of [PMP]Tf_2N/$AlCl_3$ (1.9 mol/l) on gold substrate at 25 °C. The electrode potential was scanned from the open circuit potential at 0,5 V in the negative direction at a scan rate of 10 mV/s. At a potential of -1.9 V (v.s. Al/Al(III)), the cathodic current increases due to the bulk deposition of Aluminium. Upon scan reversal, a cross-over was observed at -0.8 V, which is typical for the nucleation process. The small anodic wave recorded on the reverse scan at a potential of about -0.3 V, is attributed to the incomplete stripping of the electrodeposited Aluminium.

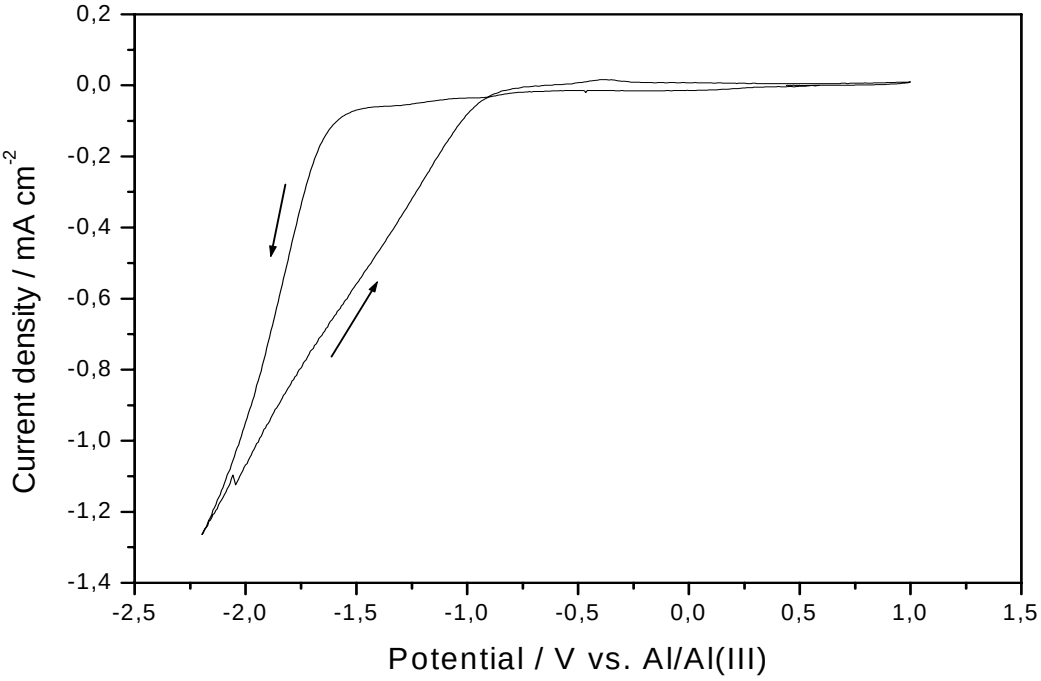

Fig.10: Cyclic voltammogram of the upper phase of [PMP]$Tf_2N/AlCl_3$ (1.9 mol/l) on Au(111) at 25 °C, v = 10 mV/s.

Figure 11 shows the effect of temperature on the electrochemical behaviour of [PMP]$Tf_2N/AlCl_3$ (1.9 mol/l). The employed liquid remains stable up to at least 300 °C under inert gas conditions, a practical temperature limit on a longer timescale might be around 150 °C where the evaporation of $AlCl_3$ slowly begins. Cyclic voltammograms were scanned at 25, 50, 100, 125 and 150 °C.

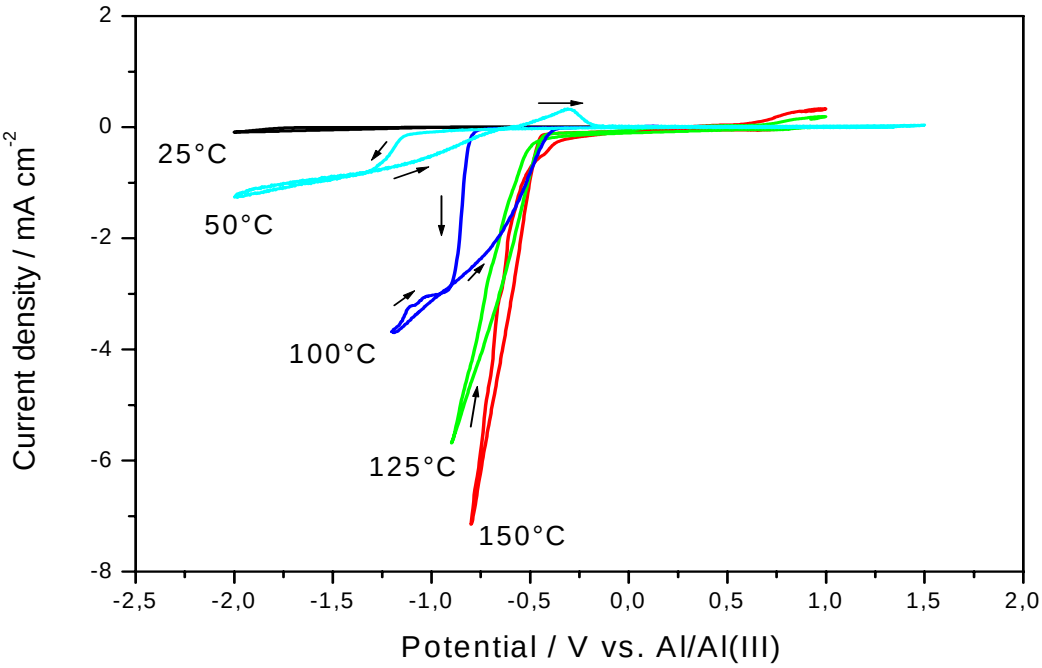

Fig.11: Cyclic voltammograms of [PMP]Tf_2N/$AlCl_3$ (1.9 mol/l) on Au(111) at various temperatures from 25 to 150 °C, v = 10 mV/s.

Cyclic voltammograms recorded at higher temperatures exhibit a similar behaviour as the one at room temperature. At 50 °C, current rises steep at -1.2 V and less steeply at -1.3 V. These process are correlated to the Al deposition, the reduction of the organic cation begins after -2.0 V v.s. Al/Al(III). The same steep rise of current was observed at -0.85 V and less steeply at -0.9 V at 100 °C. At 125 and 150 °C bulk deposition of Aluminium started at -0.6 V and current rises rapidly by higher 150°C. Anodic peaks observed around 1.0 V at 125 and 150 °C are attributed to the oxidation of gold substrate. Similar to [BMP]Tf_2N/$AlCl_3$ **[65]**, there is a sharp decrease of the overvoltage for Aluminium deposition by increasing the temperature. The irreversibility of Aluminium deposition process is always the same.

Well-adhering Aluminium deposits were obtained at temperatures higher than 100 °C. In order to explain why Aluminium can not be deposited at lower temperatures, viscosity and conductivity measurements at different temperatures would be suitable experiments.

The Al electrodeposits were investigated by high resolution field-emission scanning electron microscope (SEM). Visually, the deposits appear to be thick, shiny and well-adhering to the gold substrate. Figure 12 shows SEM pictures of Aluminium deposits obtained from [PMP]Tf_2N/$AlCl_3$(1.9 M) at 100 °C (a) and at 125 °C (b).

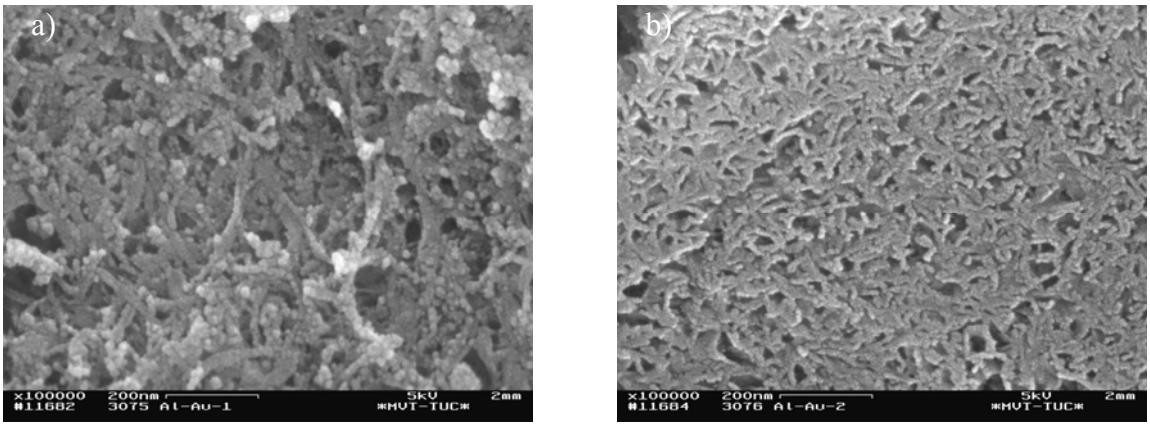

Fig.12: SEM micrographs of nanoscale Al electrodeposits made from [PMP]Tf_2N/$AlCl_3$(1.9 M) (a) at -0.9 V for 1 h; 100 °C; (b) at -0.8 V for 1 h; 125 °C.

In both cases nanoscale Al electrodeposits were obtained with a grain size of about 20 – 50 nm. The deposits seem to be porous. The EDX analysis of the electrodeposits reveals ~80 atom% Al and ~18 atom% O.

5.1.1.3 Viscosity Measurements of the Upper Phase of [PMP]Tf_2N/$AlCl_3$

Viscosity and electrical conductivity are two physical properties, which mostly affect the quality and properties of the deposit. The information about viscosity of pure ionic liquids can be found in literature, but there is no study on the viscosity of the upper phase of [PMP]Tf_2N/$AlCl_3$. The electrochemical deposition occurs in the upper phase of the mixture of ionic liquid / $AlCl_3$. In order to explain the nature of the process, it is necessary to measure viscosity of electrolyte used for electrochemical experiments.

Viscosity measurements were performed inside an inert gas glove box with Falling Ball Viscometer. Viscometer was calibrated with the pure [BMP]Tf_2N and [EMIm]Tf_2N ionic liquids. These liquids are well-known and it is easy to compare the obtained results with the literature.

The viscosity measured for [BMP]Tf_2N is 86.1 mPa s at 22 °C, which is in good agreement with viscosity reported by Tokuda **[188]**: 96.2 mPa s at 20 °C and 74.9 mPa s at 25 °C. In the case of [EMIm]Tf_2N the measured viscosity is 35.5 mPa s at 22 °C, which is similar to the reported values **[63]**: 36 mPa s at 20 °C and 32 mPa s at 25 °C. This indicates that the viscosity measurements were accurate and practical.

The viscosity measured for the upper phase of the mixture of [PMP]Tf_2N / 1.9 mol/l $AlCl_3$, which has been used for the electrochemical experiments, are presented in figure 13.

The density of the upper phase of the mixture was measured to be 1.3 g/cm^3. The first series of measurements were performed right after adding of the solution in the viscosimeter tube inside the glove box. The second series of the values were obtained after about 30 minutes. The next two series were recorded after about 14 and 16 hours. An aging of the solution was found. A small increasing of the viscosity during one series of the measurement can be explained by water absorption from the glove box.

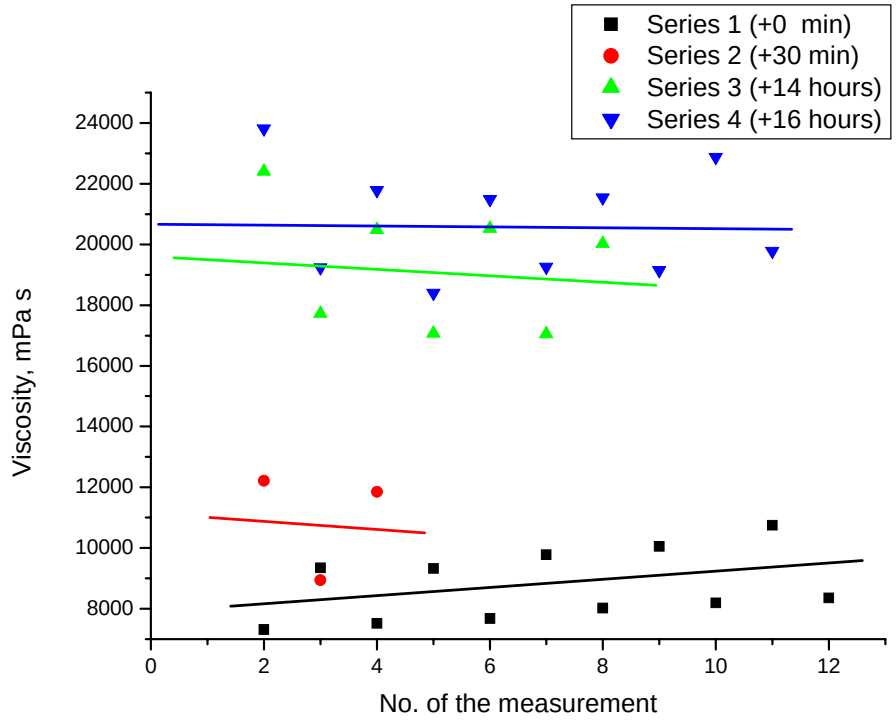

Fig.13: Viscosity of [PMP]Tf_2N / 1.9 mol/l $AlCl_3$

The measured viscosity of the mixture [PMP]Tf_2N / 1.9 mol/l $AlCl_3$ is about 9000 mPa·s, which is at least 100-fold higher than that of pure ionic liquids and can not be detected by our viscosimeter. The viscosity of pure [BMP]Tf_2N measured by MacFarlane was 85 mPa·s **[9]**.

It is also very interesting to observe that measurements in different directions (even and uneven measurements) are different. It shows that the upper phase is unequally viscose at room temperature.

Upper phase with volume 40 ml is formed after 3 weeks. It was observed that solid particles, probably of pyrrolidinium cation – $AlCl_4^-$ species, dissipate in upper phase, which accordingly affects the measurement at room temperature.

Because of time limitation, viscosity measurements of other liquids were not performed.

5.1.2 [HMP]$Tf_2N/AlCl_3$

5.1.2.1 Phase Behaviour of [HMP]$Tf_2N/AlCl_3$

To study the phase behaviour of $AlCl_3$ in [HMP]Tf_2N, the mixtures were prepared similar to [PMP]$Tf_2N/AlCl_3$. The [HMP]$Tf_2N/AlCl_3$ system is monophasic at a concentration of $AlCl_3$ of about 1 mol/l. However starting from 1.3 mol/l of $AlCl_3$ the solution shows biphasic behaviour. Figure 14 presents the phase behaviour of the solution [HMP]Tf_2N / 1.5 mol/l $AlCl_3$ as a function of time after its preparing that includes mixing, heating at 100°C and then cooling of the solution.

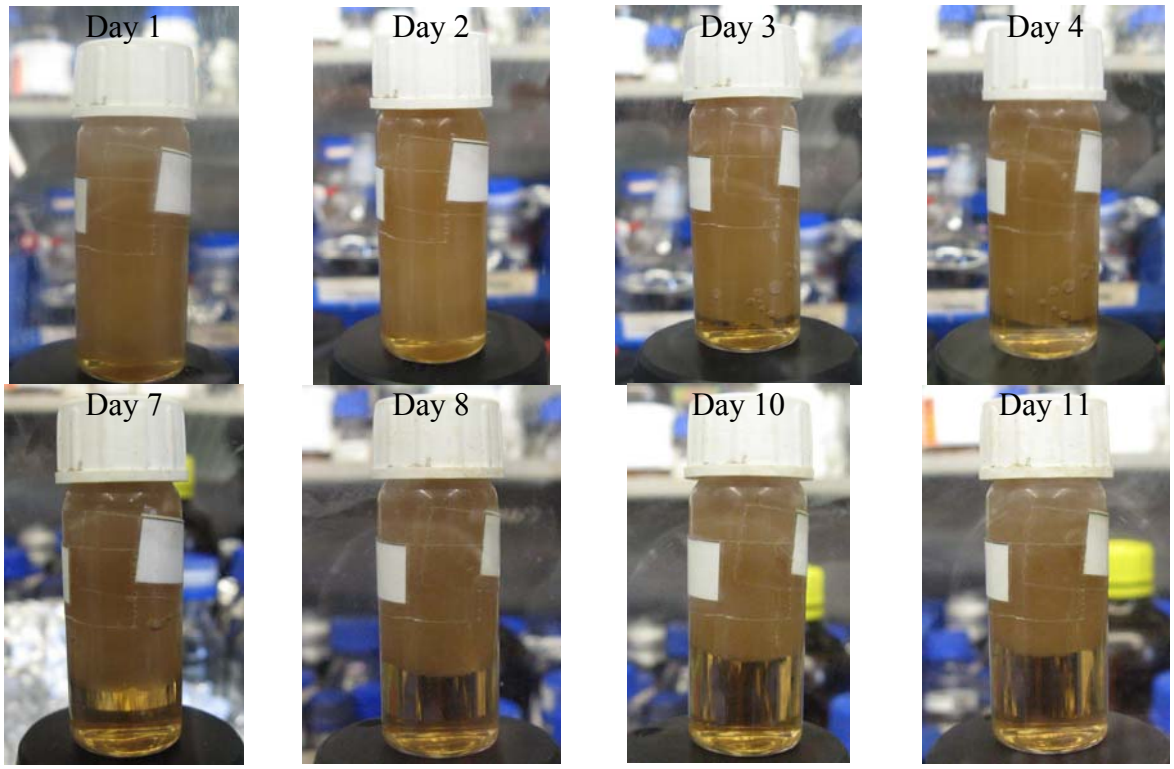

Fig.14: Phase behaviour of [HMP]$Tf_2N/AlCl_3$ (1.5 mol/l) as a function of time

As can be seen, the separation on two phases occurs very slowly. Similar to [PMP]$Tf_2N/AlCl_3$ (1.9 M), the upper phase of the [HMP]$Tf_2N/AlCl_3$ (1.5 M) is “milky” and looks to have a colloidal structure.

5.1.2.2 Electrodeposition of Al on Au (111)

Figure 15 shows the typical cyclic voltammogram of the upper phase of the biphasic mixture of [HMP]$Tf_2N/AlCl_3$ (1.5 mol/l) on gold substrate at 25 °C. The electrochemical behaviour is similar to [PMP]$Tf_2N/AlCl_3$ system, namely irreversible. The onset of bulk

Aluminium deposition starts at a potential of about -1.6 V but it shows very small values of current density at this temperature, due to high viscosity.

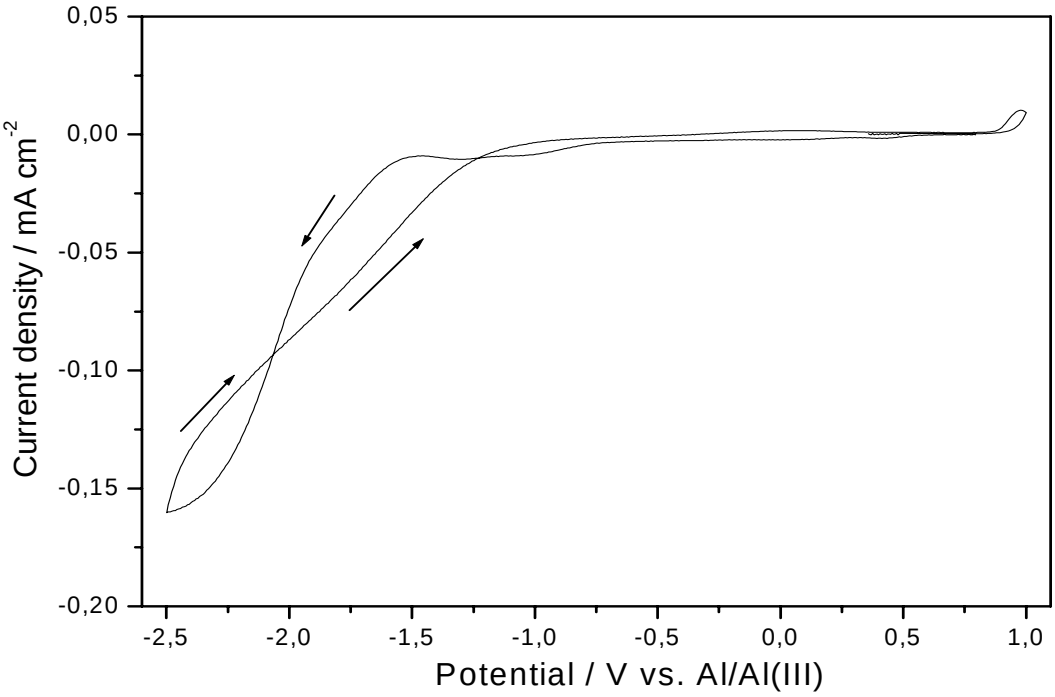

Fig.15: Cyclic voltammogram of the upper phase of [HMP]Tf_2N/$AlCl_3$ (1.5 mol/l) on Au(111) at 25 °C, at a scan rate v = 10 mV/s

The cyclic voltammograms of the ionic liquid [HMP]Tf_2N containing 1.5 mol/l $AlCl_3$ on gold substrates at different temperature that is, 50, 75, 100 and 150 °C, are shown in Figure 16. All cyclic voltammogramms are similar to that recorded at 25 °C. The onset of Aluminium deposition occurs at less negative potential and cathodic current increases as the temperature increases.

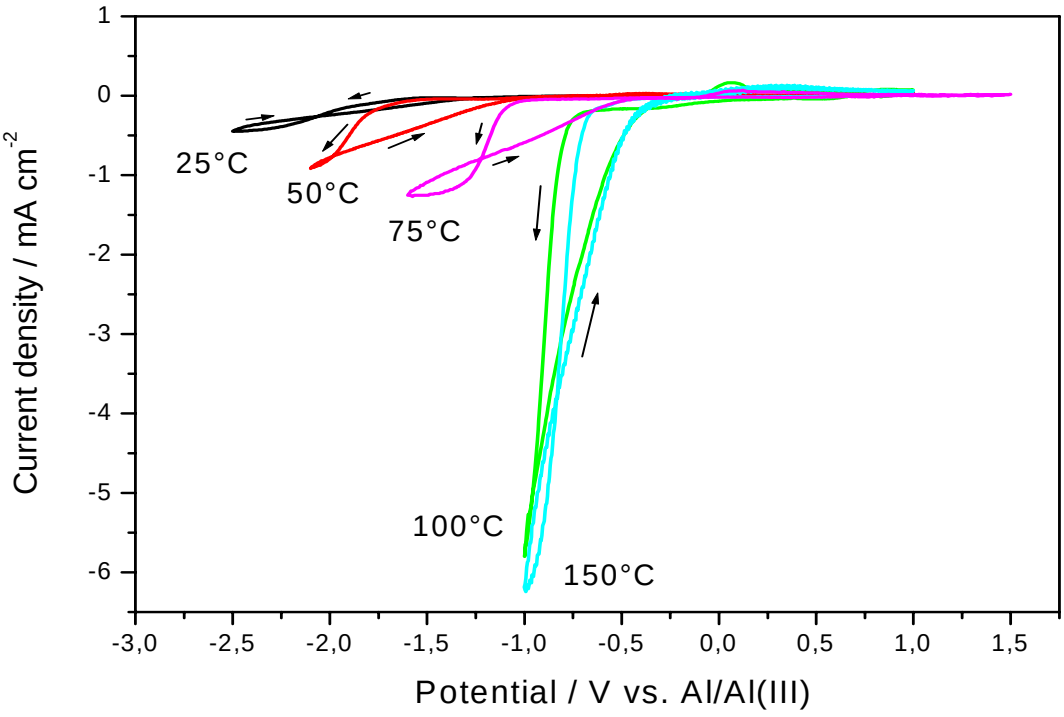

Fig.16: Cyclic voltammograms of [HMP]Tf_2N/$AlCl_3$ (1.5 mol/l) on Au(111) at various temperatures from 25 to 150 °C, v = 10 mV/s.

The Al electrodeposits obtained in [HMP]Tf_2N/$AlCl_3$ (1.5 mol/l) were investigated by high resolution field-emission scanning electron microscope (SEM). Visually, the deposits are powdery, and thin with a silver colour and poor adhesion to the gold substrate. Figure 17 shows a SEM micrograph of the layer obtained at -0.9 V for 1 h at 100 °C. It is clear that Aluminium grain size is much smaller than it can be recognized from this image. However, due to a very thin coating and poor adhesion, a higher resolution of the deposit is not possible as the deposited layer is easily destroyed by electrons at high resolutions. The EDX analysis reveals ~22 atom% Al, ~20 atom% Cl due to remains of $AlCl_3$, and ~58 atom% O.

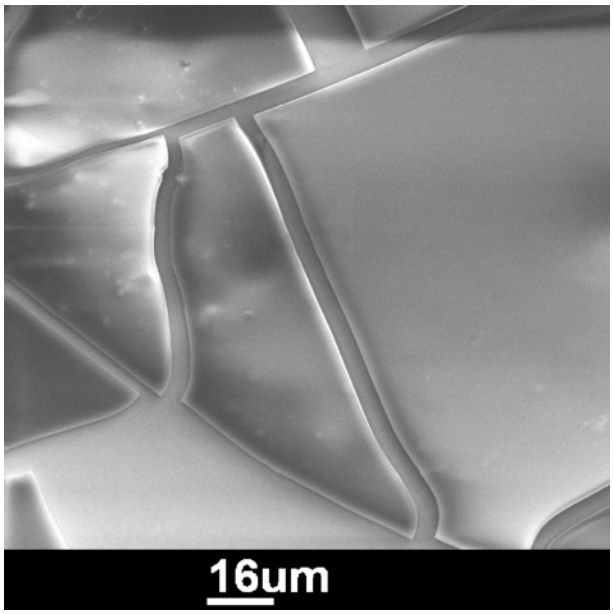

Fig.17: Aluminium deposition in [HMP]Tf_2N/$AlCl_3$ (1.5 mol/l); 100°C; -0,9V

Since Al and Au have similar 2Θ angle in XRD pattern, gold substrate affects Aluminium pattern. Therefore, to study a grain size of the electrodeposit with XRD more suitable substrate for Aluminium coating is needed. Glassy carbon seems to be an appropriate substrate for such investigations. However, the experiments to measure XRD-pattern of deposited Aluminium on glassy carbon in [HMP]Tf_2N/$AlCl_3$ at various temperature failed, due to functionality of our diffractometer and limited time of a study.

5.1.3 $[OMP]Tf_2N/AlCl_3$

5.1.3.1 Phase Behaviour of $[OMP]Tf_2N/AlCl_3$

In this part of the work, the phase behaviour of the mixture $[OMP]Tf_2N/AlCl_3$ was studied. The preparation of the solutions was the same as in the previous chapter. Interestingly, the biphasic behaviour of $[OMP]Tf_2N/AlCl_3$ is obtained at higher concentrations of $AlCl_3$ i.e. between 2.0 and 3.0 mol/l (Figure 18). The upper phase is "milky" and at higher concentration of $AlCl_3$ the bottom phase of the solution can be completely colourless. A small yellow tint of all liquids was due to organic impurities that are present in the ionic liquid.

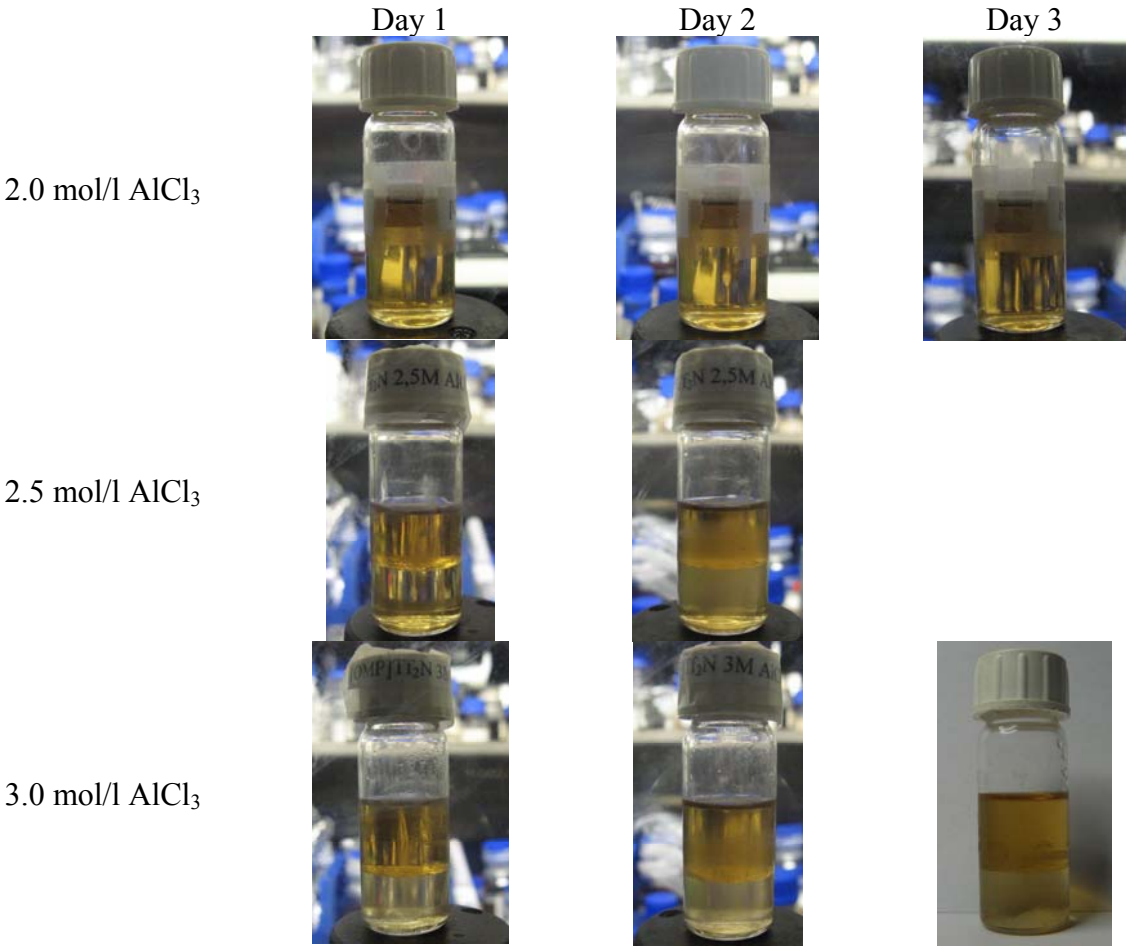

Fig.18: Phase behaviour of $[OMP]Tf_2N/AlCl_3$ as a function of time and concentration

5.1.3.2 Electrodeposition of Al on Au (111)

Figure 19 exhibits the typical cyclic voltammogram of the ionic liquid $[OMP]Tf_2N$ containing 4 mol/l $AlCl_3$ at 100 °C. The electrochemical behaviour is different for this system. It is a small oxidation peak at 0.1V. The electrochemistry seems to be reversible.

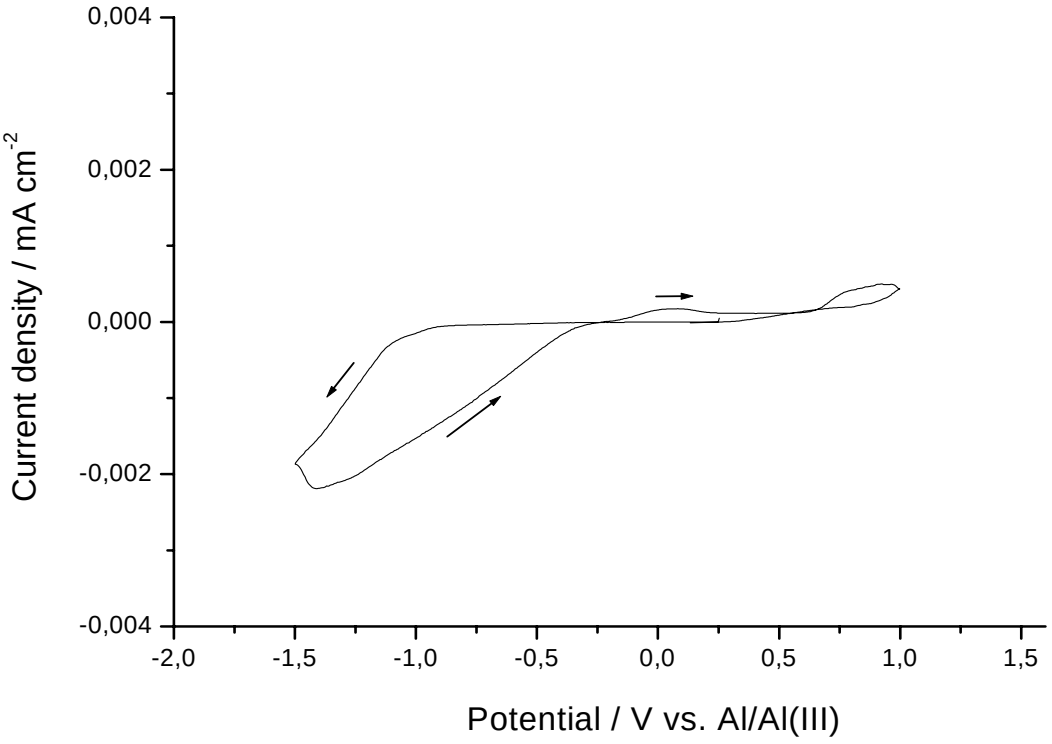

Fig.19: Cyclic voltammogram of the upper phase of [OMP]Tf_2N/$AlCl_3$ (3 mol/l) on Au(111) at 100 °C, v = 10 mV/s.

At the electrode potentials of more negative than -0.2 V a strong reduction process occurs. This process may attribute to the bulk deposition of Aluminium; however Aluminium deposits were not obtained at these electrode potentials. Instead of a well-adhering deposit, only a black layer was obtained. This layer can be easily removed from the surface by simple cleaning of the substrate with isopropanol. It might be due to the solvation layers (Chapter 2.1.7) of the ionic liquid that were adhered to the substrates preventing the electrodeposition. In this case the deposition requires more negative electrode potential. The impurities presented in the liquid can also participate in such process.

5.1.4 [HMIm]$Tf_2N/AlCl_3$

5.1.4.1 Phase Behaviour of [HMIm]$Tf_2N/AlCl_3$

Similar to other mixtures, [HMIm]$Tf_2N/AlCl_3$ solution shows biphasic behaviour with increasing concentration of $AlCl_3$ (Figure 20). The difference from other liquids is that the lower phase is solid within two weeks after the preparation of the mixture. Such behaviour is typical for imidazolium-based ionic liquids, for example [EMIm]Tf_2N **[3]**.

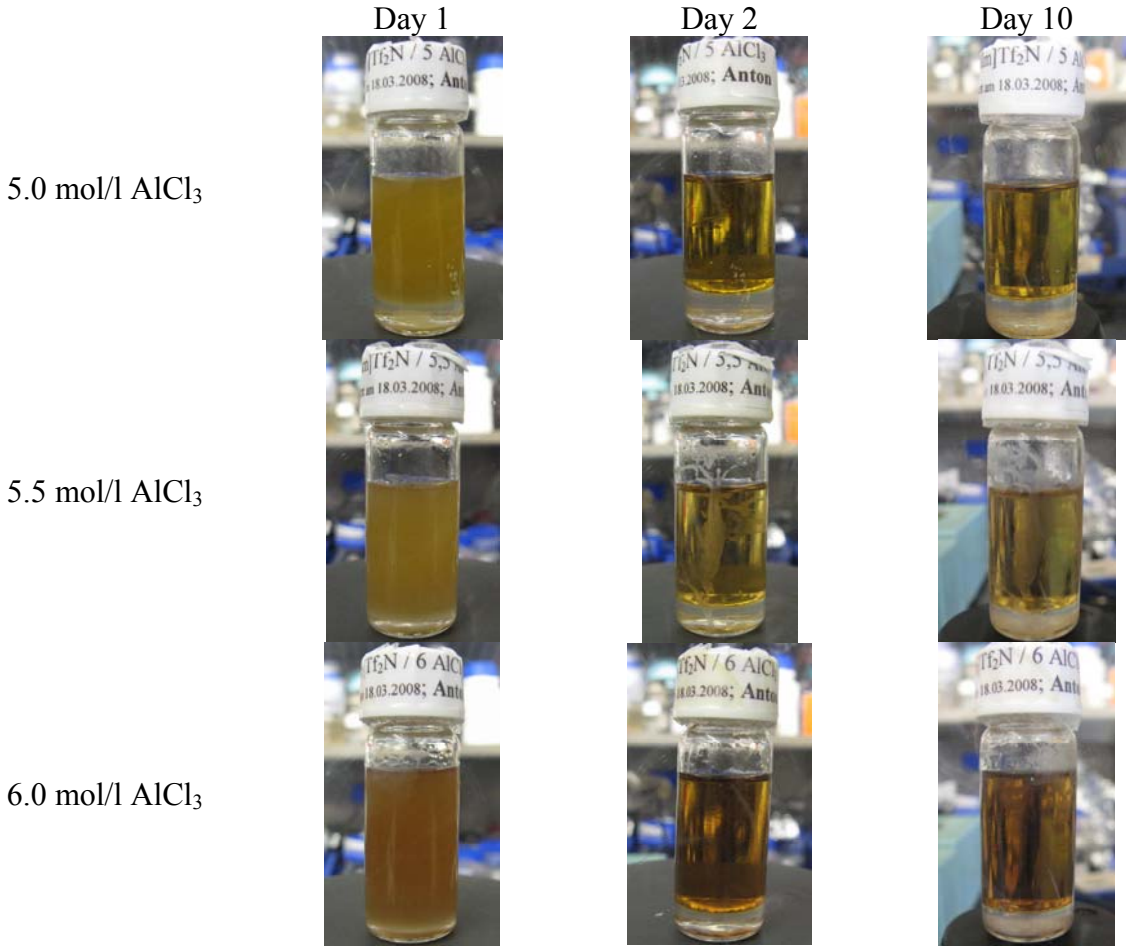

Fig.20: Phase behaviour of [HMIm]$Tf_2N/AlCl_3$ as a function of time and concentration of $AlCl_3$

5.1.4.2 Electrodeposition of Al on Au (111)

Figure 21 shows a typical cyclic voltammogram for Aluminium deposition and stripping on Au(111) in the upper phase of biphasic mixture of [HMIm]Tf_2N/$AlCl_3$ (6.0 mol/l) at room temperature. Scans were initially swept cathodically from open circuit potential (1.2 V v.s. Al/Al(III)) at a scan rate of 10 mV/s. Aluminium electrodeposition starts at about -0.2 V. The peak at +0.2 V is attributed to Aluminium stripping. A series of the small anodic peaks in the positive direction is due to the stripping of alloys and compounds, which were electrodeposited before the bulk Aluminium deposition starts.

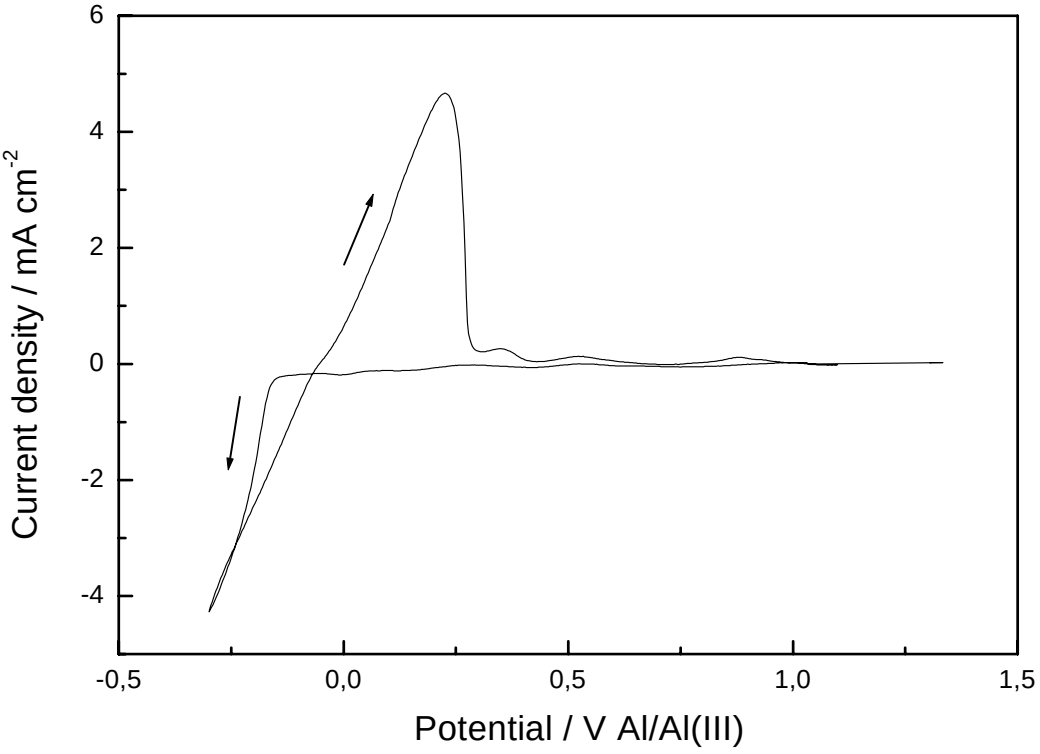

Fig.21: Cyclic voltammogram of the upper phase of [HMIm]Tf_2N/$AlCl_3$ (6.0 mol/l) on Au(111) at room temperature, v = 10 mV/s.

Figure 22 shows the cyclic voltammograms of the upper phase of the biphasic mixture of [HMIm]Tf_2N/$AlCl_3$ (6.0 mol/l) at temperatures 25 °C and 100 °C. There are more steeply cathodic and anodic peaks occurred due to Aluminium deposition and stripping when cyclic voltammogram recorded at 100°C. The interesting difference from pyrrolidinium-based mixtures is the same onset of potential for bulk Aluminium deposition at various temperatures. Such results were also obtained by Moustafa **[3]**.

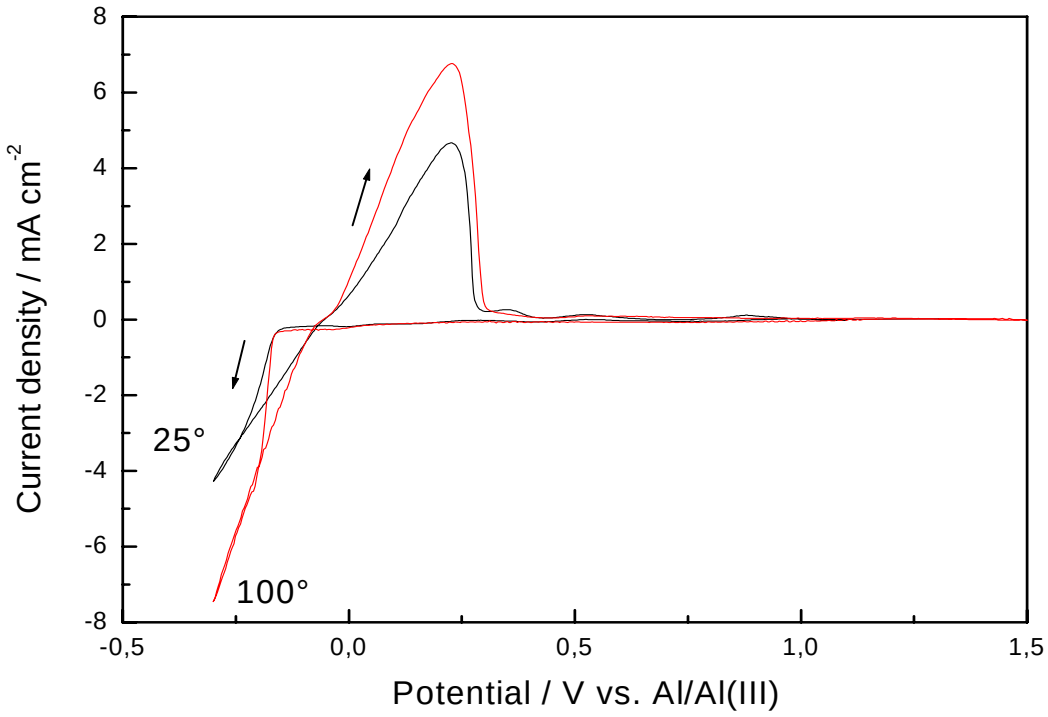

Fig.22: Cyclic voltammograms of 6.0 mol/l $AlCl_3$ in $[HMIm]Tf_2N$ on Au(111) at 25 °C and at 100 °C, v = 10 mV/s.

5.1.5 Summary and discussion

In the present work it was shown how the chain length of the ionic liquid cation influences the phase behaviour of ILs/$AlCl_3$ mixtures. For this purpose the electrodeposition of Aluminium was studied by cyclic voltammetry from its chloride in four different air- and water- stable ionic liquids, based on the same anion bis(trifluoromethylsulfonyl)amide, Tf_2N^-, and four different cations, namely, 1-hexyl-3-methylimidazolium, $[HMIm]^+$, 1-hexyl-1-methylpyrrolidinium, $[HMP]^+$, 1-octyl-1-methylpyrrolidinium $[OMP]^+$, and 1-propyl-1-methylpyrrolidinium, $[PMP]^+$. The electrodeposition of Aluminium was performed on Au(111) at various temperatures: 25 °C, 50 °C, 75 °C, 125 °C and 150 °C.

All the liquids exhibit biphasic behavior by mixture with $AlCl_3$ when the concentration of Aluminium chloride exceeded 1.6 mol/l, 1.3 mol/l, 2.0 mol/l, and 5.0 mol/l for ionic liquids $[PMP]Tf_2N$, $[HMP]Tf_2N$, $[OMP]Tf_2N$ and $[HMIm]Tf_2N$, respectively. All biphasic solutions become monophasic again when heated to a temperature of more than 80 °C. The quantity of the upper phase decreases by increasing the molar ratio of $AlCl_3$ in the solution.

All pyrrolidinium-based solutions show irreversible electrochemical behavior. In contrast, [HMIm]Tf_2N behavior is reversible. It is well-correlated with results of phase and interfacial behavior of pyrrolydinium- and imidazolium-based ionic liquids. Pyrrolidinium cations have higher interaction strength to the substrate than imidazolium cations **[24,163]** and probably prevent the reversibility on cyclic voltamogramm.

Aluminium can only be electrodeposited from the upper phase of [PMP]$Tf_2N/AlCl_3$ and the upper phase of [HMP]$Tf_2N/AlCl_3$ solutions. The best electrolyte compositions for the electrodeposition are 1.9 mol/l and 1.5 mol/l of $AlCl_3$ in [PMP]Tf_2N and [HMP]Tf_2N ionic liquid, respectively. Well-adhering thick Aluminium deposits were obtained in there solutions at temperatures higher than 100 °C. The Al electrodeposits were investigated by high resolution field-emission scanning electron microscope (SEM) and energy dispersive (EDX) X-ray analysis. In the case of [PMP]$Tf_2N/AlCl_3$ and [HMP]$Tf_2N/AlCl_3$ Al grain size seems to be in nanoscale. Unfortunately, the attempts to electrodeposit Aluminium in [OMP]$Tf_2N/AlCl_3$ and [HMIm]$Tf_2N/AlCl_3$ solutions were not successful.

As viscosity and electrical conductivity are two physical properties, which mostly affect the quality and properties of the deposit, the viscosity was measured for the upper phase of [PMP]$Tf_2N/AlCl_3$(1.9 mol/l) that seems to be the most appropriate for the electrodeposition of Aluminium under the applied conditions. The measured viscosity of the upper phase of [PMP]$Tf_2N/AlCl_3$(1.9 mol/l) at room temperature is about 9000 mPa s, which is at least 100-fold higher, than the viscosity of the pure ionic liquid [PMP]Tf_2N.

5.2 Electrodeposition of Microcrystalline Al on Spring Steel

Spring steel, due to its chemical composition, is corrosive in aggressive environments and therefore should be replaced to an expensive analog. Electrochemical deposition is a relatively simple and cheap method to protect the complex parts made of spring steel from corrosion by coating with an adherent Aluminium layer. To perform this covering, two well known mixtures of ionic liquid and $AlCl_3$: [EMIm]Tf_2N / $AlCl_3$ and [EMIm]Cl / $AlCl_3$ were used. Aluminium deposits were analyzed using SEM, EDX and metallographic preparations.

5.2.1 Influence of Pre- and Post-treatment of the Substrate on Coating

The results of the study show that the pre-treatment of the substrates plays a key role in the coating adhesion. The Aluminium coating made on conventionally pretreated spring steel does not exhibit good adherence to the substrate. Adhesion of coating on foreign substrates is of essential importance to the coating performance.

In comparison with mild steel spring steel contains silicon and chrome. Their combinations with iron and carbon build on the surface strong oxide layer which prevents Aluminium adhesion. In order to remove this layer electrochemical etching was performed **[170]**.

Figure 23 shows the cyclic voltammogram recorded on spring steel substrate in the mixture [EMIm]Tf_2N / 5.5 mol/l $AlCl_3$ at room temperature. The electrode potential was scanned from the open circuit potential in the negative direction at a scan rate of 10 mV/s. A rising cathodic current corresponding to the bulk Al deposition starts at around -0.15 V. In the reverse scan a current loop is recorded which indicates that bulk Al deposition on mild steel electrode is initiated by an overpotential driven nucleation process, which is characteristic for many of its analogues in ionic liquids. An oxidation peak is centered at about +0.3 V attributed to the stripping of Al.

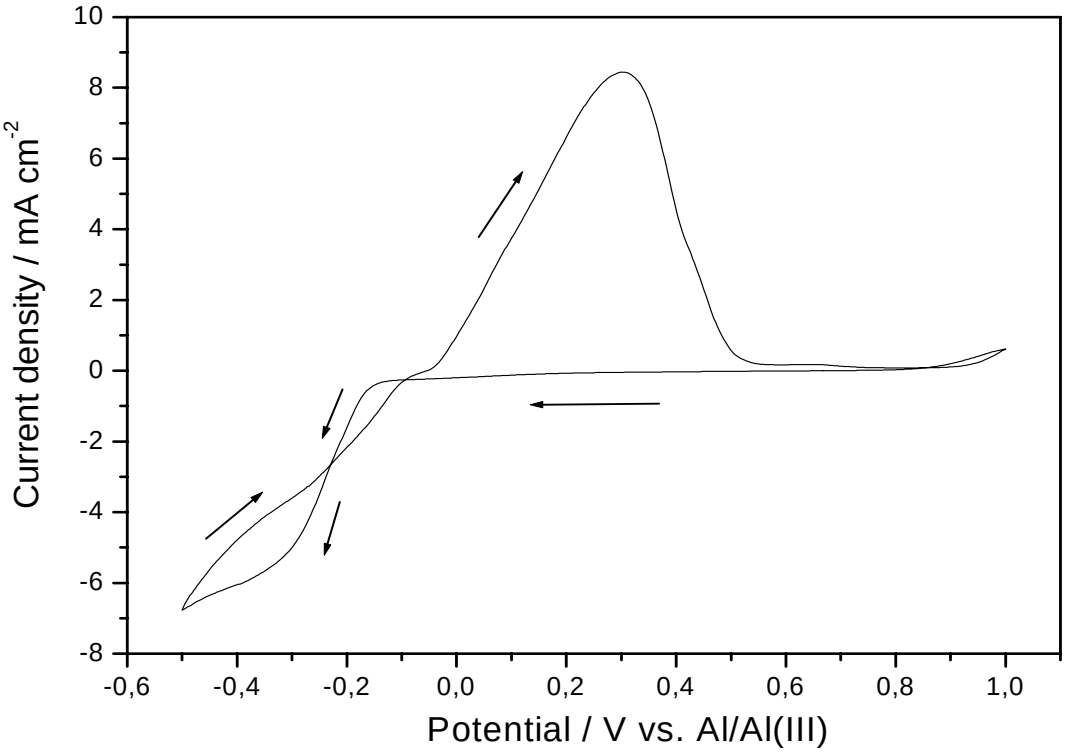

Fig.23: Typical cyclic voltammogram of [EMIm]Tf_2N / 5.5 mol/l $AlCl_3$ on spring steel at 25 °C. Scan rate is 10 mV s^{-1}.

The small peak at around +1 V shows the substrate dissolution. It can be used for removing of the oxide layer from the surface (anodic etching). First anodic etching was made at 1 V for 3 minutes. However, the subsequent electrodeposition showed that the deposited Aluminium layer does not adhere well to the surface of the substrate. Increasing of the etching time to remove more oxide from the surface does not improve the adhesion as the roughness of the surface of the sample increases due to its strong dissolution. After 10-minutes etching the holes are formed in the sample that can be seen by the naked eye. Chemical etching in HCl does not lead to good results, too.

The best results of Aluminium coating were achieved after the combination of pre-treatments. Grinding of the substrate with 800 Si-C paper and subsequent electrochemical etching for 5-7 minutes allow to obtain well-adherent coating. This coating contained black particles in covering. As it was shown by EDX (Figure 24) there are iron particles. They were removed by anodic etching and deposited again simultaneously with Aluminium.

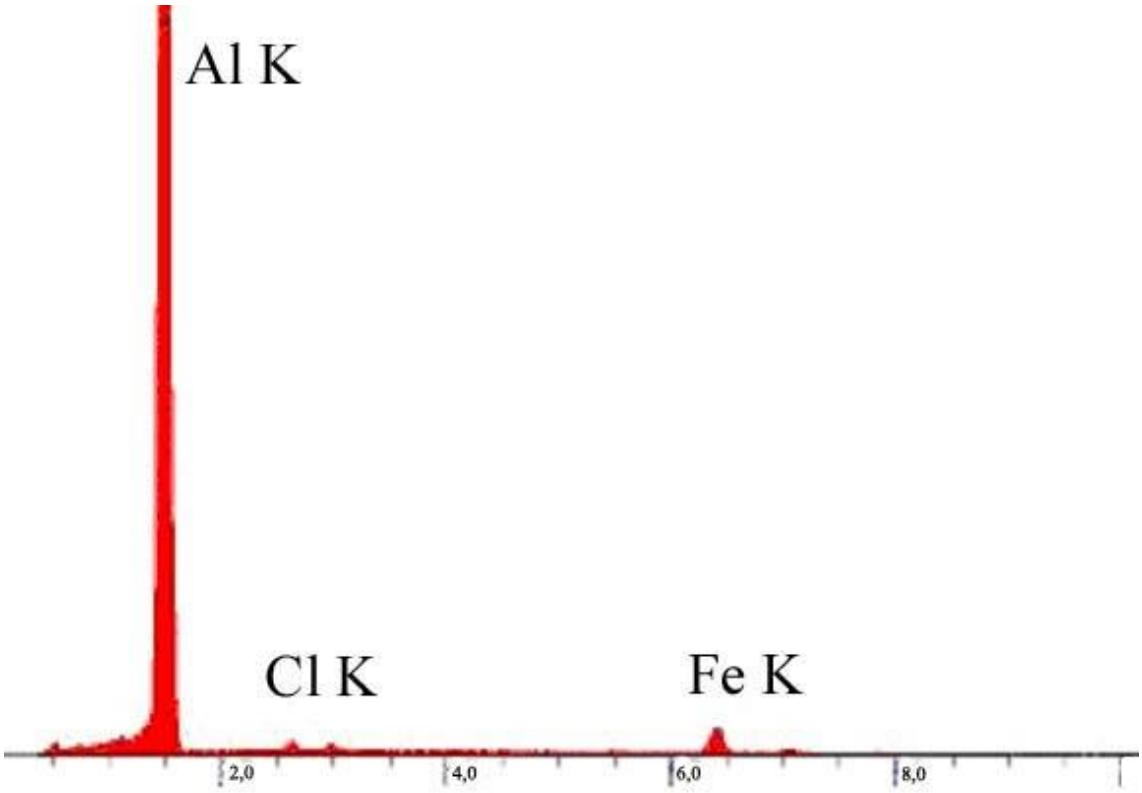

Fig.24: EDX-Spectrum of Al-coating made on spring steel substrate after mechanical pre-treatment and subsequent anodic etching

To eliminate iron deposition the electrolyte was changed after the anodic etching. This procedure leads to the well adherent 10 μm thick Aluminium layer (Figure 25). Aluminium covered spring steel was cut, the cross section was polished and investigated by optical microscopy.

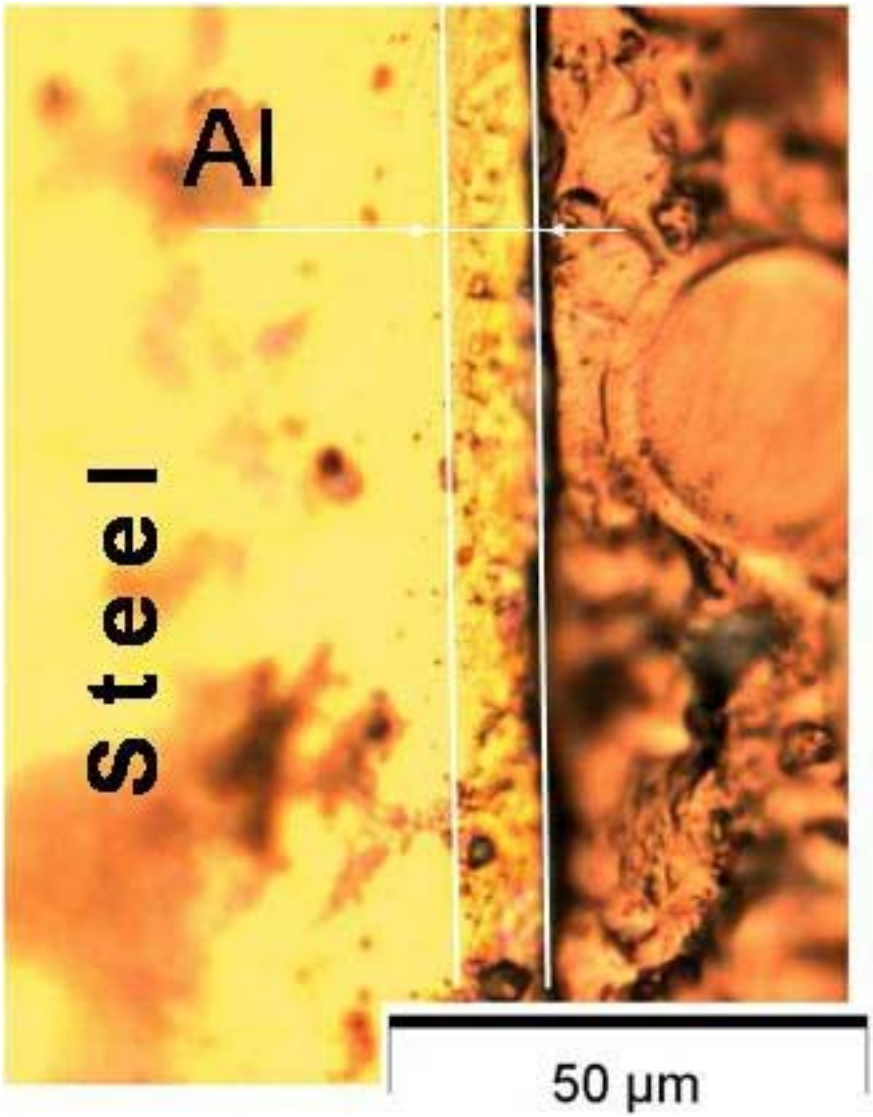

Fig.25: Cross section view of Al-electrodeposit on spring steel. Average thickness of the coating is about 10.3 µm.

To obtain thicker coatings of Al on spring steel, the deposition time was increased to more than two hours. In this case, the Aluminium deposits with the thicknesses of more than 20 µm can be obtained, where iron particles are covered by Aluminium even without electrolyte changing.

Some trails were carried out using [EMIm]Cl where spring steel was coated with Al for several hours. The result revealed that some impurities were also coated. The water content of ionic liquid and $AlCl_3$ leads to the formation different forms of Aluminium hydroxychloride precipitating on the surface in the first hours of the experiment. These impurities can be minimized by electrolysis the solution prior to coating of Al. To achieve the high quality of coats, electrolysis was carried out for 7 hours.

The post-treatment of deposits has a great importance attributed to undergone surface corrosion. The adsorption of the ionic liquid to the samples surface and their reaction with air

leads to corrosion. If the rests of the electrolyte are not removed from the surface, the coating can be even completely destroyed (Figure 26).

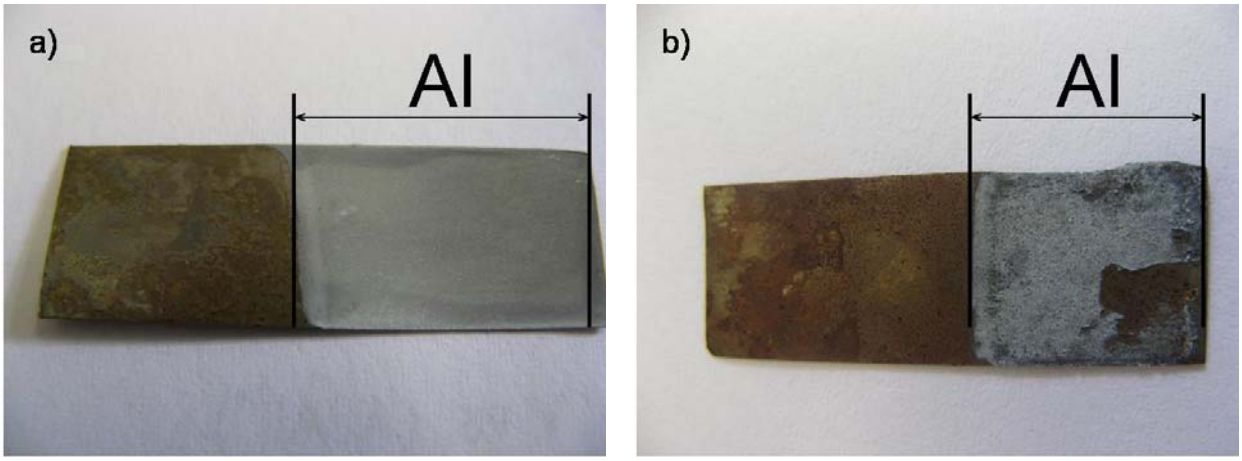

Fig.26: The photographs of the Al electrodeposits: (a) the remains of the electrolyte were completely removed from the surface; (b) the remains of the electrolyte were not completely removed from the surface.

In order to avoid such corrosion, the substrates were cleaned in isopropanol on trial and error basis. At first, the coated sample was placed in isopropanol bath for 12 hours, but it resulted in corrosion. Washing in isopropanol with ultrasonic bath was also not successful. The best results were achieved by immediately washing with isopropanol in a Soxhlett extractor. A very pure isopropanol was used for this purpose, because it is capable of dissolving the rest ionic liquid.

5.2.2 Electrodeposition of Al in [EMIm]Tf_2N /$AlCl_3$

In order to deposit Al from [EMIm]Tf_2N / 5.5 mol/l $AlCl_3$, some of experiments were performed to find the optimal parameters of the electrochemical covering. The resulted cyclic voltammogram is shown in Figure 27. The onset of the bulk deposition of Aluminium starts at a potential of about -0.2 V. First oxidation peak at about 1 V is attributed to the substrate dissolution, second one at about 0.25 V is due to the reduction of the deposited Al alloy with steel and the third one at 0 V is observed due to the Al dissolution.

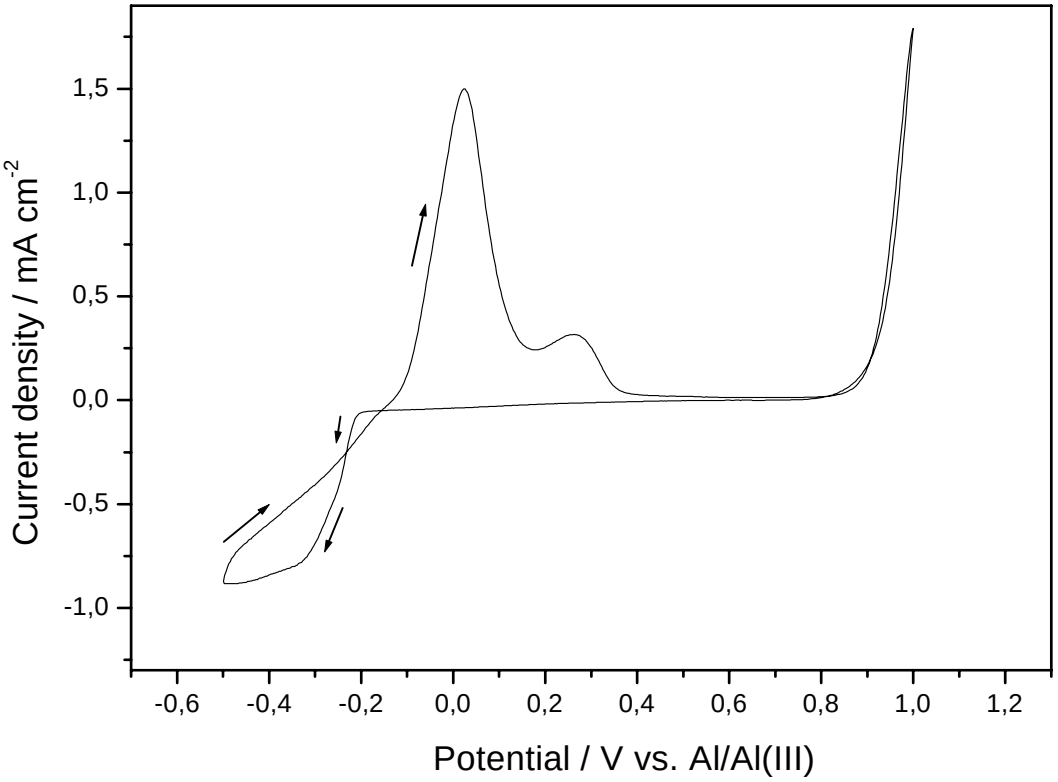

Fig.27: Cyclic voltammogram recorded at 10 mV/s on spring steel substrate in the mixture [EMIm]Tf_2N/ 5.5 mol/l $AlCl_3$ at room temperature

The SEM micrograph of an Aluminium layer electroplated on a spring steel substrate from the mixture [EMIm]Tf_2N / 5.5 mol/l $AlCl_3$ at -0.25 mA/cm^2 for 1 hour is shown in Figure 28 (a). Fine crystallites can be seen on the substrate, as shown in the figure. This deposit was obtained after grinding and etching of the substrate in HCl before the electrodeposition. The obtained layer is dark in color due to a high content of iron on the surface. EDX analysis shown in Figure 28 (b) clearly confirms the importance of anodic etching for substrate cleaning.

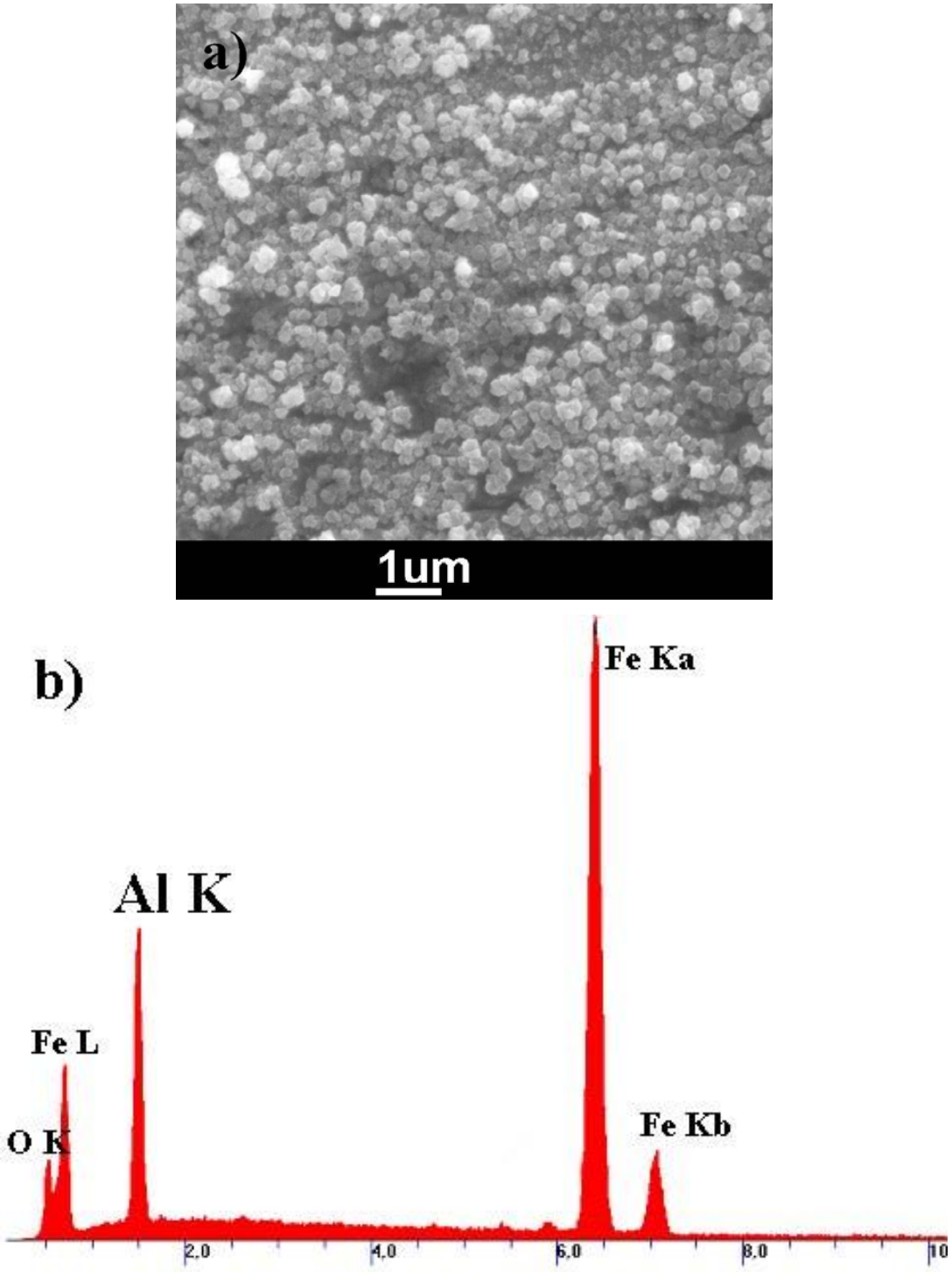

Fig.28: Aluminium layer electrodeposited on spring steel substrate at -0.25 mA/cm^2 for 1 h in [EMIm]Tf_2N / 5.5 mol/l $AlCl_3$ at 25 °C;
(a) SEM micrograph; (b) EDX profile for the area shown in the SEM micrograph.

In order to find the optimal conditions of spring steels covers, electrodepositions were performed galvanostatically at different current densities. Before electrodeposition the sample was treated by grinding, cleaning with isopropanol and anodic etching. If a small current

density is applied, -0.25 mA/cm^2 for 1 hour, the electrode potential is first reduced to -0.7 V and then increased to -0.2 V (Figure 29). The deposited layer looks thick, well-adhering and darker then usual Al coating.

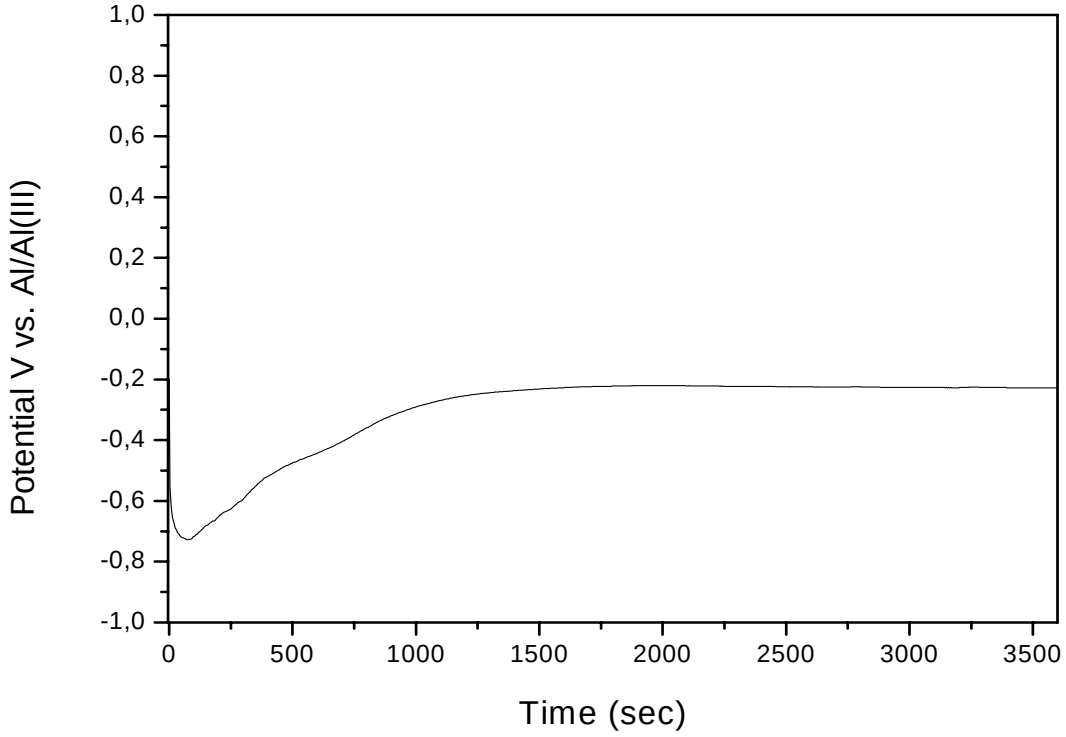

Fig.29: The potential response for chronopotentiometry measurement in [EMIm]Tf_2N/ 5,5 mol/l $AlCl_3$ on spring steel substrate at -0.25 mA/cm^2 at 25°C.

At a higher current densities, -1 mA/cm^2 for 1 hour, generally the same behaviour as in Figure 29 is obtained: first the small reduction of potential at the beginning and following increasing to -0.2 V. Resulted Aluminium layer visually looks thick, well-adhering and dark, similar to layers obtained at -0.25 mA/cm^2.

At a current density of -2.5 mA/cm^2 a well-adhered layer, brighter then before forms. There was not such strong decline of the potential at the beginning of the deposition and potential stayed at -0.2 V during the experiment. The quality of Aluminium coating is still not good enough. It was decided that the bad quality of Aluminium layer occurs due to the low concentration of $AlCl_3$ in the ionic liquid. Aluminium can only be deposited if the concentration is higher than 5.0 mol/l.

Therefore another mixture of [EMIm]Tf_2N and $AlCl_3$ containing 7.0 mol/l $AlCl_3$ was prepared. The deposition was made at the same parameters as for the previous experiments. If a current density of -2.9 mA/cm^2 is applied for 1 hour, the potential decreases a little at the beginning and then keeps at -0.2 V during the deposition. The deposited layer looks dark and

contains dark particles. EDX analysis reveals that there is a lot of iron in the dark areas and black particles are iron alloys. It means that iron, which was removed by anodic etching, can be deposited again. In order to cover this "iron layer" the electrodeposition was performed at -2.9 mA/cm^2 for 3 hours (Figure 30). The change in potential is also similar to the previous experiments.

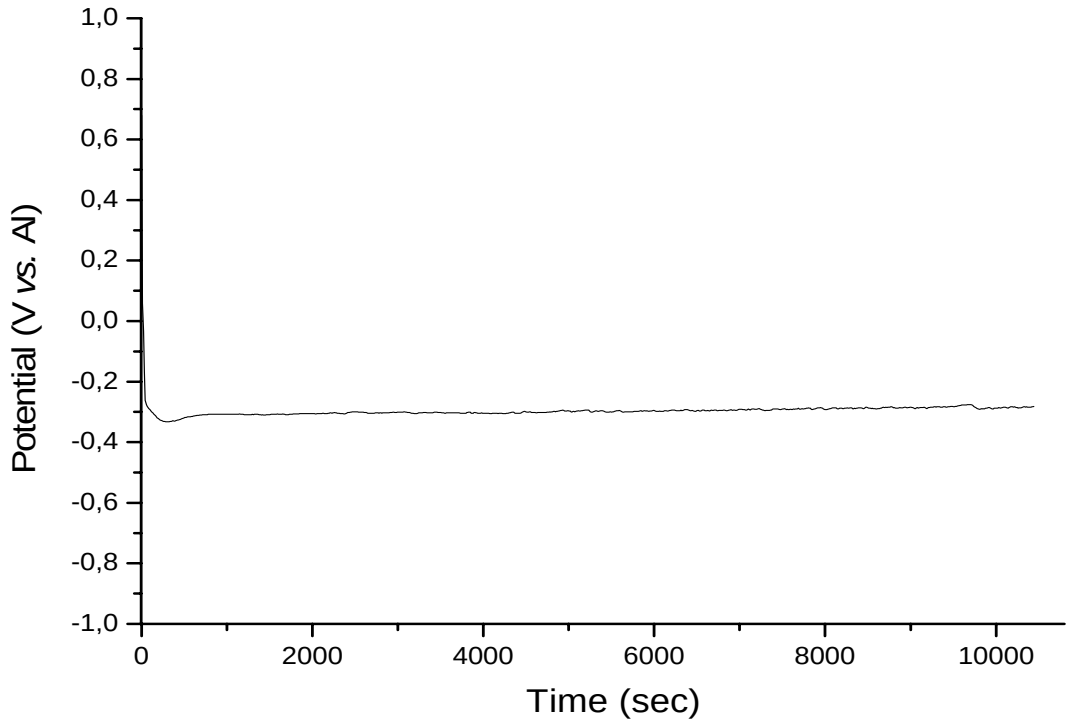

Fig.30: The potential response for chronopotentiometry measurement in [EMIm]Tf_2N/ 7.0 mol/l $AlCl_3$ on spring steel substrate at -2.9 mA/cm^2 for 3 hours at 25°C.

The layer looks much brighter than the previous one, but shows very bad adhesion, especially at the bottom edge. Adhesion of a coating on foreign substrates is very crucial for coating performance. Poor adhesion can be explained as follow. The iron compounds, especially iron oxide, under the Aluminium layer have poor adhesion with the substrate and destroy the adherence of the whole layer.

In order to remove iron compounds the electrolyte before the deposition but after anodic etching was changed. The experiments after one, two and tree hours of deposition show well-adhering, dark coverings. The cross section views of spring steel sheets with these Al coverings are shown in Figure 31.

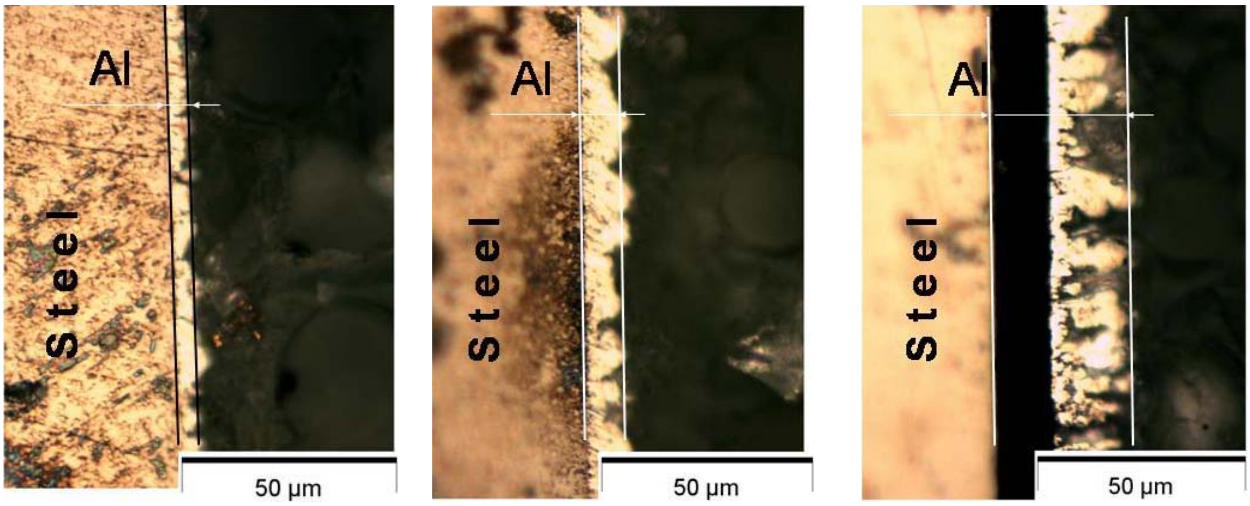

1 hour, 5,8µm **2 hours, 10,3µm** **3 hours, 30,8µm**

Fig.31: Cross section views of spring steel substrates with Al electrodeposits obtained at -2.9 mA/cm^2 in [EMIm]Tf_2N/ 7.0 mol/l $AlCl_3$ at 25 °C

As can be seen in Figure 31, the obtained deposits are irregular. The changing of the etching and deposition parameters does not influence the regularity of the deposit. For example, if the anodic etching at 1.3 mA/cm^2 for 7 minutes and deposition at -3.6 mA/cm^2 for 3 hours are performed, the deposited layer with an average thickness of about 10,8 µm, forms. The coating on the surface is still irregular. It is likely that the impurities presented in the ionic liquid influence the regularity of the deposits.

The microscopic view in Figure 32 (a) shows an Aluminium deposit on a spring steel substrate made after grinding, 5-minute anodic etching at 0.75 mA/cm^2 and 1-hour electrodeposition in the mixture [EMIm]Tf_2N / 5.5 mol/l $AlCl_3$ at -2.5 mA/cm^2. The obtained deposit contains crystallites with the grain sizes in the micrometer regime.

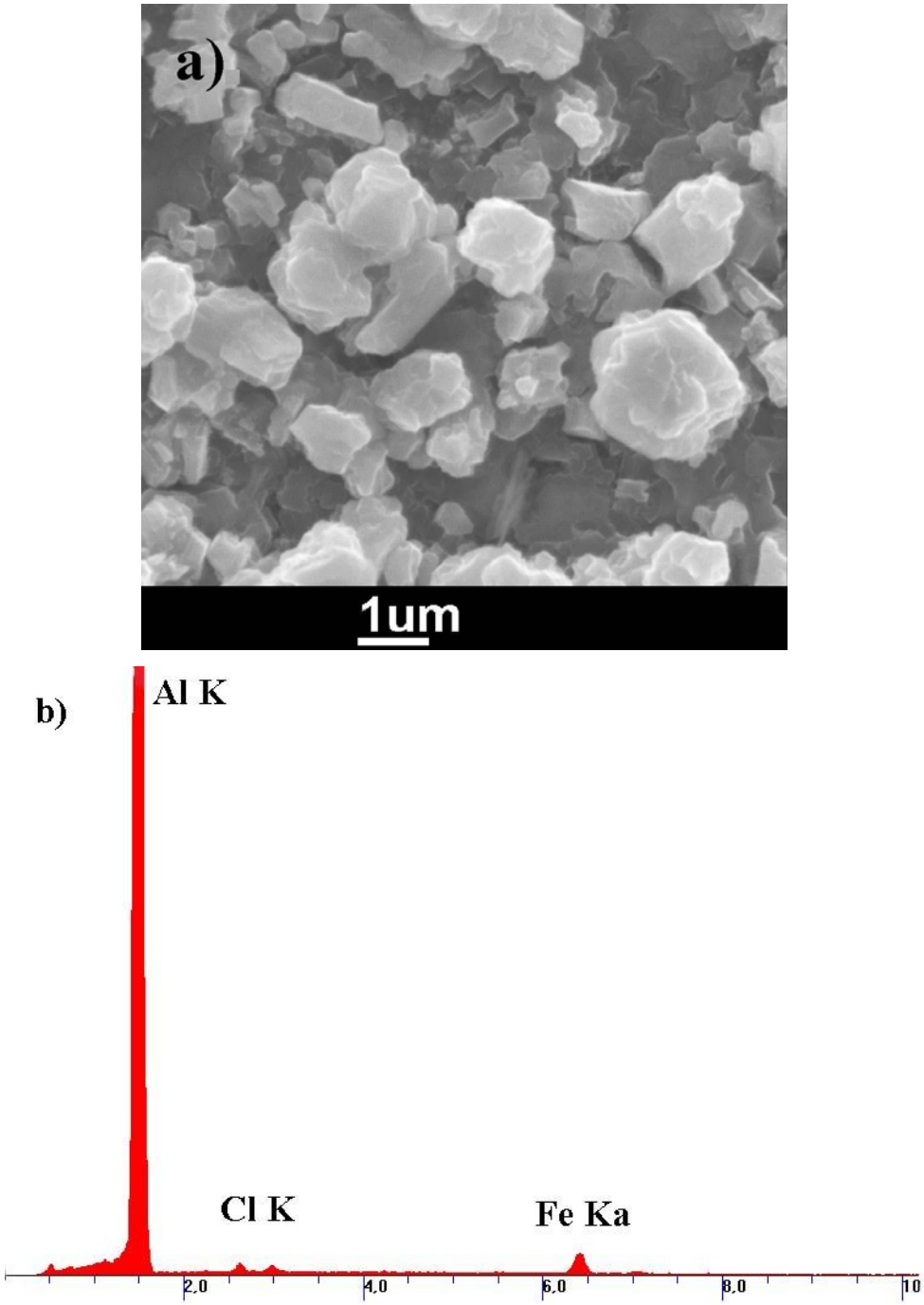

Fig.32: Aluminium layer electrodeposited on spring steel substrate at -2.5 mA/cm^2 for 1 h in [EMIm]Tf_2N / 5.5 mol/l $AlCl_3$ at 25 °C;
(a) SEM micrograph; (b) EDX profile for the area shown in the SEM micrograph.

The EDX profile in Figure 32 (b) confirms the importance of anodic etching and shows generally only Aluminium in this area.

5.2.3 Electrodeposition of Al in [EMIm]Cl/$AlCl_3$

In order to find an alternative to [EMIm]Tf_2N for Aluminium electrodeposition on spring steel, [EMIm]Cl was used. This ionic liquid has two advantages in comparison with [EMIm]Tf_2N: it is cheaper and easier to prepare. Figure 33 shows the typical cyclic voltammogram recorded on spring steel substrate in the mixture [EMIm]Cl/$AlCl_3$ at room temperature. Aluminium electrodeposition starts at about -0.15 V-. A clear nucleation loop was observed in the backward scan. The electrodeposition of Aluminium is totally reversible with a stripping peak centered at around 0.4 V and a tail on its positive side. The stripping of Aluminium takes place over a relatively broad potential range, which might originate from a certain surface alloying between Aluminium and iron.

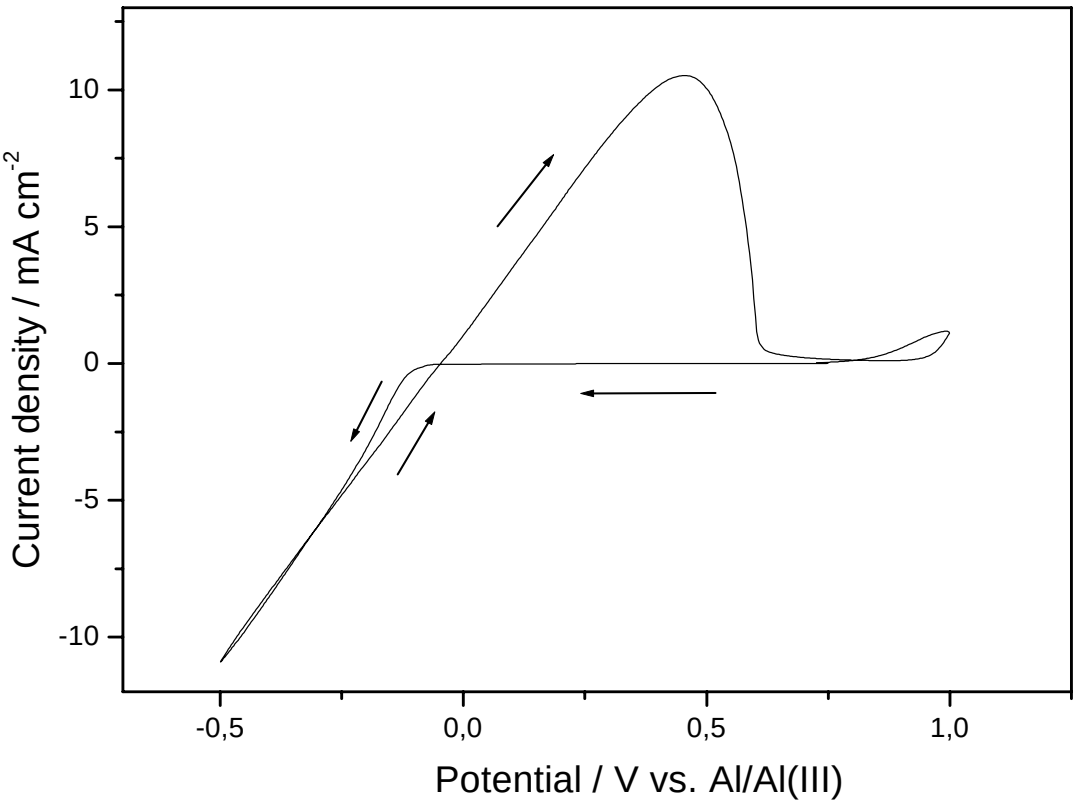

Fig.33: Typical cyclic voltammogram recorded on spring steel substrate in the mixture [EMIm]Cl/$AlCl_3$ at room temperature, 10 mV/s

Oxidation peak appeared at 1 V due to substrate dissolution that can be used for anodic etching to remove thin iron oxide layer which forms after the pre-treatment step.

In order to investigate the influence of current density on Aluminium deposits, a sequence of samples at varying current density from -1.5 mA/cm^2 to -4.3 mA/cm^2 were made

on the spring steel substrates. As is shown below, microcrystalline Aluminium is obtained in all classes.

First the deposit was prepared galvanostatically at a current density of -1.5 mA/cm^2 for one hour. The deposited layer looks shiny and shows poor adhesion. Aluminium layer was almost completely removed by post-treatment. In order to improve the quality of coating the current density was increased to -3.1 mA/cm^2. At higher current density, -4.3 mA/cm^2, the deposit contains black particles on the surface. It is iron oxide, which was removed by the anodic etching and formed again during the deposition step due to iron and Aluminium codeposition. The EDX analysis shows that the black layer consists mostly of iron. In order to cover such steel pieces, 3-hour deposition was made (Figure 34).

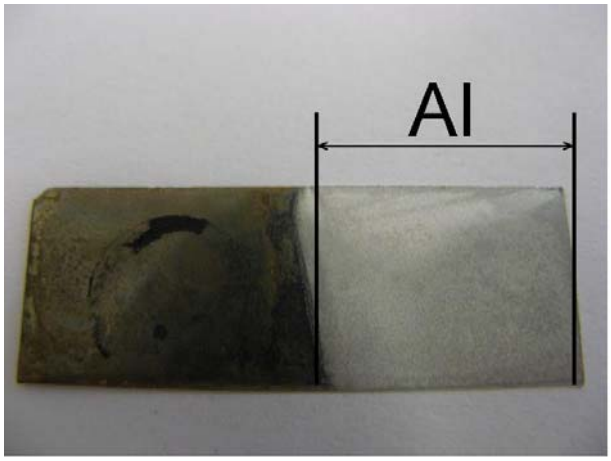

Fig.34: The photograph of the spring steel substrate with Al electrodeposit made in [EMIm]Cl/ $AlCl_3$ at -4.3 mA/cm^2 for 3 hours at 25 °C.

The adhesion of Al coating is not the same at the different parts of the substrate and becomes worse at the bottom edge of the sample (right edge in the picture). It can be explained by the fact that this place is difficult to grind or because of "redeposition" of etched oxide layer, which was subsequently covered by Al. Figure 35 shows EDX-spectrum and SEM-picture of this sample.

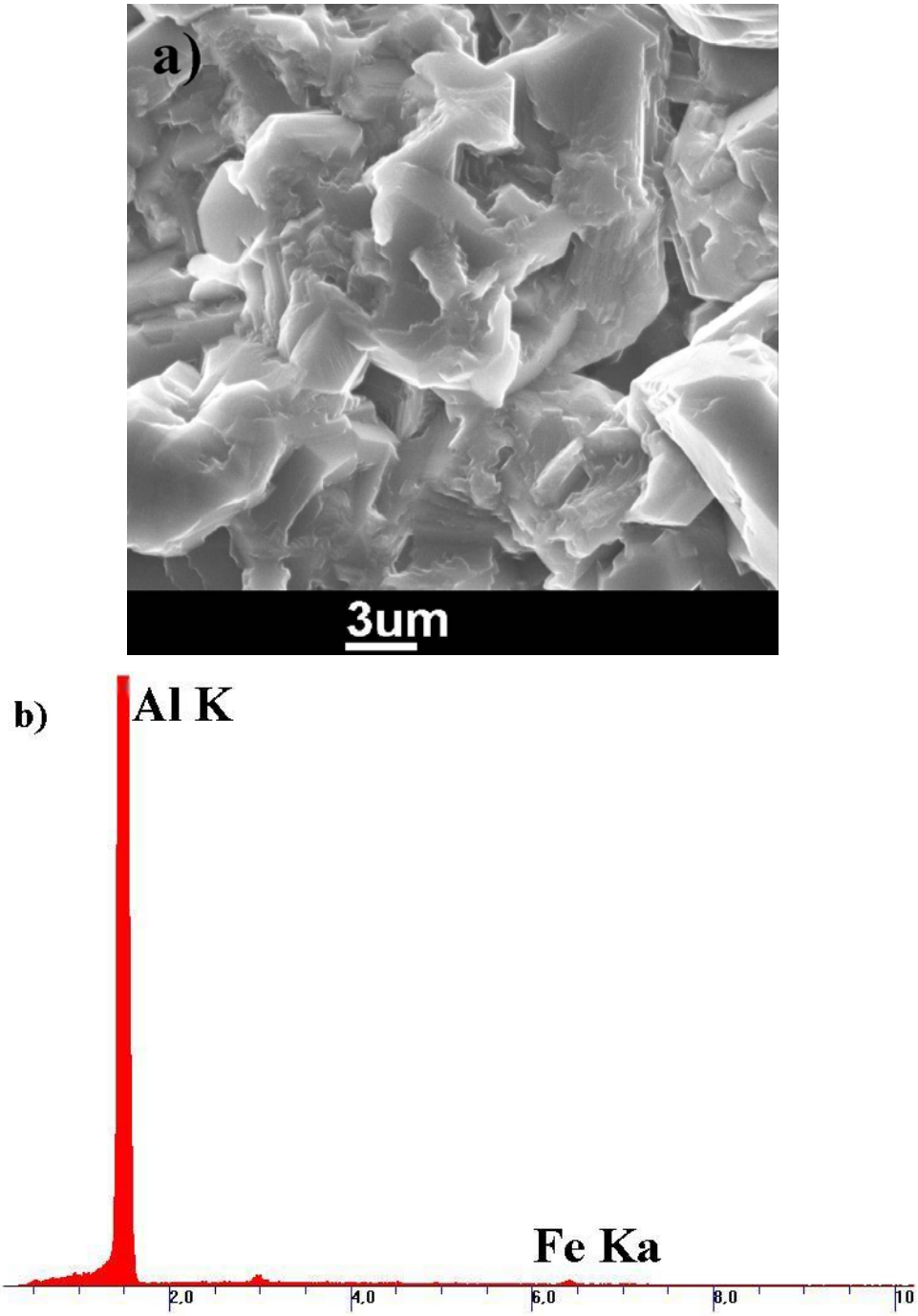

Fig.35: Aluminium deposit made on spring steel substrate at -4.3 mA/cm^2 for 3 h in [EMIm]Cl / $AlCl_3$ at 25 °C;
(a) SEM micrograph; (b) EDX profile for the area shown in the SEM micrograph.

SEM micrograph (Figure 35 (a)) shows the microcrystalline deposit. The layer seems to be porous. EDX profile contains mostly Aluminium on the surface. It proves that the iron-compounds deposited first and then are covered by Aluminium.

In order to investigate the influence of deposition time on the thickness of Aluminium deposits, the time of the deposition was varied from 1 to 3 hours. Figure 36 shows cross section views of three deposits obtained at -3.1 mA/cm^2 for 1, 2 and 3 hours, respectively.

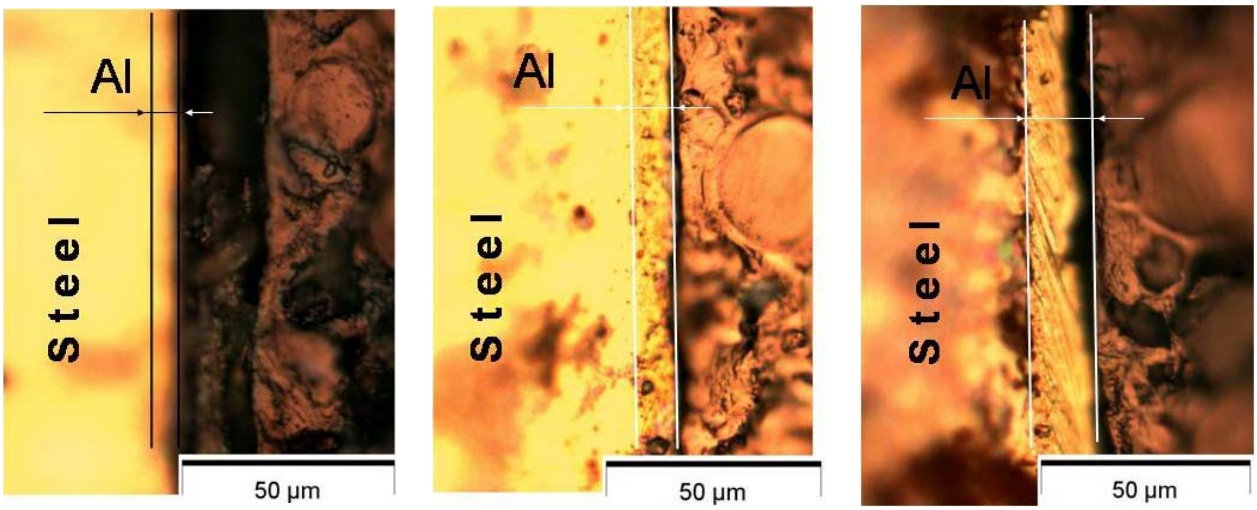

1 hour, 5,7µm **2 hours, 10,3µm** **3 hours, 17,3µm**

Fig.36: Cross section views of spring steel substrates with Al electrodeposits obtained at 25°C in [EMIm]Cl/$AlCl_3$ at -3.1 mA/cm^2 for (a) 1 hour, (b) 2 hours, (c) 3 hours.

The thicknesses of the Aluminium coating are 5.7 µm, 10.3 µm and 17.3 µm for 1, 2 and 3 hours of the electrodeposition, respectively. The thickness of the coatings after 1 and 2 hours of the deposition is the same as for the coatings obtained at the same conditions in [EMIm]Tf_2N/$AlCl_3$. The Aluminium layer obtained after 3 hours of the electrodeposition in [EMIm]Tf_2N/$AlCl_3$ is thicker than the deposit made in [EMIm]Cl/$AlCl_3$, but also looks more porous (Figure 31).

Figure 37 shows the cross section view of the Aluminium electrodeposit obtained on spring steel substrate in the mixture [EMIm]Cl/$AlCl_3$ at room temperature with electrolyte changing between anodic etching and electrodeposition. The anodic etching at 1.4 mA and electrochemical deposition at –3.6 mA/cm^2 for 3 hours were carried out.

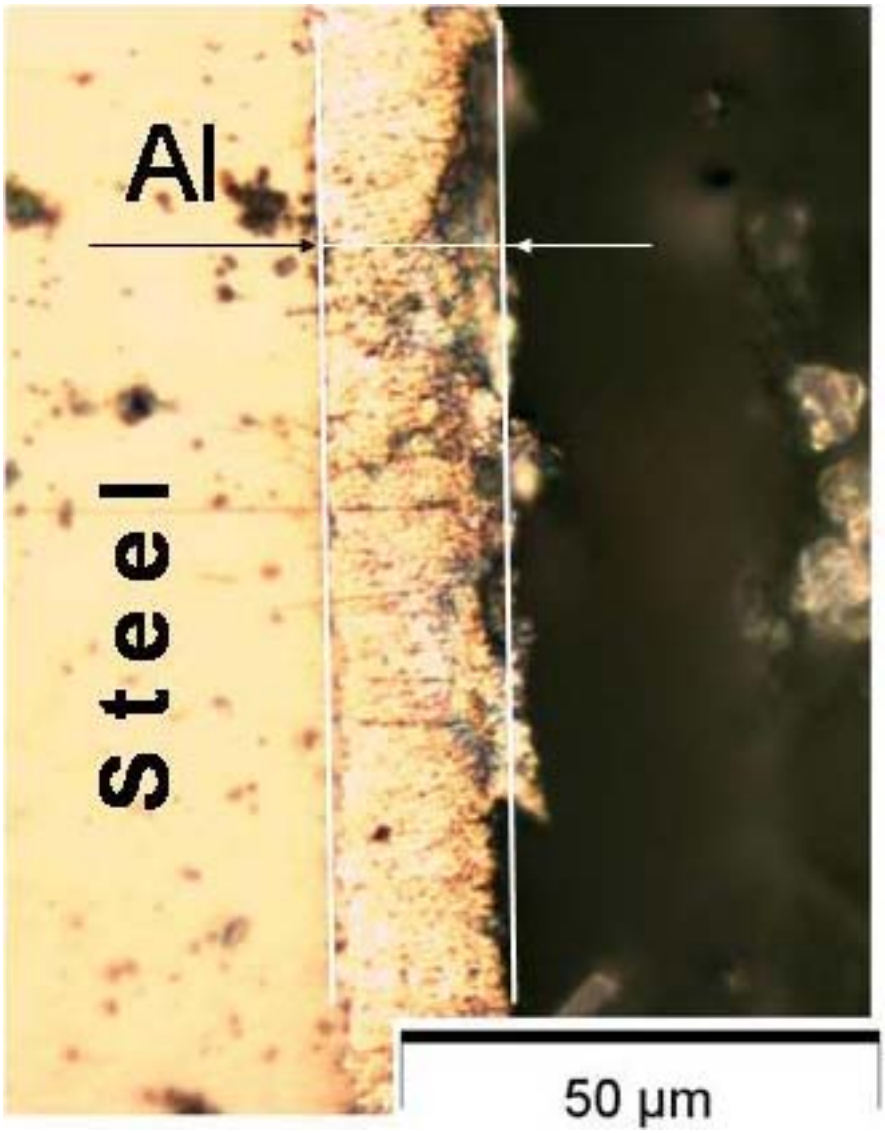

Fig.37: Cross section views of spring steel substrates with Al electrodeposit obtained at 25°C in [EMIm]Cl/$AlCl_3$ at -3.6 mA/cm^2 for 3 hours. The electrolyte has been changed prior the deposition step.

The deposited layer looks bright, without black particle and shows good adhesion. The coating also has different thickness depending on the side of the sample. The average thickness of the deposited layer is 17.6 µm, maximum value is 25.1 µm and minimum is 6.7 µm. The difference in average thickness must be cleared by the difference in current density, when the substrate is not situated in the middle of the beaker.

The Aluminium deposit made at the similar conditions but without electrolyte changing prior the deposition step is shown in Figure 36 (c). Average thickness of this coating is 17.3 µm. From the light of these results it might be concluded that the quality of the Aluminium deposit can be significantly improved when the anodic etching is applied to remove the existing oxide layer and the electrolyte for the electrodeposition is changed prior

to the deposition step. In this case the deposits do not contain black particles, however the cross section view shows that the coatings are more irregular.

The thickness required for electroplating is usually 10 μm that can be perfectly obtained after 2-hour electrodeposition. Optimal electrochemical parameters for well-adhering, shiny covering are 7-minut anodic etching for removing the oxide layer from the surface and galvanostatically Aluminium deposition at -3.5 mA/cm^2. It is necessary to change the electrolyte before the electrodeposition, because after anodic etching the electrolyte contains impurities, which were removed from the surface of the substrate. Otherwise they can be codeposited with Aluminium affecting the adhesion or enhancing the corrosion.

5.2.4 Summary and discussion

It was shown that spring steel substrates can be electroplated with Aluminium. Aluminium can be electrodeposited on spring steel substrates from Aluminium chloride in two ionic liquids, namely, upper phase of 1-ethyl-3-methylimidazolium bis(trifluoromethylsulfonyl)amide, [EMIm]Tf_2N, and 1-ethyl-3-methylimidazolium chloride, [EMIm]Cl. The Aluminium deposits were analyzed by high resolution field-emission scanning electron microscope (SEM) and energy dispersive (EDX) X-ray analysis.

The pre-treatment of the spring steel substrates plays an important role in the coating adhesion. Before the electrodeposition, the substrates were grinded with emery paper SiC 800 and anodically etched in the employed electrolyte at +1.0 V vs. Al/Al(III) for 7 minutes to remove the oxide layer. Aluminium deposit of more than 10 μm thick can be made galvanostatically on spring steel substrate in the upper phase of [EMIm]$Tf_2N/AlCl_3$(5.5 M) and in [EMIm]$Cl/AlCl_3$ solutions. It was found that iron removed by anodic etching can be re-deposited again simultaneously with Aluminium during electrodeposition resulting in black particles of iron in the deposit that influenced the quality of the coating. The iron content is strongly decreased by changing of the electrolyte prior to the electrodeposition. In the case of [EMIm]$Cl/AlCl_3$, the iron content in the deposit is lower than in the case of [EMIm]$Tf_2N/AlCl_3$. Aluminium coatings of better qualities are obtained in [EMIm]$Cl/AlCl_3$ comparing with the upper phase of [EMIm]$Tf_2N/AlCl_3$.

For more adhesive Aluminium layer, other surface pre-treatment that allows complete removal of oxide layer from the substrate is required. As an alternative to anodic etching, literature showed that it is possible to remove the native oxide layer in only a few minutes using plasma etching **[189]**.

5.3 Electrodeposition of Micro- and Subsequently Nano- Crystalline Aluminium on Spring Steel

Nanocrystalline metals show often better corrosion resistance as microcrystalline **[65].** However nanocrystalline layer is usually very thin and can be easily destroyed with mechanical attack. To achieve higher thickness of the covering microcrystalline Aluminium was electrodeposited on spring steel substrate following by the electrodeposition of nanocrystalline Aluminium. The coverings were studied using SEM, EDX and XRD.

In order to obtain the spring steel substrate covered by a layer of nanocrystalline Aluminium, which, in one's turn, is deposited on the microcrystalline Aluminium film, the following experiment was performed. Grinded spring steel substrate was immersed into the electrolyte (upper phase of [BMP]Tf_2N / 1.7 mol/l $AlCl_3$) at 90°C The cyclic voltammogram of the upper phase of [BMP]Tf_2N / 1.7 mol/l $AlCl_3$ on spring steel at 90°C is presented in Figure 38. The electrode potential was scanned from the open circuit potential in the negative direction at a scan rate of 10 mV/s. As can be seen, a rising cathodic current corresponding to the bulk Al deposition occurs at about -0.6 V. In the reverse scan an oxidation peak at +0.2 V is attributed to the stripping of Al. Irreversible deposition is characteristic for many of the pyrrolidinium-based ionic liquids, according to adsorption of pyrrolydinium-cation to the substrate surface (Chapter 2.1.7).

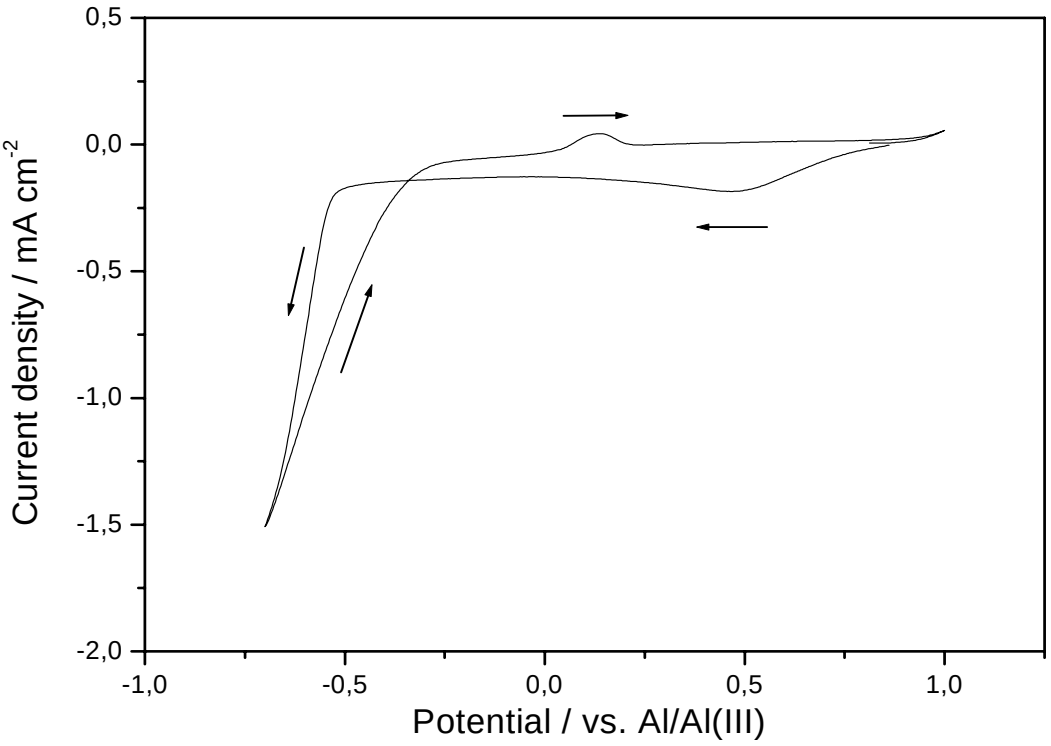

Fig.38: Cyclic voltammogram recorded on spring steel substrate in the mixture [BMP]$Tf_2N/AlCl_3$ at 90°C. Scan rate is 10 mV/s.

In order to obtain a well-adherent Aluminium electrodeposit an anodic etching was carried out for 7 minutes before the electrodeposition at a current density of -0.3 mA/cm^2 for 2 hours was performed. Visually, the deposit appears to be thick, yellow in colour and well-adhering to the steel substrate. The obtained deposit was investigated with a high resolution field-emission scanning electron microscope (SEM) (Figure 39).

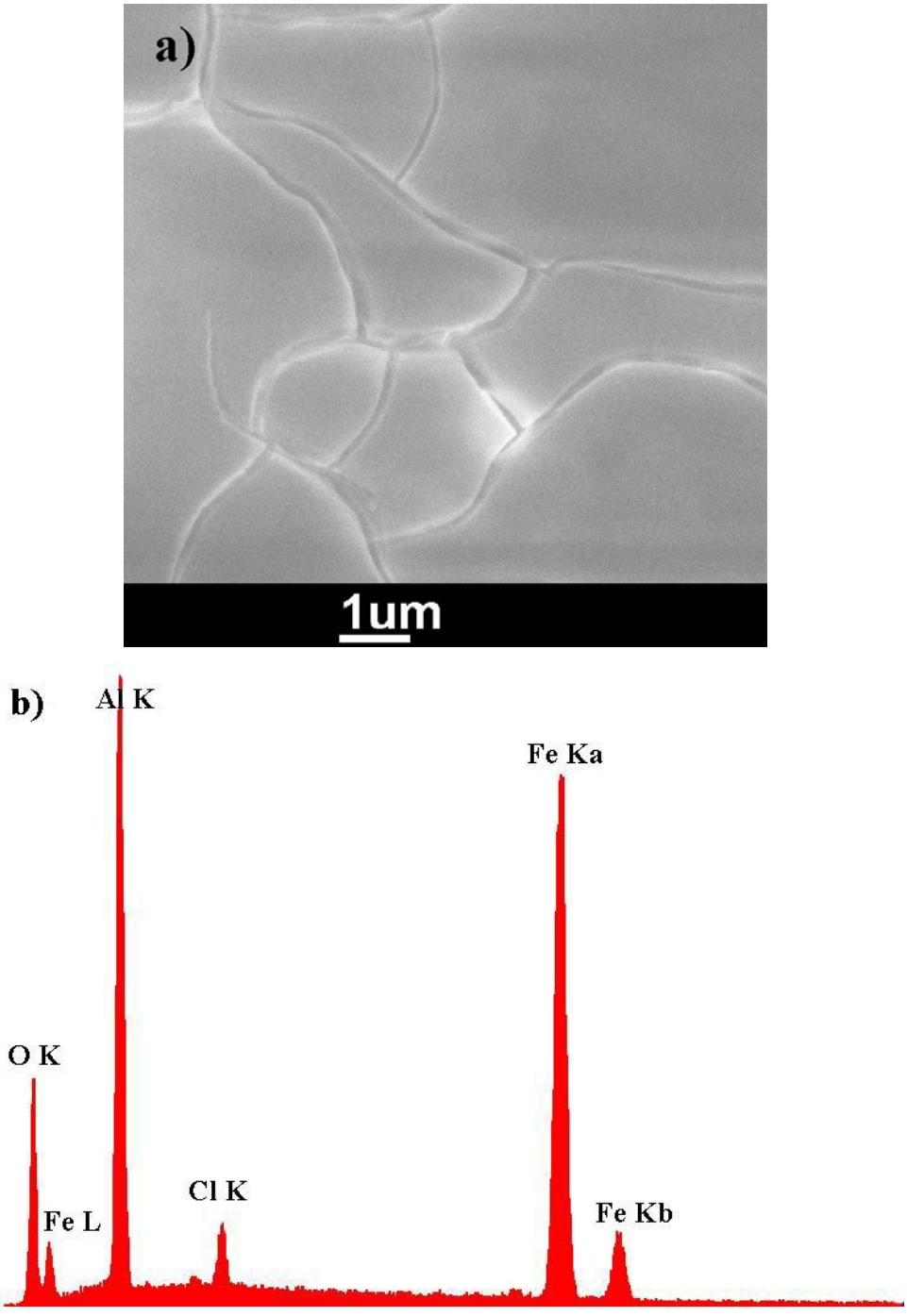

Fig.39: Aluminium deposit made on spring steel substrate at -0.3 mA/cm^2 for 2 h in [BMP]Tf_2N / $AlCl_3$ at 90 °C;
(a) SEM micrograph; (b) EDX profile of the area shown in the SEM micrograph.

There are a lot of black particles on the surface of the deposit, which are iron oxide that was removed by the anodic etching and formed again during the deposition step due to iron and Aluminium codeposition. It happens when the anodic etching and the electrodeposition are performed from the same electrolyte. EDX analysis of the surface gives both Aluminium and iron. Unfortunately, the resolution of the microscope does not allow recognising the nanocharacter of grains.

Figure 40 shows the SEM micrographs and EDX pattern of Aluminium layer made in the following way: After 7-minuts anodic etching, the grinded sample was covered by microcrystalline Al at -4.5 mA/cm^2 for 1 hour in [EMIm]Cl/$AlCl_3$ at 25 °C and then by nanocrystalline Al at -0,2 mA/cm^2 for 1 hour in [BMP]Tf_2N/$AlCl_3$ at 90 °C. Visually, the obtained deposit has yellow colour. As can be seen from Figure 40 (a) Aluminium deposition occurs on the traces of grinding. Such phenomenon was not found for the deposition of microcrystalline Aluminium. It points to the probable dissolution of microcrystalline Al layer by nanocrystalline Al deposition.

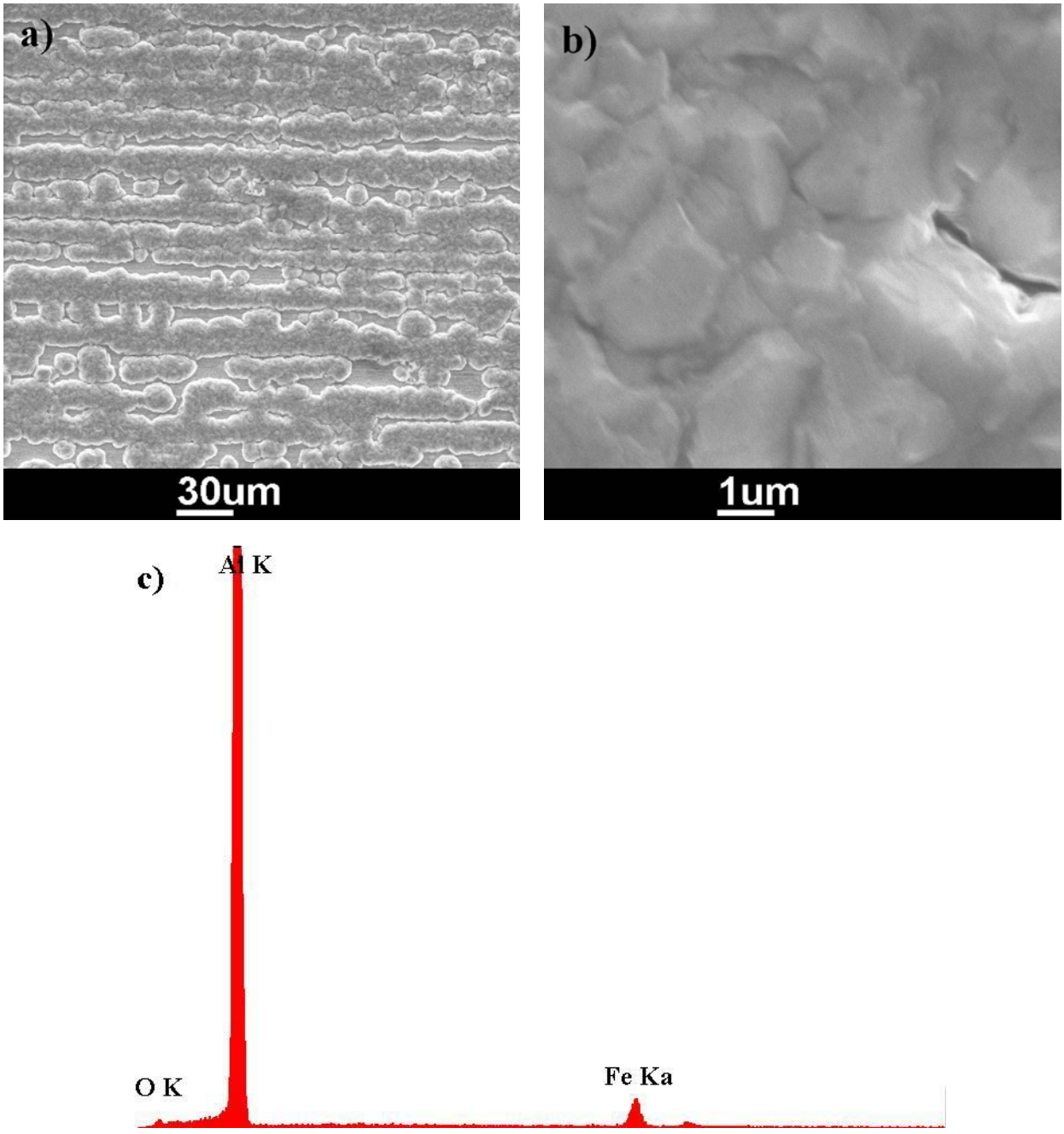

Fig.40: Aluminium deposit made on spring steel substrate by two-step deposition: first at -4.5 mA/cm^2 for 1 h in [EMIm]Cl / $AlCl_3$ at 25 °C and then at -0.2 mA/cm^2 for 1 hour in [BMP]Tf_2N/$AlCl_3$ at 90°C.
(a), (b) SEM micrographs; (c) EDX profile for the area shown in the SEM micrograph.

Attempts were made to polish one side of the sample and see the difference in adhesion (Figure 42). Some cracks and clusters without microcrystalline Aluminium were found on the surface by the simple analysis of the sample. Probably the nanocrystalline Aluminium deposition takes place at the dissolution of the microcrystalline Aluminium layer. The microcrystalline Aluminium deposition time was increased to check the nature of the

process (Figure 41). The deposition was performed at similar conditions, except microcrystalline deposition that was made for 2 hours.

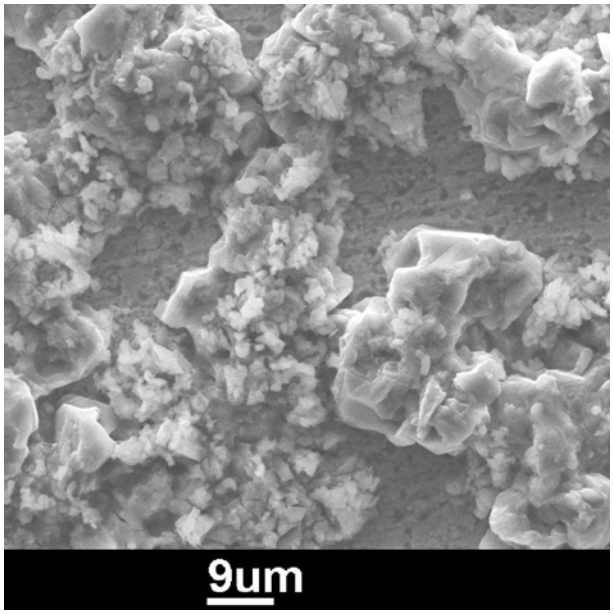

Fig.41: SEM image of Aluminium deposit made on spring steel substrate by two-step deposition: first at -3.0 mA/cm^2 for 2 h in [EMIm]Cl / $AlCl_3$ at 25 °C and then at -0.13 mA/cm^2 for 1 hour in [BMP]Tf_2N/$AlCl_3$ at 90°

There are still some cracks in the microaluminium layer. The color of the deposit becomes silverish. The SEM micrograph in figure 42 shows the Aluminium crystals and surface of the spring steel substrate.

In order to check the influence of surface morphology on two-step Aluminium deposition one side of the grinded spring steel substrate was polished. After cleaning the sample was immersed into the electrolyte [EMIm]Cl / $AlCl_3$ at room temperature. After making of 7-minute anodic etching, the electrolyte was changed with a new one and the electrodeposition was performed at -4.0 mA/cm^2 for 1 hour (Figure 42). So the microcrystalline Aluminium was deposited. Subsequently, to deposit nanocrystalline Aluminium, the sample was immersed into the upper phase of [BMP]Tf_2N / 1.7 mol/L $AlCl_3$ and the deposition was performed at -0.13 mA/cm^2 for 1 hour at 90 °C.

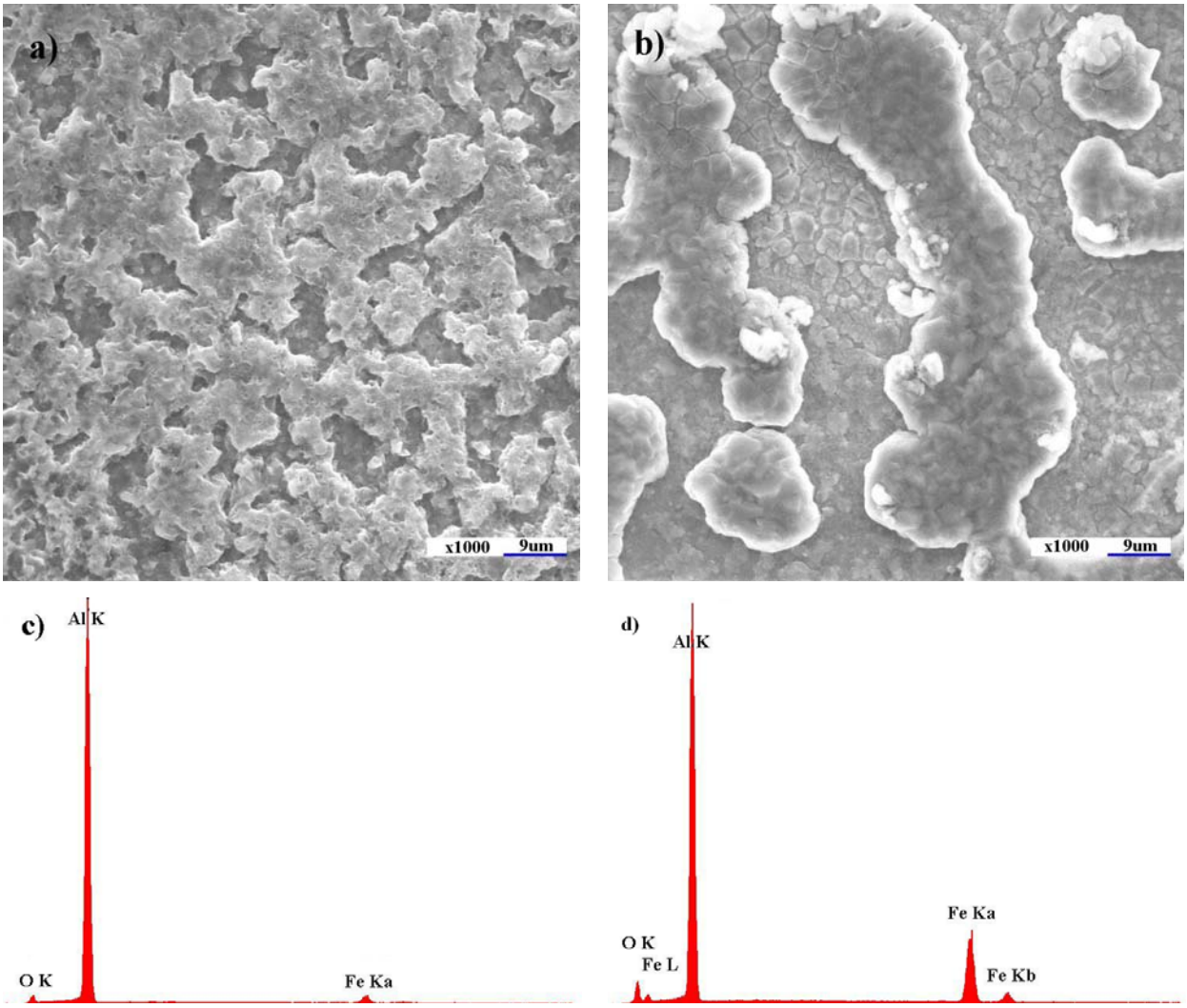

Fig.42: SEM images of Aluminium deposit made on spring steel substrate by two-step deposition: first at -4.0 mA/cm^2 for 1 h in [EMIm]Cl / $AlCl_3$ at 25 °C and then at -0.13 mA/cm^2 for 1 hour in [BMP]Tf_2N/$AlCl_3$ at 90°
(a) SEM micrograph of the deposit made on the grinded side of the sample;
(b) SEM micrograph of the deposit made on the polished side of the sample;
(c) EDX profile of the deposit made on the grinded side of the sample;
(d) EDX profile of the deposit made on the polished side of the sample.

Deposited microcrystalline Aluminium layer is very thin and the spring steel surface can be seen through the deposit. The time of microaluminium electrodeposition was increased and a couple of experiments were made under similar conditions.

The SEM micrographs and EDX analyses show no difference by 2-hour microcrystalline Aluminium deposition case for the layers deposited on the grinded and on the polished sides of the sample. The SEM micrograph in Figure 43 shows the deposit obtained on the polished side of the sample. EDX analyses were made at two points of deeper area of the sample with different contrasts.

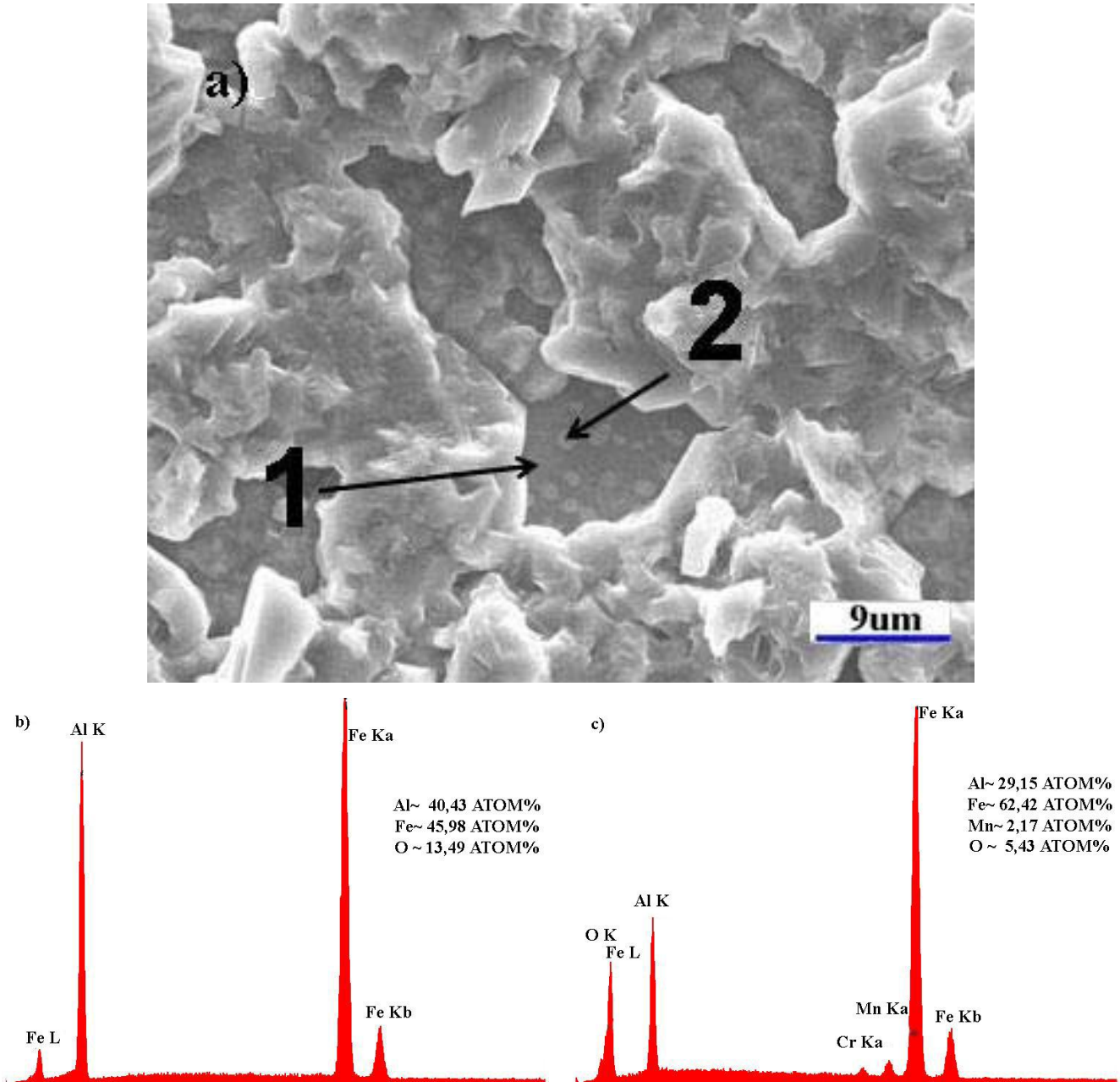

Fig.43: (a) SEM micrograph of Aluminium layer deposited on the polished side of the spring steel substrate by two-step deposition: first at -3.0 mA/cm^2 for 2 h in [EMIm]Cl / $AlCl_3$ at 25 °C and then at -0.13 mA/cm^2 for 1 hour in [BMP]Tf_2N/$AlCl_3$ at 90°;
(b) EDX profile of Aluminium layer made in point 1 in Fig. 43(a)
(c) EDX profile of Aluminium layer made in point 2 in Fig. 43(a).

The EDX analyses in two different points show that there is more Aluminium in the first point (Figure 43). EDX analysis revealed that the sample at point 2 could be the particle of the alloy, which was in the electrolyte and deposited together with Aluminium.

Figure 44 shows the SEM micrographs of Aluminium elecrodeposit made on spring steel substrate by two-step deposition: first at -3.0 mA/cm^2 for 1 h in [EMIm]Cl / $AlCl_3$ at 25 °C and then at -0.13 mA/cm^2 for 1 hour in [BMP]Tf_2N/$AlCl_3$ at 90

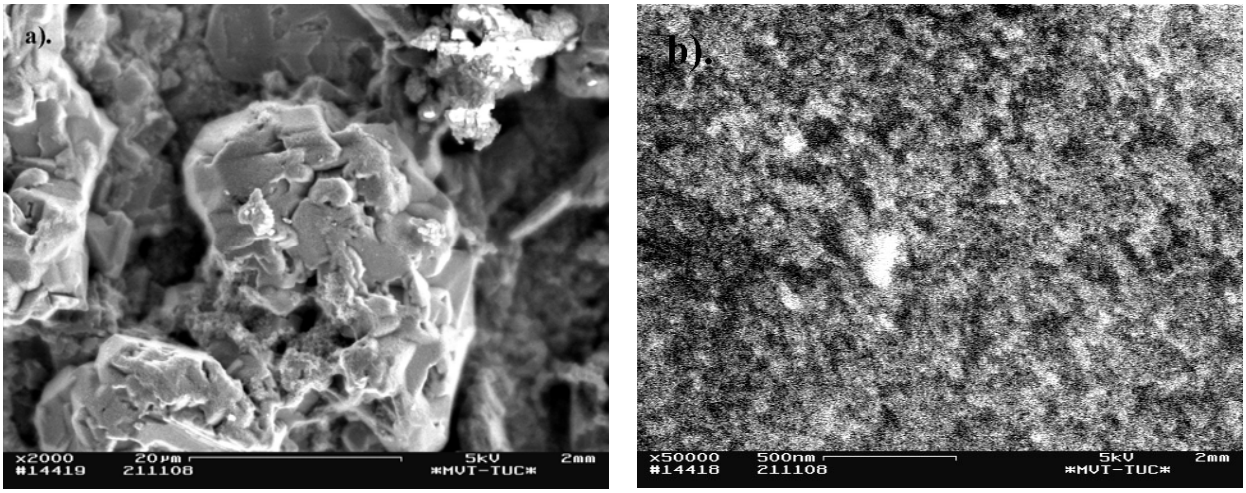

Fig.44: SEM micrographs of Aluminium layer deposited on spring steel substrate by two-step deposition: first at -3.0 mA/cm^2 for 1 h in [EMIm]Cl / $AlCl_3$ at 25 °C and then at -0.13 mA/cm^2 for 1 hour in [BMP]Tf_2N/$AlCl_3$ at 90°.
(a) SEM image at x2000; (b) SEM image at x50000

The micrograph in Figure 44(a) shows like in Figure 46 the spring steel samples covered with microcrystalline Aluminium. By the increasing of the magnification (Figure 44 (b)) the nanostructure of covering can be clearly seen. Generally, the electrodeposited layer contains very fine crystallites in the nanometer regime.

To evaluate the grain size of the deposited Aluminium, X-ray diffraction (XRD) measurements were made. Figure 45 shows the XRD pattern of Aluminium film obtained galvanostatically on spring steel substrate in [EMIm]Cl/$AlCl_3$ at room temperature after 1-hour deposition at a current density of -4.5 mA/cm^2 and subsequently in [BMP]Tf_2N/$AlCl_3$ at 90°C after 1-hour deposition at -0.2 mA/cm^2. The peaks are broad, indicating the small size of the electrodeposited Aluminium. The average grain sizes of Aluminium are 28.2 nm, determined from the full width at half maximum of the 100% peak using the Scherrer equation. This average grain size is quite similar to the grain size of 34 nm obtained for Aluminium electrodeposited in [BMP]Tf_2N/$AlCl_3$ at 100 °C **[65]**.

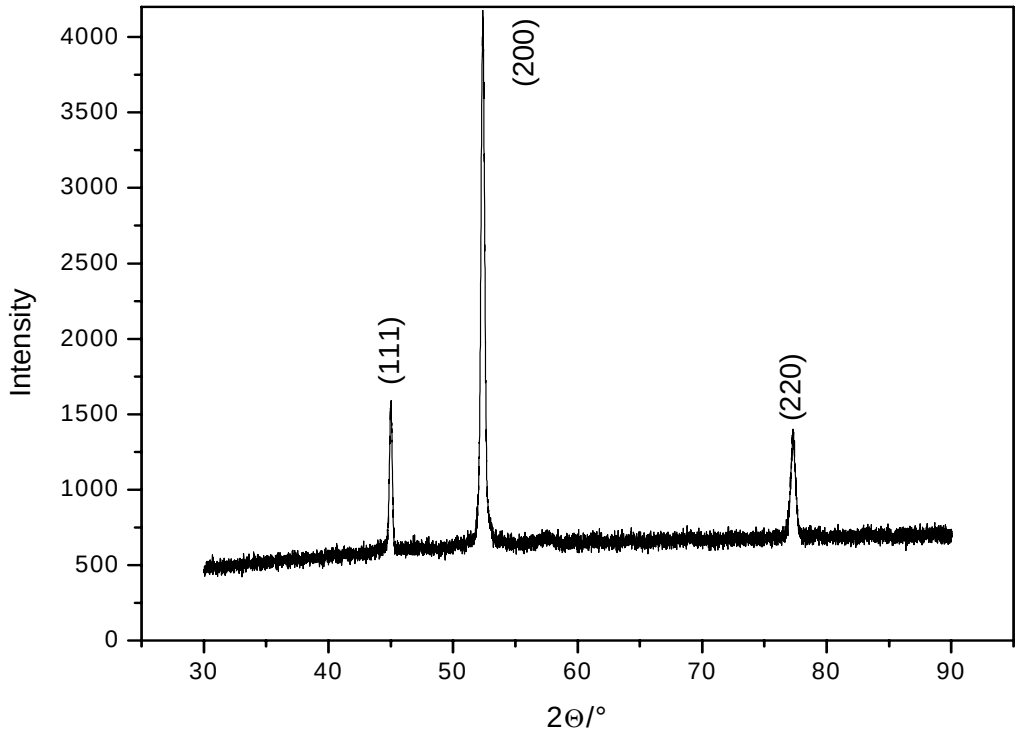

Fig.45: XRD pattern of Aluminium deposited on spring steel substrate by two-step deposition: first at -4.5 mA/cm^2 for 1 h in [EMIm]Cl / $AlCl_3$ at 25 °C and then at -0.2 mA/cm^2 for 1 hour in [BMP]Tf_2N/$AlCl_3$ at 90°.

In order to establish the difference in average grain sizes between grinded and polished sample XRD measurements were made. Aluminium layer has been made on spring steel substrate by two-step deposition: first at -3.0 mA/cm^2 for 2 h in [EMIm]Cl / $AlCl_3$ at 25 °C and second at -0.13 mA/cm^2 for 1 hour in [BMP]Tf_2N/$AlCl_3$ at 90°. One side of this sample was subsequently polished after grinding before the deposition. The average grain size

of Aluminium layer electrodeposited on the grinded and on the polished sides of the sample are 29.1 nm and 29.2 nm, respectively. Thus, this measurement shows that there is no difference in the grain size of Aluminium layer electrodeposited on the grinded and on the polished side of the sample. The measurement also confirms the value of average grain size, which is about 30 nm.

It is also quite interesting to determine the grain size of microcrystalline Aluminium electrodeposit. For this purpose one side of the spring steel substrate was polished after grinding. Electrodeposition was performed on this substrate in the mixture [EMIm]Cl/$AlCl_3$ at room temperature at a current density of -3.5 mA/cm^2 for 2 hours. The average grain size of Aluminium deposits made on the grinded and on the polished sides of the sample are 31.8 nm and 37.8 nm, respectively. These values are also lying in the nanometre scale at about 30 nm. In is quite interesting that the average grain size of Aluminium electrodeposit for all samples is of about 30 nm.

Figure 46 and Figure 47 show high resolution SEM micrographs of microcrystalline Aluminium deposited on spring steel substrate in the mixture [EMIm]Cl/$AlCl_3$ at room temperature at -3.5 mA/cm^2 for 2 hours.

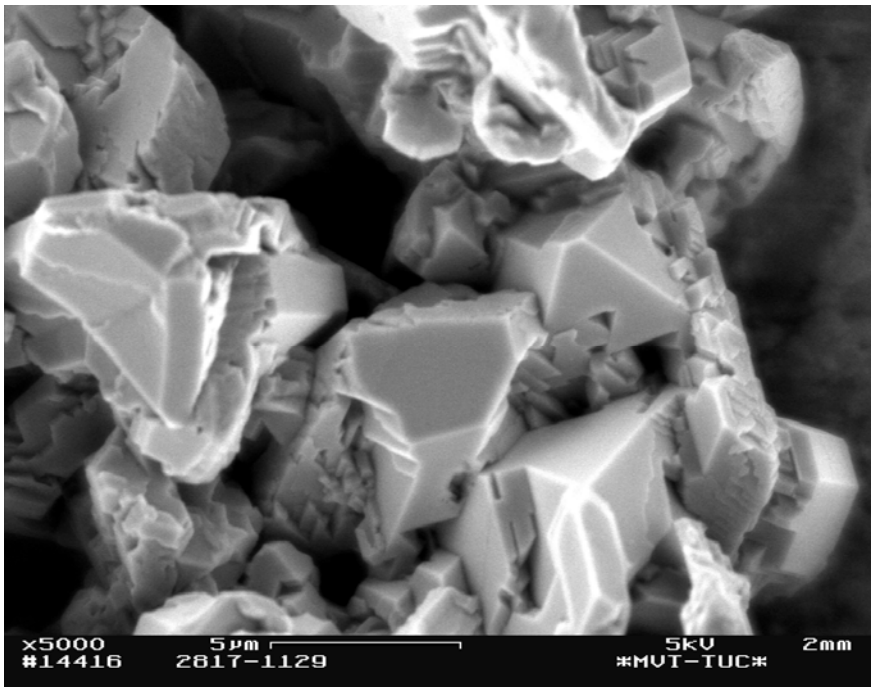

Fig.46: SEM micrograph of Aluminium deposit made on spring steel substrate at -3.5 mA/cm^2 for 2 hours in [EMIm]Cl / $AlCl_3$ at 25 °C.

The microcrystalline Aluminium grains can be clearly seen. Figure 47 shows another place of the deposit.

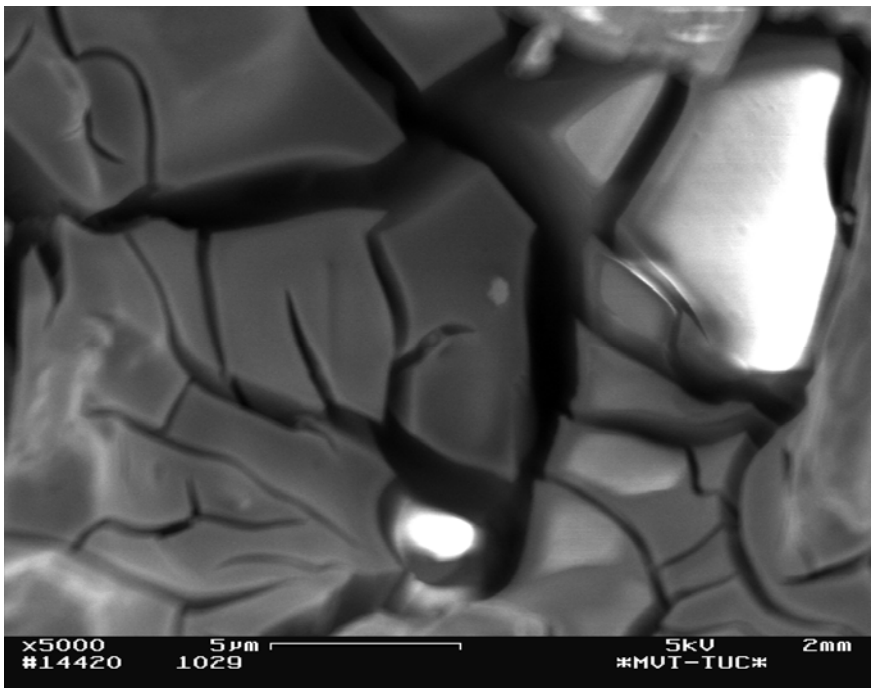

Fig.47: SEM image of Aluminium deposit made on spring steel substrate at -3.5 mA/cm^2 for 2 hours in [EMIm]Cl / $AlCl_3$ at 25 °C.

There are a lot of cracks together with Aluminium grains. It points at internal stresses in the coated layer, **due to them the XRD-results look the same**. During the

electrodeposition of metals or alloys, internal or residual stress almost always appears. The stress can originate from intrinsic film stress and from interfacial stress between the deposit and the substrate. Generally, this may be attributed to a number of factors, such as coalescence of the crystallites, inclusion of foreign species or generation of structural defects **[190]**.

5.3.1 Summary and discussion

It shown that nanocrystalline Aluminium can be electrodeposited on spring steel plates covered by microcrystalline Aluminium. To get such a coating the spring steel substrate was first electroplated with the microcrystalline Aluminium followed by the electroplating with the nanocrystalline Aluminium. The microcrystalline Aluminium was electrodeposited galvanostatically on spring steel substrate in [EMIm]Cl/$AlCl_3$ at room temperature for 2-hours at a current density of -4.5 mA/cm^2. Then the nanocrystalline Aluminium was deposited galvanostatically in [BMP]Tf_2N/$AlCl_3$ at 90°C for 1-hour at -0.2 mA/cm^2. The deposits were studied by SEM, EDX and X-ray diffraction (XRD). Internal stresses appear during the electrodeposition and XRD measurements always show the average grain size of deposited Al about 35 nm.

6 Conclusions

The present thesis shows that room temperature air- and water stable ionic liquids are well suited for the electrochemical deposition of Aluminium. It can not be mentioned that the quality of the deposits depends on the chain length of ionic liquid cation applied as a solvent media for the electrodeposition. To study the influence of the chain length of ionic liquid cation on the grain size of the deposited Aluminium four ionic liquids, namely, 1-propyl-1-methylpyrrolidinium bis(trifluoromethylsulfonyl)amide, [PMP]Tf_2N, 1-hexyl-1-methylpyrrolidinium bis(trifluoromethylsulfonyl)amide, [HMP]Tf_2N, 1-octyl-1-methylpyrrolidinium bis(trifluoromethylsulfonyl)amide, [OMP]Tf_2N, and 1-hexyl-3-methylimidazolium bis(trifluoromethylsulfonyl)amide, [HMIm]Tf_2N, based on the same anion and different cations were employed. $AlCl_3$ was added in these ionic liquids as a precursor for Aluminium. All the liquids exhibit a biphasic behaviour in mixtures with $AlCl_3$ and become monophasic at around 80 °C. Aluminium can only be electrodeposited from the upper phase of [PMP]$Tf_2N/AlCl_3$ and the upper phase of [HMP]$Tf_2N/AlCl_3$ solutions. The best electrodeposits are made in [PMP]$Tf_2N/AlCl_3$ (1.9 M) and in [HMP]$Tf_2N/AlCl_3$ (1.5 M) ionic liquid at 100 °C. Nanoscale Al deposit is obtained in [PMP]$Tf_2N/AlCl_3$. It is found that the viscosity of the upper phase of [PMP]$Tf_2N/AlCl_3$ (1.9 M) is about 9000 mPa·s, which is at least 100-fold higher, as the viscosity of the pure ionic liquid [PMP]Tf_2N.

All pyrrolidinium-based solutions show irreversible electrochemical behavior. In contrast, [HMIm]Tf_2N behavior is reversible. It is well-correlated with results of phase and interfacial behavior of pyrrolydinium- and imidazolium-based ionic liquids **[24,163]**.

Spring steel substrates can be electrochemical covered by Aluminium. Aluminium has been electroplated from upper phase of two solutions of $AlCl_3$ with ionic liquids, namely, 1-ethyl-3-methylimidazolium bis(trifluoromethylsulfonyl)amide, [EMIm]Tf_2N, and 1-ethyl-3-methylimidazolium chloride, [EMIm]Cl. The pre-treatment of the spring steel substrates plays a key role in the coating adhesion. Before the electrodeposition, the substrates have to be grinded with emery paper SiC 800 and anodically etched in the employed electrolyte at +1.0 V vs. Al/Al(III) for 7 minutes to remove the existing oxide layer. Adherent Aluminium deposit of more than 10 μm thick can be made galvanostatically on spring steel substrate in the upper phase of [EMIm]$Tf_2N/AlCl_3$ and in [EMIm]$Cl/AlCl_3$ solutions. Furthermore, nanocrystalline Aluminium can be electrodeposited on the spring steel plates covered by microcrystalline Aluminium. Microcrystalline Aluminium is obtained galvanostatically at 25 °C in [EMIm]$Cl/AlCl_3$. The deposition of nanocrystalline Aluminium

was performed galvanostatically in the upper phase of [BMP]$Tf_2N/AlCl_3$ at 90°C. Internal stresses appear during the electrodeposition.

References

1 Y.Zhao, T.J. Vandernoot, *Electrochim. Acta,* 42(1), 1997, 3

2 A.R. Brukin, *Production of Aluminium and Alumina, Critical reposts in Applied Chemistry,* Vol. 20. John Wiley, Chichester, U.K, 1987

3 E.M. Moustafa, *Dissertation, Technische Universität Clausthal, Clausthal-Zellerfeld*, 2007

4 A.P. Abbot, I. Dalrymple, F. Endres, D.R. MacFarlane, *Electrodeposition from ionic liquids*, ed. F. Endres, D. MacFarlane, A, Abbott, Wiley-VCH, Weinheim, 2008, 1-13

5 F.Endres; S. Zein El Abedin, *PCCP*, 2006, 8, 2101-2116

6 P.C. Trulove and R.A. Mantz, in *Ionic Liquids in Synthesis*, ed. P. Wasserscheid and T.Welton, Wiley-VCH, Weinheim, 2003, pp. 103-126

7 S. Carda-Broh, A. Berthod and D.W. Armstrong, *Anal. Bioanal. Chem*., 2003, 375, 191

8 P. Bonhote, A. Dias, N. Papageorgiou, K. Kalyanasundaram and M. Grätzel, *Inorg. Chem.*, 1996, 35, 1168

9 D.R. MacFarlane, P. Meakin, J. Sun, N. Amini and M. Forsyth, *J. Phys. Chem. B*, 1999, 103, 4164

10 P.Wasserscheid, R. Van Hal, A. Boesman, *Green Chem*., 2002, 4, 400

11 P.A.Z. Suarez, S. Einloft, J.E.L. Dullius, R.F. De Souza and J. Dupont, *J. Chim. Phys.*, 1998, 95, 1626

12 K.N. Marsh, J.A. Boxall and R. Lichtenthaler, *Fluid Phase Equilib*., 2004, 219, 93

13 R.A. Mantz and P.C. Trulove, in *Ionic Liquids in Synthesis*, ed. P. Wasserscheid and T.Welton, Wiley-VCH, Weinheim, 2003, pp. 56-68

14 Crosthwaite, J. M.; Muldoon, M. J.; Dixon, J. K.; Anderson, J. L.; Brennecke, J. F. *J. Chem. Thermodyn.* 37 , 559-568, 2005

15 J.G. Huddleston, A.E. Visser, W.M. Reichert, H.D. Wllauer, G.A. Broker and R.D. Rogers, *Green Chem*., 2001, 3, 156

16 P. Wasserscheid and W. Keim, *Angew. Chem*., Int. Ed., 200, 39,3772

17 J. Fuller, R.T. Carlin and R.A. Osteryoung, *j. Electrochem. Soc*., 1997, 144, 3881

18 J.D. Hlbrey and R.D. Rogers, in *Ionic Liquids in Synthesis*, ed. P. Wasserscheid and T.Welton, Wiley-VCH, Weinheim, 2003, pp. 41-45

19 M.E. Van Valkenburg, R.L. Vaughn, M. Williams and J.S. Wilkes, *15th Symposium on Thermophysical properties*, 2003

20 K.R. Seddon, A. Stark and M.J. Torres, *Pure Appl. Chem*., 200, 72, 2275

21 U. Shröder, J.D. Wadhawan, R.G. Compton, F. Marken, P.A.Z. Suarez, C.S. Consorti, R.F. de Souza and J. Dupont, *New J. Chem*., 2000, 24, 1009

22 M.Mezger, H.Schröder, H.Reichert, S. Schramm, J.S. Okasinski, S. Schröder, V. Honkimäki, M. Deutsch, B.M. Ocko, J. Ralston, M. Rohwerder, M. Stratmann, H. Dosch, *Science*, 2008, 322, p.424

23 R.Atkin, G.G. Warr, *J. Phys. Chem. C*, 2007, 111, 5162

24 R.Atkin, S.Zein El Abedin, R. Hayes, L.H.S. Gaparotto, N. Borissenko, F. Endres, *J. Phys. Chem. C*, 2009, 113, 13266

25 Y. Katayama, S. Dan, T. Miura and T. Kishi, *J. Electrochem. Soc*., 2001, 148, C102

26 P. He, H. T. Liu, Z. Y. Li, Y. Liu, X. D. Xu and J. H. Li, *Langmuir*, 2004, 20, 10260

27 P.-Y. Chen and I.-W. Sun, Electrochim. Acta, 2000, 45, 316332

28 P.-Y. Chen and I.-W. Sun, *Electrochim. Acta*, 1999, 45, 441

29 M.-H. Yang and I.-W. Sun, *J. Appl. Electrochem*., 2003, 33, 1077

30 M.-H. Yang, M.-C. Yang and I.-W. Sun*, J. Electrochem. Soc*., 2003, 150, C544

31 S.-I. Hsiu and I.-W. Sun, *J. Appl. Electrochem*., 2004, 34, 1057

32 I. Mukhopadhyay, C. L. Aravinda, D. Borissov and W. Freyland, *Electrochim. Acta*, 2005, 50, 1275

33 N. Koura, T. Endo and Y. Idemoto, *J. Non-Cryst. Solids*, 1996, 205, 650

34 L. Simanavicius, A. Stakenas and A. Starkis, *Electrochim. Acta*, 1997, 42, 1581

35 Y.-F. Lin and I.-W. Sun, *Electrochim. Acta*, 1999, 44, 2771

36 P.-Y. Chen, M.-C. Lin and I.-W. Sun, *J. Electrochem. Soc*., 2000, 147, 3350

37 P.-Y. Chen and I.-W. Sun*, Electrochim. Acta*, 2001, 46, 1169

38 S. I. Hsiu, J. F. Huang, I.-W. Sun, C. H. Yuan and J. Shiea, *Electrochim. Acta*, 2002, 47, 4367

39 J. F. Huang and I.-W. Sun, *Adv. Funct. Mater*., 2005, 15, 989

40 J. F. Huang and I.-W. Sun, *Chem. Mater*., 2004, 16, 1829

41 H. Y. Hsu and C. C. Yang, *Z. Naturforsch*., B, 2003, 58b, 1055

42 J. F. Huang and I.-W. Sun, *Eectrochim. Acta*, 2004, 49, 3251

43 J. F. Huang and I.-W. Sun, *J. Electrochem. Soc*., 2004, 151, C8

44 J. F. Huang and I.-W. Sun, *J. Electrochem. Soc*., 2003, 150, E299

45 J. F. Huang and I.-W. Sun, *J. Electrochem. Soc*., 2002, 149, E348

46 A. P. Abbott, G. Capper, D. L. Davies, H. L. Munro, R. K. Rasheed and V. Tambyrajah, *Chem. Commun*., 2001, 7, 1010

47 A. P. Abbott, G. Capper, D. L. Davies and R. K. Rasheed, *Chem.-Eur. J*., 2004, 10, 3769

48 A. P. Abbott, G. Capper, D. L. Davies, R. K. Rasheed, J. Archer and C. John, *Trans. Inst. Met. Finish.,* 2004, 82, 14

49 N. Borisenko, A. Ispas, E. Zschippang, Q. Liu, S. Zein El Abedin, A. Bund, F. Endres, *Electrochimica Acta*, 54, 2009, 1519–1528

50 L. H. S. Gasparotto, N. Borisenko, N. Bocchi, S. Zein El Abedin, F. Endres, . *Chem. Chem. Phys*., 2009, 11, 11140–11145

51 G. T. Cheek, W. E. O'Grady, S. Zein El Abedin, E. M. Moustafa, F. Endres, *Journal of The Electrochemical Society,* 155, 1, D91-D95, 2008

52 S. Zein El Abedin, A.Y. Saad, H.K. Farag, N. Borisenko, Q.X. Liu, F. Endres, *Electrochimica Acta,* 52, 2007, 2746–2754

53 N. Borisenko, S. Zein El Abedin, F. Endres, *J. Phys. Chem.,* B 2006, 110, 6250-6256

54 F. Endres, S. Zein El Abedin, A. Y. Saad, E. M. Moustafa, N. Borissenko, W. E. Price, G. G. Wallace, D. R. MacFarlane, P. J. Newman and A. Bund; *Phys. Chem. Chem. Phys.*, 2008, 10, 2189–2199

55 R. Al-Salman, J. Mallet, M. Molinari, P. Fricoteaux, F. Martineau, M. Troyon, S. Zein El Abedin, F. Endres, *Phys. Chem. Chem. Phys*., 2008, 10, 6233–6237

56 R. Al-Salman, S. Zein El Abedin, F. Endres, *Phys. Chem. Chem. Phys*., 2008, 10, 4650–4657

57 T. Carstens, S. Zein El Abedin, F. Endres*, ChemPhysChem* 2008, 9, 439 – 444

58 MacFarlane, D. R.; Meakin, P.; Sun, J.; Amini, N.; Forsyth, M. *J. Phys. Chem.* B 103 , 4164-4170, 1999

59 MacFarlane, D. R.; Meakin, P.; Amini, N.; Forsyth, M. *J. Phys. Condens. Matter*., 13 , 8257-8267, 2001

60 www.merck-chemicals.de

61 Kandil, M. E.; Marsh, K. N.; Goodwin, A. R. H. *J. Chem. Eng.* Data 52 , 2382-2387, 2007

62 Ngo, H. L.; LeCompte, K.; Hargens, L.; McEwen, A. B. *Thermochim.* Acta 357-358 , 97-102, 2000

63 Crosthwaite J. M.; Muldoon M. J.; Dixon J. K.; Anderson J. L.; Brennecke J. F., *J Chem. Thermodyn*. 37 , 2005, 559-568

64 Qi-Xian Qin and M. Skyllas-Kazacos, *J. Electroanal. Chem*., 168, 1984, 193

65 S.Z. El Abedin, E.M. Moustafa, R. Hempelmann, H. Natter, F. Endres, *ChemPhysChem* 2006, 7, 1535-1543

66 Bolkan, S. A.; Yoke, J. T. J. Chem. Eng. Data 31 , 194-197, 1986

67 M. Galova, *Surface Technology*, 11, 1980, 357

68 M.W.M. Graef, *J. Electrochem. Soc*., 132, 1985, 1038

69 T. Garai. *Mater. Chem. Phys.* 8,1983, 399

70 M.I. Konovalov, V.A. Plotnikov, *J. Russ. Phys. Chem. Soc*., 31, 1899, 1020

71 V.A. Plotnikov, *J. Russ. Phys. Chem. Soc*., 34, 1902, 466

72 S. Simanavicius, *Chemija*, 178, 1990, 3

73 D.E. Couch, A. Brenner, *J. Electrochem. Soc*., 99, 1952, 234

74 A. Brenner, D.E. Couch, *U.S. patern 2*, 651, 608, 1953

75 A. Brenner*, in Advances in Electrochemistry and Electrochemical Engineering (Edited by C.W. Tobias)*, vol. 5, p. 217. Interscience, New York, 1967

76 A. Brenner, *J. Electrochem. Soc.*, 106, 1959, 148

77 D.E. Couch, A. Brenner, *J. Electrochem. Soc*., 103, 1956, 657

78 M. Galova, *Surface Technology*, 11, 1980, 357

79 F.J. Schmidt, I.J. Hess, *Electroforming Aluminium for solar energy concentrators*, NASA Tech. Rep. CR-197, 1965

80 A.G. Buschow, I.J. Hess, F.J. Schmidt, *Electroforming Aluminium for solar energy concentrators*, NASA Tech. Rep. CR-66322, 1967

81 F.J. Schmidt, I.J. Hess, *Plating*, 53, 1966, 229

82 W.C. Schickner, *Steel*, 133, 1953, 125

83 R.N. Hanson, D.G. Du pree and K. Lui*, Plating*, 55, 1968, 247

84 J.C. Withers, E.F. Abrams, *Plating*, 55, 1968, 605

85 F.A. Clay, W.B. Harding, C.J. Stimetz, *Plating*, 56, 1969, 1027

86 A.L. Levinskas, J.J. Sinius, *Elektrokhimiya*, 8, 1972, 1053

87 B.I. Ingaunite, A.L. Levinskas, *Issled. Obl. Elektroosazhd. Met*., 2, 1973, 140

88 A.G. Buschow, C.H. Esola, *Plating*, 55, 1968, 931

89 A.L. Leviskas, J.J. Sinius, *C.A.,* 72, 1970, 62161y

90 J.Hess, J.F.Betz, *Metal Finish*, 69, 1971, 38

91 N. Ishibashi, M. Yoshio, *Electrochim. Acta*, 17, 1972, 1343

92 M. Yoshio, N. Ishibashi, *J. Appl. Electrochem*., 3, 1973, 321

93 H.J. Eckert, H. Kslling, *Wiss. Z. Tech. Univ. Dresden*, 24, 1975, 19

94 T. Kurata, R. Kawabata, K. Katayama, E. Takeshima, *Jpn. Patent 73 44*, 608, 1973

95 T. Kurata, R. Kawabata, K. Katayama, E. Takeshima, *Jpn. Patent 73 44*, 609, 1973

96 T. Kurata, R. Kawabata, K. Katayama, E. Takeshima, *Jpn. Patent 74 00*, 018, 1974

97 M. Yoshio, *Mat. Finish*, 7, 1987, 33

98 S.P. Sidelnikova, V.N. Sherstkina, A.N. Jakubetz, *Izv. Akad. Nauk Mold. SSR, Ser. Fiz.-Tekh. Mat. Nauk*, 1, 1979, 69

99 E. Eckert, *Dechema-Monografhien*, Vol. 125, p. 425, VCH Verlagsgesellschaft, Winheim, 1992

100 M.C. Lefebvre, B.E. Conway, *J. Electroanal. Chem*., 480, 2000, 34

101 M.C. Lefebvre, B.E. Conway, *J. Electroanal. Chem*., 480, 2000, 46

102 F.H. Hurley, T.P. Wier, *J. Electrochem. Soc*., 98, 1951, 207

103 W. Safranek, W. Schickfier, C. Faust*, J. Electrochem. Soc*., 99, 1952, 53

104 L.E. Simanavicius, P.P. Dobrovolskis, *Issled. Obl. Elektroosazhd. Met*., 1, 1971, 192

105 L.E. Simanavicius, P.P. Dobrovolskis, *USSR Patent 382*, 761, 1972

106 L.E. Simanavicius, P.P. Dobrovolskis*, Issled. Obl. Elektroosazhd. Met*., 2, 1973, 131

107 E. Peled, E. Gileadi, *J. Electrochem. Soc*., 123, 1976, 15

108 E. Peled, E. Gileadi, *Plating*. 62, 1975, 342

109 L.E. Simanavicius, A. Stakenas, A. Sarkis, *Electrochim. Acta*, 46, 2000, 499

110 G.A. Capuano, W.G. Davenport, *J. Electrochem. Soc*., 118, 1971, 1688

111 G.A. Capuano, W.G. Davenport, *Plating*, 60, 1973, 251

112 W.G. Davenport, G.A. Capuano, in J.H.E. Jeff and R.J. Tait (eds.), *Proc. Richardson Conf. on the Physical Chemistry of Process Metallurgy, London, 1973, Institution of Mining and Metallurgy, London,* 1973, p.77

113 G.A. Capuano, W.G. Davenport, *Can. Patent 4375*, 1971

114 L.E. Simanavicius, A.M. Levinskiene, *Elektrokhimiya*, 2, 1966, 353

115 L.E. Simanavicius, A.P. Karpavicius, *Issled. Obl. Elektroosazhd. Met*., 1, 1968, 164

116 L.E. Simanavicius, A.P. Karpavicius*, Nauchn. Tr. Vyssh. Uchebn. Zaved. Lit. SSR*, Ser. B, 4, 1970, 139

117 L.E. Simanavicius, A.M. Levinskiene, *Tr. Akad. Nauk Litov. SSR*, Ser. B, 4, 1966, 39

118 V.A. Kazakov, V.N. Titova, N.V. Petrova, *Elektrokhimija*, 12, 1976, 576

119 V.A. Larchenko, V.A. Kazakov, V.N. Titova, V.F. Chuvajev, *Elektrokhimija*, 14, 1978, 588

120 E. Bokor, *Proc. 29th Meet. Of ISE, Budapest, 1978. MTA Kozponti Kemiai Kunato Intezet, Budapest*, 1978, p.1182

121 S.P. Shavukunov, T.L. Strugova, *Russ. J. Electrochem*., 39, 2003, 642

122 G.A. Capuano, *J. Electrochem. Soc*., 138, 1991, 484

123 H: Lehmkuhl, *Dissertation, Rheinisch-Westfalische Technische Hochschule, Achen*, 1954

124 K. Ziegler, H. Lehmkuhl, *Z. Anorg. Allg. Chem*., 283, 1956, 414

125 K. Ziegler, H. Lehmkuhl, *C.A. 52*, 1958, 19619d

126 R. Dötzer, *Chem.-Ing.-Tech*., 45, 1973, 653

127 G. Ivantscheff, R. Dötzer, *Werkstattstechnik*, 9, 1972, 10

128 R. Dötzer, E. Todt, H.G. Hauschildt, *Ger. Offe, Patent 2553830*, 1976

129 J.P. Pereira-Ramos, *Dissertation, University of Paris* 12, 1988

130 T.R. Griffins, *J. Chem. Soc. Comm*., 1222, 1967

131 J. Hennion, J. Nicole, *J. Bull. Soc. Chim. Fr*., 426, 1978

132 J.P. Pereira-Ramos, R. Messina, J. Perichon, *J. Electroanal. Chem*., 209, 1986, 283

133 L. Legrand, A. Tranchant, R. Messina, *Electrochim. Acta*, 39, 1994, 1427

134 L. Legrand, A. Tranchant, R. Messina, *J. Electrochem. Soc*., 141, 1994, 378

135 L. Legrand, A. Tranchant, R. Messina, F. Romain, M. Lautie, *Inorg. Chem*., 35, 1996, 1310

136 J. Fransaer, E. Leunis, T. Hirato, J.-P. Celis, *J. Appl. Electrochem*., 32, 2002, 123

137 G.R. Stafford, *J. Electrochem. Soc*., 136, 1989, 635

138 R. Bunsen, *Poggendorf's Ann*., 97, 1854, 648

139 V.A. Plotnikov, V.P. Mashovets, N.S. Fortunatov, *Zhur. Khim. Prom*., 7, 1930, 1476

140 V.A. Plotnikov, N.N. Gratsianskii, *Zhur. Khim. Prom*., 8, 1931, 829

141 V.A. Plotnikov, N.N. Gratsianskii, *Legkie Metally*, No 2-3, 1933, 47

142 Y.F. Chittum, *U.S. 1*, 927, 772, 19 Sep 1933

143 S.N. Orleva, V.I. Lainer, *Legkie Metally*, No 12, 1935, 9

144 W.H. Wade, G.O. Tellmeyer, L.F. Yntema, *Trans. Electrochem. Soc*., 78, 1940, 77

145 R. Wehrmann, L.F. Yntema, *J. Phys. Chem*., 48, 1944, 259

146 R.G. Verdieck, L.F. Yntema, *J. Phys. Chem*., 48, 1944, 268

147 Yu.K. Delimarskii, A.V. Chetverikov, V.F. Makogon, *USSR, No 178 257*, 8 Jan 1966

148 A.V. Chetverikov, Yu.K. Delimarskii, V.F. Makogon, *Dopovidi Akad. Nauk SSSR – S.B. 2*, 1967, 447

149 A.V. Chetverikov, V.F. Makogon, Yu.K. Delimarskii, *Fizicheskaya khimia i elektrokhimia rasplavlennykh solei i shlakov, Khimia, Moscow*, 1968

150 A. Miyata, H. Okubo, Ch. Tomito, A. Suzuki, *U.S. 3*, 470, 073, 30 Sep 1969

151 *Japan Steel and Tube Corp., Fr. 1*, 549, 879, 13 Dec 1968

152 V.V. Kuzmovich, V.F. Makogon, Yu.B. Kazakov, *Ukr. Khim. Zhur*., 34, 1968, 344

153 V.V. Kuzmovich, V.F. Makogon, Yu.B. Kazakov, *Ukr. Khim. Zhur*., 35, 1969, 258

154 Yu. K. Delimarskii, V.F. Makogon, V.V. Kuzmovich, *Zashchita Metallov*, 4, 1968, 743

155 Yu.K. Delimarskii, V.V. Kuzmovich, *Ukr. Chim. Zhur*., 36, 1970, 776

156 L.W. Austin, M.G. Vucich, E.J. Smith, *Electrochem. Technology*, 1, 1963, 267

157 Yu.K. Delimarskii, V.V. Kuzmovich, *Zhur. Fiz. Khim*., 46, 1972, 2567

158 C.S. Charlton, N.F. Murphy, *U.S. 2*, 807, 575, 24 Sep 1957

159 M. Paucirova, K. Matiasovsky, *Electrodeposition and Surface Treatment*, 3, 1975, 121

160 G.R. Stafford, *J. Electrochem. Soc*., 141, 1994, 945

161 R.J. Gale, R.A. Osteryoung, *Inorg. Chem*., 18, 1979, 1603

162 J. Robinson, R.A. Osteryoung, *J. Electrochem. Soc*., 127, 1980, 122

163 P. Eiden, Q. Liu, S. Zein El Abedin, F. Endres, I. Krossing, *Chem. Eur. J*., 2009, 15, 3426-3434

164 T. Tsuda, C.L. Hussey, G.R. Stafford, *J. Electrochem. Soc*., 151, 6, 2004, C379

165 T. Tsuda, C.L. Hussey, G.R. Stafford, J.E. Bonevich, *J. Electrochem. Soc*., 150, 4, 2003, C234

166 T.Tsuda, C.L. Hussey, G.R. Stafford, O. Konhstein, *J. Electrochem. Soc*., 151, 7, 2004, C447

167 Q. Zhu, C.L. Hussey, G.R. Stafford, *J. Electrochem. Soc*., 148, 2, 2001, C88

168 T. Tsuda, C.L. Hussey, G.R. Stafford, *J. Electrochem. Soc*., 152, 9, 2005, C620

169 T. Jiang, M.J.C. Brym, G. Dube, A. Lasia, G.M. Brisard, *Surface and Coatings technology*, 201, 1-2, 2006, 1

170 Q.X. Liu, S.Z. El Abedin, F. Endres, *Surface and Coatings Technology*, 201, 3-4, 2006, 1352

171 Q. Zhu, C.L. Hussey, *J. Electrochem. Soc*., 148, 5, 2001, C395

172 Q. Zhu, C.L. Hussey, *J. Electrochem. Soc*., 149, 5, 2002, C268

173 F. Endres, M. Bukowski, R. Hempelmann, H. Natter, *Angew. Chem. Int. Ed*., 42, 2003, 3428

174 D. Floreani, D. Stech, J. Wilkes, J. Williams, B. Piersma, L. King, R. Vaughn, *Proc. Power Sources Symp*., 30, 1982, 84

175 P.K. Lai, M. Skyllas-Kazacos, *J. Electroanal. Chem*., 248, 1988, 413

176 R.T. Carlin, W. Crawford, M. Bersch, *J. Electrochem. Soc*., 139, 10, 1992, 2720

177 G.R. Stafford, *J. Electrochem. Soc*., 144, 3, 1997, 936

178 J. Robinson, R.A. Osteryoung, *J. Electroanal. Chem*., 248, 1988, 413

179 P.K. Lai, M. Skyllas-Kazacos, *Electrochim. Acta*, 32, 10, 1987, 1443

180 J. Robinson, R.A. Osteryoung, *J. Electrochem. Soc*., 127, 1, 1980, 122

181 Chao-Cheng Yang, *Materials Chemistry and Physics*, 37, 1994, 355

182 M.R. Ali, A. Nishikata, T. Tsuru, *Electrochim. Acta*, 42, 12, 1997, 1819

183 M.R. Ali, A. Nishikata, T. Tsuru, *Electrochim. Acta*, 42, 12, 1997, 2347

184 N.Borisenko *Dissertation, Technische Universität Clausthal, Clausthal-Zellerfeld*, 2007

185 Flegler, Heckman, Klomparens, *Elektronenmikroskopie - Grundlagen, Methoden, Anwendungen*, Spektrum Akademischer Verlag, 1995

186 www.reotec.de

187 P. Scherrer, Göttinger Nachrichten, 2, 1918, 98

188 Tokuda H.; Tsuzuki S.; Susan M. A. B. H.; Hayamizu K.; Watanabe M., *J. Phys. Chem.*, B 110 (39), 19593-19600, 2006

189 C. Martinez, S. Kyrsta, R. Cremer, D. Neuschütz, *Surf. Interface Anal*., 2002, 34, 396-399

190 F. Czerwinski, *J. Electrochem. Soc.*, 143, 3327, 1996

Abbreviations

$AlCl_3$ - Aluminium chloride

BF_4^- - tetrafluoroborate anion

NO_3^- - nitrate anion

[BMIm]PF_6 - 1-Butyl-3-methylimidazolium hexafluorophosphat

[BMIm]BF_4 - 1-Butyl-3-methylimidazolium tetrafluoroborat

[BMIm]Tf_2N - 1-Butyl-3-methylimidazolium bis(trifluoromethylsulfonyl]amide

$[EEIm]^+$ - 1-Ethyl-3-ethylimidazolium cation

$[BEIm]^+$ - 1-Butyl-3-ethylimidazolium cation

PF_6^- - hexafluorophosphate anion

TFA^- - trifluoroacetic anion

$[CH_3SO_3]^-$ - methanesulfonate anion
$CF_3CO_2^-$ - trifluoroacetate anion
$CF_3SO_3^-$ - trifluoromethylsulfonate anion
$C_3F_7CO_2^-$ - heptafluorobutyrate anion

$DMSO_2$ - dimethylsulfone

$BuPy^+$ - butylpyridinium cation

[PMP]Tf_2N -1-Propyl-1-methylpyrrolidinium bis(trifluoromethylsulfonyl)amide

[HMP]Tf_2N -1-Hexyl-1-methylpyrrolidinium bis(trifluoromethylsulfonyl)amide

[OMP]Tf_2N -1-Octyl-1-methylpyrrolidinium bis(trifluoromethylsulfonyl)amide

[OMIm]Tf_2N -1-Octyl-3-methylimidazolium bis(trifluoromethylsulfonyl)amide

[EMIm]Tf_2N -1-Ethyl-3-methylimidazolium bis(trifluoromethylsulfonyl)amide

[EMIm]Cl -1-Ethyl-3-methylimidazolium chloride

[BMP]Tf_2N -1-Butyl-1-methylpyrrolidinium bis(trifluoromethylsulfonyl)amide

$(CF3SO_2)_2N^-$=Tf_2N=TFSA=TFSI - bis(trifluoromethylsulfonyl]amide anion

Anton Fomin

Persönliche Daten

Geburt:	20.02.1982, Ramenskoe (Moskau Gebiet), Russland
Nationalität:	Russisch

Hochschulstudium

Promotion

10/2006 – 10/2010	Doktorantur an der TU Clausthal, Abteilung Grenzflächenprozesse http://www.mvt.tu-clausthal.de/ , Doctorthesis: „Elektrochemische Aluminium Abscheidung aus verschiedenen Wasser- und Luftstabilen Ionischen Flüssigkeiten“

Diplomstudiengänge

10/2004 – 10/2006	Studium des Werkstoffwissenschaften an der TU Clausthal http://www.tu-clausthal.de/ Gesamtnote 2,2
	Diplomstudiengang: Werkstoffwissenschaften
09/1999 – 06/2006	Studium an der Moskauer Staatlichen Hochschule für Stahl und Legierungen (Technologische Universität) www.misis.ru/en Fakultät für Physik und Chemie. 11 Semester lang, Gesamtnote 4,2*
	Diplomstudiengang: Metallphysik
09/2003 – 11/2003	Studienarbeit: “Untersuchungen vom Einfluss Ionenstrahlen auf die Substruktur der Stahl mit 12% Cr“
10/2005 – 10/2006	Diplomarbeit: „Mechanische Eigenschaften von Ti-6Al-4V in feinlamellaren, globularen und bimodalen Zustände nach verschiedenen Oberflächebehandlungen.“ Note 1,3.

Schulausbildung

09/1989 – 06/1999	Zhukovsky Gymnasium №1 mit erweiterten Mathematik- und Physikunterrichten, Moskau Gebiet, Russland
Abschluss:	Allgemeine Hochschulreife, Gesamtnote 4,4*

* Das *russische Notensystem* beruht auf einer Fünferskala, wobei "5" die beste Note ist.